Dysregulation of metabolic pathways by KSHV and metabolic sensors in cancer

by

Tingting Li

BA, Hunan Normal University, 2014

MS, University of Southern California, 2016

Submitted to the Graduate Faculty of the

School of Medicine in partial fulfillment

of the requirements for the degree of

Doctor of Philosophy

University of Pittsburgh

2020

UNIVERSITY OF PITTSBURGH

SCHOOL OF MEDICINE

This thesis was presented

by

Tingting Li

It was defended on

March 16, 2020

and approved by

Patrick S. Moore, Distinguished Professor, Department of Microbiology and Molecular Genetics

Fred L. Homa, Professor, Department of Microbiology and Molecular Genetics

Masahiro Shuda, Assistant Professor, Department of Microbiology and Molecular Genetics

Man-Tzu Wang, Assistant Professor, Department of Pharmacology and Chemical Biology

Dissertation Director: **Shou-Jiang Gao**, Professor, Department of Microbiology and Molecular Genetics

Dysregulation of metabolic pathways by KSHV and metabolic sensors in cancer

Tingting Li, PhD

University of Pittsburgh, 2020

Cancer cells reprogram cellular metabolic pathways to provide bioenergetics and anabolic demands to sustain uncontrolled cell proliferation. Fluctuations in metabolites are sensed by metabolic sensors such as mTORC1, AMPK and sirtuins that coordinate biological networks essential for cell survival and proliferation. Oncogenic viruses induce oncogenesis often by targeting the same pathways that are deregulated in cancer. Indeed, both metabolic pathways and sensors are hijacked by KSHV to support viral persistence, replication and cellular transformation. During my Ph.D. training, I studied the metabolic alterations of arginine metabolism and citrulline-NO cycle in KSHV-transformed cells, which later led to me to explore arginine sensing by mTORC1 and CASTOR1 in KS and other types of cancer.

In **Chapter 1.1** of this thesis, I introduce some essential concepts and recent advances in KSHV dysregulation of cellular metabolic pathways and sensors. **In Chapter 1.2**, I discuss recent works on sensing of the nutrients by mTORC1 and how these mechanisms might be relevant to cancer and aging. In **Chapter 2.0** to **4.0**, I summarize my research progress. In **Chapter 2.0**, I demonstrate how *de novo* arginine synthesis and the citrulline-NO cycle are hijacked by KSHV-encoded miRNAs, which is essential for STAT3 activation and therefore KSHV-driven cell proliferation and transformation. In **Chapter 3.0**, I show that KSHV-encoded miR-K4-5p and likely -K1-5p directly target CASTOR1 for degradation, leading to mTORC1 activation, and contributing to KSHV-induced cellular transformation. In **Chapter 4.0**, I present the results that support a distinct mechanism by which the inhibitory effect of CASTOR1 on

mTORC1 is released in KSHV-negative cancer. In details, AKT1 directly binds to and phosphorylates CASTOR1 at S14, which enhances its interaction with E3 ubiquitin ligase RNF167 and therefore promotes its ubiquitination and degradation. Significantly, AKT1- and RNF167-mediated CASTOR1 degradation activates mTORC1 and promotes breast cancer progression. In **Chapter 5.0**, I list the experimental methods that I have used in my studies. Finally, I discuss the significance of my works and potential future directions in **Chapter 6.0**.

A list of publications and other academic contributions are presented in **Appendix C**.

Table of Contents

List of Tables

List of Figures

Acknowledgement

This thesis was completed under the careful guidance of my advisor Dr. Shou-Jiang Gao. The selection of the thesis, the experimental design, and the analysis of the experimental results all combine Dr. Gao's wisdom, efforts and sweat. Dr. Gao has deeply influenced me with his solid theoretical foundation, meticulous scientific thinking, rigorous research attitude and persistent self-dedication. It will also have a positive impact on my future study and life. Every step along the way relies on Dr. Gao's concern and guidance. Here, I would like to express my highest respect and sincere gratitude to my instructor Dr. Shou-Jiang Gao. I've been very proud of being one of his students!

Thanks to my committee members, Dr. Patrick S. Moore, Dr. Fred Homa, Dr. Masa Shuda and Dr. Man-tzu Wang. In the process of completing my thesis, they have been giving lots of valuable suggestions. Their thinking, profound knowledge and insights into the frontiers of science, positive attitude towards life, and enthusiasm for students have benefited me a lot. Here, I would like to express my heartfelt thanks and respect to them.

I am grateful to our previous lab mates and friends neighboring to our lab in USC, Dr. Ying Zhu, Dr. Fan Cheng, Dr. Meilan He, Dr. Brandon Tan, Dr. Hongfeng Yuan, Dr. Hui Liu, Ruoyun Gao, Dr. Jianning Ge and Meng Li. They taught me all basic experimental skills and interested me to scientific research. More importantly, they took care of me besides lab work. I am also very grateful to our current lab mates, Dr. Suzane Ramos, Dr. Enguo Ju, Shan Wei, Dr. Xinquan Zhang, Luping Chen, Qin Yan, Xian Wang, Jian Feng, Wen Meng, Xinghong Gao, Xiaofei Zhu, Wan Li and Fei Zhang. Because of their accompany, my research life is meaningful.

I would like to particularly thank my best friends Jie Chen and Xiang Li. Although they are in China, they have been giving me enormous encouragements since I was an undergraduate student. I've been very lucky to have them as my lifelong friends.

Thanks to PMI program directors and coordinator, Dr. Jennifer M. Bomberger, Dr. Robert Juilan Binder and Ms. Kristin M. Digiacomo for their guidance and instruction, I can quickly meet the program requirements and graduate smoothly.

The five and half years in Dr Gao's lab have been the best memories of my life. I sincerely thank all the teachers in the Graduate Department for their care and help in my study and life!

Finally, I am especially grateful to my family for their long-standing support and encouragement for my studies.

1.0 Introduction

Cancer is recognized as a metabolic disease since a defining hallmark of cancer is uncontrolled proliferation that demands surplus bioenergetics and biosynthetic precursors [1]. To meet these demands, cancer cells have rewired metabolic pathways, which can be achieved by dysregulating tumor suppressors or oncogenes. Conversely, cancer cells produce certain metabolites that further regulate metabolic sensors including mTOR complex 1 (mTORC1), AMPK and sirtuins to support cell proliferation and survival [2]. Among them, mTORC1 is most widely studied and has been implicated in most types of cancer. By sensing the changes of cancer cell metabolites, mTORC1 will execute a command that eventually promote cancer progression. Likewise, the chronic infection of oncogenic viruses also rewires the metabolic pathways and hence metabolic sensors of host cells to induce cellular transformation and tumorigenesis. As cancer virus, Kaposi's sarcoma-associated herpesvirus (KSHV) directly hijacks metabolic enzymes to alter the metabolic pathways and dysregulates metabolic sensors to divert the ways that cells respond to the environmental inputs. The interests on cancer metabolisms have recently been accelerated with the developments of new techniques. In this chapter, I will summarize the recent advances on the metabolic pathways and metabolic sensors with a focus on mTORC1 that are reprogrammed by KSHV and in cancer.

1.1 KSHV hijacks cellular metabolic pathways and sensors

According to the assessment of the International Agency for Research on Cancer, viral infection accounts for up to 11% of human cancer worldwide [3]. Oncoviruses induce tumorigenesis by chronically infecting host cells and consequently inducing persistent epigenetic alterations as well as changes in some cellular oncogenic pathways. KSHV is an oncogenic herpesvirus and its lifelong latent infection leads to cellular transformation and tumorigenesis [4]. It has been observed for long time that viral infection reprograms the host cell metabolic pathways [5]. Emerging evidence has shown that KSHV hijacks the cellular catabolic and anabolic pathways to support cell survival and proliferation. In this subsection, I summarize the main aspects of metabolic alterations that occur in KSHV-infected and -transformed cells and the related signaling pathways potentially underlying the metabolic reprogramming. Throughout, we discuss important questions that remains to be resolved in future studies in the field of KSHV-reprogrammed metabolism.

1.1.1 Cancer metabolism

The recent resurgence of cancer metabolism is arisen from the advances in the newly developed biomedical and biological tools, which expands our understanding of the underpinning mechanisms and functional consequences of altered metabolism in cancer. Tumor cells often show increased consumption of glucose, accompanied by a switch of energy metabolism from oxidative phosphorylation to aerobic glycolysis even when exposed to ambient oxygen, the so-called Warburg effect [6]. Although the aerobic glycolysis has low energy yield, it is widely regarded as a way to effectively provide precursors such as NADPH and ribose-5-

phosphate for the synthesis of biologically relevant macromolecules [7]. Glutamine is a primary source of both carbon and nitrogen for *de novo* synthesis of diverse nitrogen-containing building blocks including nucleotides, fatty acids and nonessential amino acids (arginine, proline, asparagine) [2]. Proliferating cancer cells are highly addicted to glutamine leading to accelerated glutamine uptake and glutaminolysis [2, 7]. Hence, glutamine deprivation often lead to cancer cell death and decreased cell proliferation, which is countered by glutamine anaplerosis [7]. DNA replication is the basis of cancer cell proliferation, which demands rapid nucleotides synthesis driven by c-Myc through upregulation of nucleotide biosynthesis enzymes [7]. Acetyl-CoA, which is derived from glucose and glutamine, is the building block of fatty acids and cholesterol. With the rapid division of cancer cells, the membrane synthesis supported by *de novo* fatty acids synthesis is increased. Additionally, one-carbon metabolism is a universal metabolic process in eukaryotes and across organs, and is frequently enhanced in cancer cells to support the biosynthesis of nucleic acids, defend the reactive oxygen species (ROS) and control the concentration of three amino acids: glycine, methionine and serine [8, 9]. Further, as the only supply of the methyl group, one carbon metabolism is frequently upregulated in cancer to provide the methyl group required for DNA, RNA and histone modifications, which supports tumor progression by dysregulating gene expression [10]. Although the reprogramming of metabolic activities in cancer is widely documented, most data are obtained *in vitro*. How and to what extent this explains tumorigenesis *in vivo* remains largely unclear. A breakthrough in techniques that allow better determination of the *in vivo* conditions is urgently required.

1.1.2 KSHV and KSHV-associated human diseases

Kaposi's sarcoma-associated herpesvirus (KSHV), discovered in 1994 by Chang and Moore [11], is one of seven oncogenic viruses and the causative agent of Kaposi's sarcoma (KS), primary effusion lymphoma (PEL), multicentric Castleman's diseases (MCD) and KSHV-associated inflammatory cytokine syndrome (KICS) [12, 13]. The life cycle of KHSV comprises two phases, known as the latent and lytic phases. During latency, KSHV only expresses a few genes including LANA (ORF73), vCyclin (ORF72) and vFLIP (ORF71) together with 25 microRNAs (miRNAs) derived from a cluster of 12 precursor miRNAs (pre-miRNAs) named KSHV-miR-K12-1-12 (hereafter referred to as miR-K1-12) [4, 14]. Among them, LANA is essential for KSHV episome maintenance in host cells by mediating viral genome replication and tethering viral genome to chromosomes to ensure appropriate segregation during mitosis [15]. By contrast, there are many lytic genes and among them RTA is the key transactivator that initiates KSHV replication [4].

KS tumors are spindle-shaped expressing vascular endothelial, lymphatic endothelial, precursor and mesenchymal markers [16]. Most KS and PEL tumors are latently infected by KSHV, suggesting that KSHV latent infection is critical for KSHV-induced tumorigenesis [4]. There is currently no effective drug for inhibiting latent KSHV infection and for treating KSHV-induced cancers. A comprehensive illustration of how the KSHV latent genes manipulate cellular metabolic pathways and metabolic sensors might help develop treatments for KS tumors.

1.1.3 KSHV reprograms glucose metabolism

The first characterization of metabolic changes in tumors cells dated back to 100 years ago when the Germany physiologist Otto Warburg observed that cancer cells consume a large amount of glucose and secrete excessive lactate even in the presence of oxygen, which only yields 2 ATP per glucose [6]. In contrast, normal cells under normoxia preferentially catabolize glucose to pyruvate that is subsequently transported into mitochondria to fuel the tricarboxylic acid cycle (TCA) coupled with oxidative phosphorylation to generate 36 ATP (**Figure 1A**). Cancer patients undergoing aerobic glycolysis have poor survival [17]. Recently the positron emission tomography (PET)-based imaging to monitor the uptake of a radiolabeled glucose analog, ^{18}F-fluorodeoxyglucose (^{18}F-FDG), has been successfully applied clinically to diagnose and stage tumors. The combination of PET with ^{18}F-FDG and computed tomography (^{18}F-FDG PET/CT) provides valuable functional information regarding the uptake of glucose and glycolytic processes of cancer cells, which benefits cancer recurrence detection and treatments [18].

Viruses rely on metabolites and energy of host cells to generate progeny, which requires the rewiring of cellular metabolic pathways to prevent metabolic exhaustion. To assess the effect of KSHV infection on glucose catabolism, Delgado et al. infected telemerase-immortalized microvascular endothelial cells (TIME cells) and primary dermal microvascular endothelial cells (1° hDMVECs) with KSHV for 48 hours and observed the induction of Warburg effect in KSHV-infected cells, which had an increased glucose uptake, decreased oxygen consumption and lactate secretion in KSHV- versus mock-infected cells [19] (**Figure 1B**). Inhibitors of aerobic glycolysis specifically induce cell death by apoptosis in KSHV-infected TIME cells, which is partially rescued by inhibiting oxidative phosphorylation, suggesting that the Warburg

effect is essential for maintaining the survival of KSHV-infected cells. Hexokinase 2 (HK2) is the rate-limiting enzyme that catalyzes the first step of glycolysis and is upregulated following 48-hours of KSHV infection [19], and KSHV infection alone for 48 hours fails to induce the glucose transporter 3 (GLUT3) that is only stabilized after adding hypoxia mimics. These authors did not observe notable differential cell death in KSHV-negative Burkitt's lymphoma BJAB versus KSHV-infected BJAB cells after inhibiting aerobic glycolysis [19]. Singh et al. later confirmed these results by showing that hypoxia-stabilized HIF1α can be upregulated by KSHV-encoded vGPCR, leading to increased aerobic glycolysis in KSHV-infected BJAB cells [20]. Additionally, the induction of hypoxia significantly changed the gene profiles of PEL cells involved in the metabolism of fatty acids and amino acids, suggesting that the KSHV-HIF1α axis might reprogram these metabolic pathways [20]. Similarly, Ma et al. reported that KSHV induces Warburg effect in human umbilical vein endothelial cells (HUVEC) by enhancing the HIF1α-mediated upregulation of pyruvate kinase 2 (PKM2), which is a key step in pyruvate production and aerobic glycolytic efflux [21]. Yogev et al. found that KSHV-encoded miRNA cluster induces Warburg effect in lymphatic endothelial cells (LEC) by stabilizing HIF1α and inhibiting mitochondrial biogenesis through downregulating EGLN2 and HSPA9 [22] (**Figure 1B**).

Nevertheless, all these studies rely on the short-term KSHV infection that don't lead to cellular transformation. As a result, the above system might not recapitulate the *in vivo* metabolic characteristics of KS tumors. In 2012 Jones et al. successfully immortalized and transformed primary rat metanephric mesenchymal precursor cells (MM) by chronic KSHV infection alone [23]. This breakthrough, for the first time, has made it possible to delineate viral genes and cellular pathways required for KSHV-induced cellular transformation and tumorigenesis. By

applying this model, Zhu et al. found that KSHV-encoded miRNAs and vFLIP concomitantly activate NF-κB signaling pathway to suppress aerobic glycolysis and oxidative phosphorylation by downregulating both GLUT1 and GLUT3 [24] (**Figure 1C**). Of note, the authors also showed that the Warburg effect is likewise reduced in several KSHV-positive PEL cells and KSHV-infected BJAB cells [24]. The independence on glucose of KSHV-transformed cells (KMM) is essential for them to survive in glucose-deprived tumor microenvironment. This controversy in glycolysis between KSHV-infected and -transformed cells might be explained by differential metabolic status during distinct stages of KSHV infection, which may reflect that the glycolytic activities are highly dynamic in different stages of KS tumors. Although the alteration of glucose metabolism is ensured, the exact mechanism by which KSHV latent product directly impacts glycolysis remains unclear.

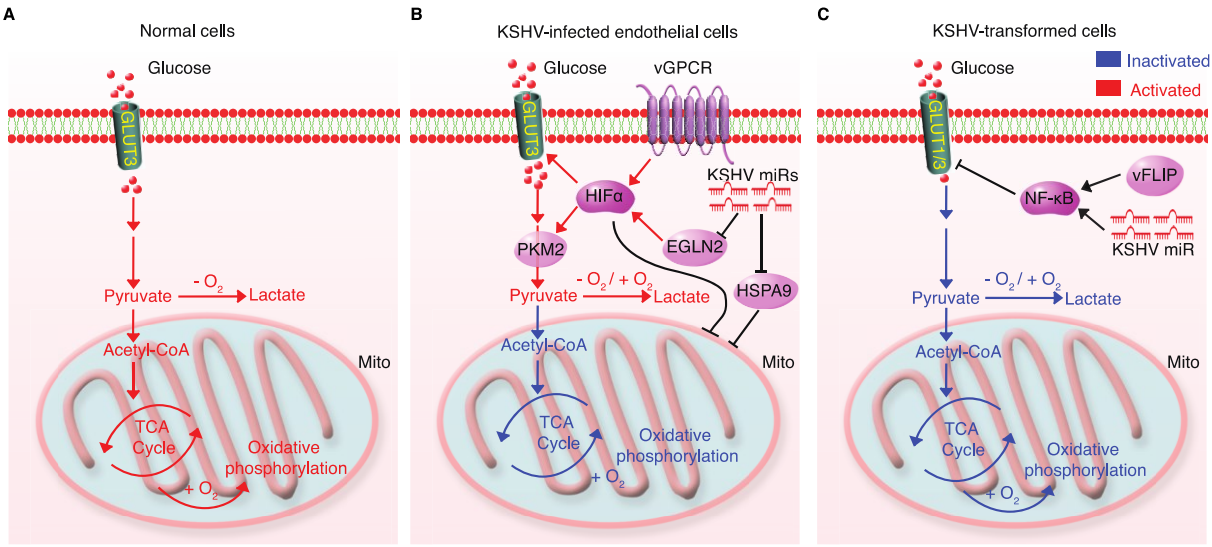

Figure 1: The glycolytic pathway in normal and KSHV-infected and –transformed cells.

(**A**) The glycolysis is highly regulated by oxygen levels in normal cells. Under normoxia, the glucose is metabolized to pyruvate that fuels the TCA cycle and is coupled with oxidative phosphorylation to generate copious ATP. Under hypoxia, the glucose is metabolized to pyruvate and subsequently converted to lactate. (**B**) KSHV-encoded miRNA cluster and vGPCR induce the aerobic glycolysis in short-term KSHV-infected endothelial cells by upregulating HIF1α and inhibiting mitochondria. (**C**) KSHV-encoded miRNA cluster and vFLIP suppress the glycolysis and oxidative phosphorylation by activating NF-κB-mediated GLUT1 and GLUT3 downregulation.

1.1.4 KSHV enhances glutaminolysis and the urea cycle efflux

Glutamine is a very versatile amino acid, acting as energy fueling as well as a precursor to synthesize many biological macromolecules. GLS and GLS2 hydrolyze glutamine to glutamate that is further exported by antiporter xCT coupled with cysteine import [25, 26]. Inhibition of GLS and GLS2, which are at the early steps of glutamine pathway, causes cell cycle arrest in several cancer cells, indicating the importance of glutaminolysis in tumorigenesis [27-29]. The promotion of glutaminolysis by xCT, which is upregulated by KSHV miRNA cluster, replenishes intracellular glutathione and antagonizes reactive nitrogen species (RNS)-induced

cell death [30-32] (**Figure 2**). Whether KSHV-mediated xCT upregulation promotes glutamine uptake, catabolism and glutamate secretion is unknown.

Veettil et al. observed an increased secretion of glutamate into medium following KSHV latent infection, which is essential for the proliferation of KSHV-infected cells [33]. Mechanistically, RE-1 silencing transcription factor (REST), a transcriptional repressor of the metabotropic glutamate receptor 1 (mGluR1), interacts with and is sequestered by KSHV-encoded Kaposin A in the cytoplasm accounting for mGluR1 upregulation in KSHV-infected cells [33]. However, more direct evidence is required to confirm the essentiality of mGluR1 in KSHV-induced glutamate secretion. Alternatively, the authors illustrated that KSHV LANA upregulates GLS by inducing c-Myc expression, which leads to increased glutamine hydrolysis in KSHV-infected cells [33] (**Figure 2**). Sanchez et al. further observed an increased uptake of glutamine following KSHV primary infection of TIME cells, which is mediated by KSHV-upregulated c-Myc that increases glutamine transporter SLC1A5 by transcriptionally inducing MondoA [34] (**Figure 2**). Glutamine deprivation or SLC1A5 silencing selectively causes KSHV- rather than mock-infected apoptosis, which is partially rescued by cell-permeable a-ketoglutarate (α-KG) anaplerosis [34]. As a key intermediate metabolite of glutaminolysis, α-KG is produced by two steps: GLS catalyzes glutamine to glutamate that is subsequently converted to α-KG through glutamate dehydrogenase 1 and 2 (GLUD1 and GLUD2). The rescue experiment demonstrated that KSHV-infected cells rely on glutaminolysis for survival possibly because glutamine fuels the TCA cycle.

By contrast, Zhu et al. found that KSHV-transformed cells are addicted to glutamine rather than glucose to sustain cell proliferation, survival and transformation [35]. Compared to mock cells, KSHV-transformed MM cells have increased consumption of glutamine and

upregulation of several key glutaminolytic enzymes including GLS, GLUD1 and glutamic-oxaloacetic transaminase 2 (GOT2) [35] (**Figure 2**). Intriguingly, whereas the supplementation of asparagine alone but neither any other NEAA nor α-KG fully rescues glutamine deprivation in KMM cells while the combination of α-KG, glutamate and nucleosides mimics the effect of asparagine [35] (**Figure 2**). This indicates that glutamine provides a nitrogen source for nucleotide synthesis and a carbon source for the TCA cycle and aspartate synthesis in KSHV-transformed cells [35]. The high consumption of glutamine in KSHV-transformed cells requires tight regulation and timely clearance of excess nitrogen to avoid accumulation of toxic byproducts, which can only be achieved by the citrulline-nitric oxide (NO) cycle. Indeed, we have found that KSHV-encoded miRNAs accelerate the citrulline-NO cycle by upregulating the rate-limiting enzyme argininosuccinate synthase 1 (ASS1) [36]. Knockdown of ASS1 suppresses cell proliferation and abolishes colony formation in soft agar of KSHV-transformed cells, which is mimicked by inducible nitric oxide synthase (iNOS) knockdown [36]. Furthermore, ASS1 is required for KSHV activation of the STAT3 pathway by maintaining intracellular NO level, which is essential for KSHV-induced abnormal cell proliferation and transformation [36] (**Figure 2**). Despite the advances in understanding the glutamine metabolism and the urea cycle in KSHV-infected and -transformed cells, the specific viral genes responsible for manipulating these pathways are elusive.

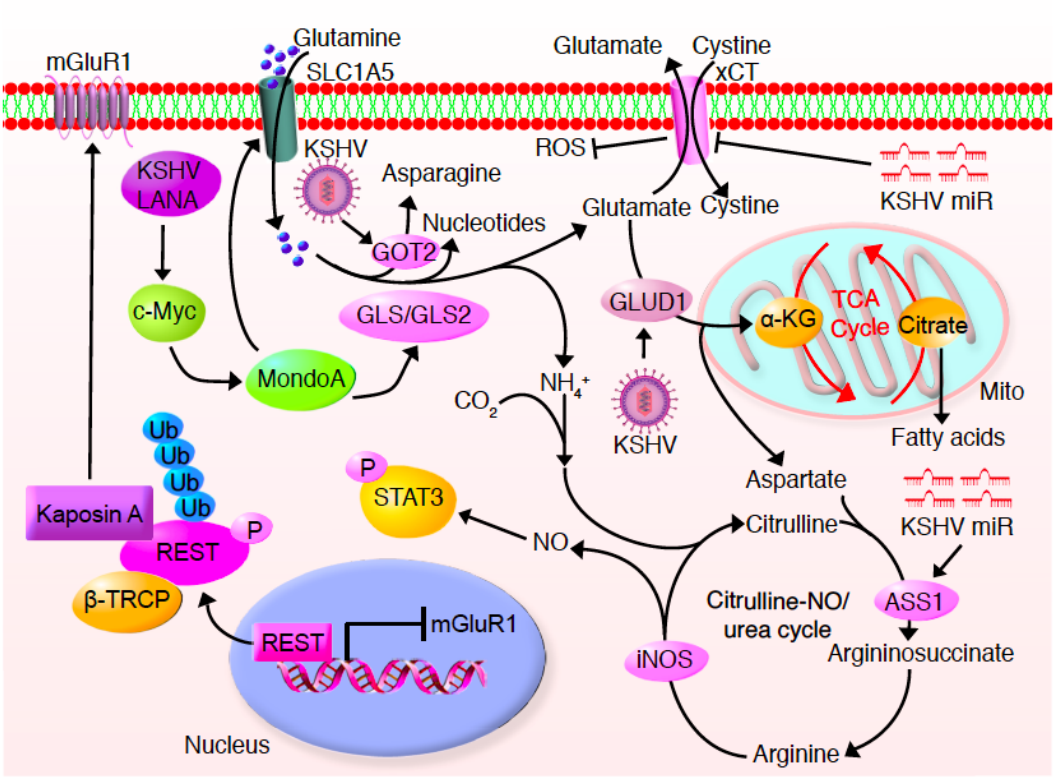

Figure 2: The glutaminolysis is upregulated in KSHV-infected and -transformed cells.

KSHV promotes glutamine uptake by upregulating glutamine transporter SLC1A5; KSHV enhances glutaminolysis by upregulating several glutaminolytic enzymes including GLS1/2, GLUD1 and GOT2; KSHV Kaposin A mediates mGluR1 upregulation to promote glutamate secretion; the citrulline-NO cycle is accelerated by KSHV miRNAs mediated ASS1 upregulation and KSHV-mediated iNOS upregulation.

1.1.5 KSHV promotes fatty acid synthesis

Cancer cells have a high demand for fatty acids used for membrane synthesis. Acetyl-CoA is the obligate substrate for fatty acid synthesis (FAS), which can be derived from the catabolism of glucose and glutamine. Bhatt et al. is the first to report that KSHV-infected PEL cells have upregulated fatty acid synthase and FAS compared to KSHV-negative primary B lymphocytes, which is essential for PEL cell proliferation and survival [37]. Additionally, the authors pointed out that the upregulated aerobic glycolysis in PEL cells is intimately linked to

FAS as inhibition of one pathway blocks another. Both processes are highly dependent on the abnormally activated PI3K/AKT signaling pathway [37] (**Figure 3**). One underpinning hypothesis for these observations is that aerobic glycolysis might provide the building blocks such as acetyl-CoA for FAS.

Sphingosine is a class of cell membrane lipids and can be phosphorylated by sphingosine kinases (SphK) to form a signaling lipid called sphingosine-1-phosphate (S1P) that elicits pro-proliferative and pro-survival signaling. Qin et al. showed that the inhibition of SphK1 specifically induced the apoptosis of PEL and KSHV-infected endothelial cells, hinting the important role of lipid metabolism [38]. Moreover, Angius et al demonstrated that KSHV-infected HUVEC cells had an increased level of neutral lipids, and the inhibition of cholesterol esterification decreased the tubular formation of KSHV-infected HUVEC cells, indicating that neutral lipids might be involved in neo-angiogenesis [39]. Nevertheless, there is no direct evidence linking KSHV infection to the altered lipogenesis until Delgado et al. profiles the global metabolites in cells before and after KSHV infection [40]. The authors showed at a molecular level that the short-term KSHV infection of TIME cells induces nearly all intermediates for FAS and finally increases the *de novo* synthesis of long-chain fatty acids, which is essential for the survival of KSHV-infected cells [40] (**Figure 3**). A follow-up study further confirmed the utilization and the necessity of fatty acids in KSHV-infected cells by integrating transcriptomic, proteomic and metabolomic analyses. It was found that cells infected by KSHV for 96 hours had increased the biogenesis of peroxisomes in which the β-oxidation and breakdown of fatty acids occurred [41]. The peroxisome-mediated lipid oxidation is essential for the survival of KSHV-infected cell as knockdown of two involved enzymes ABCD3 and ACOX1 specifically sensitized KSHV-infected cells to death [41] (**Figure 3**). However, the

functional importance of metabolites derived from peroxisome-mediated fatty acids oxidation and the mechanisms by which KSHV promotes FAS are yet unclear.

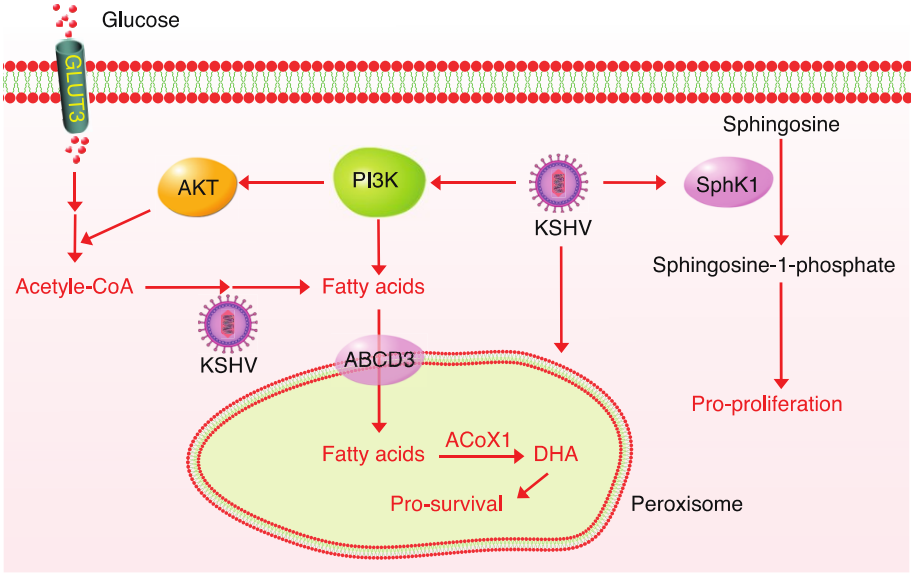

Figure 3: KSHV enhances lipogenesis and peroxisome-mediated ß-oxidation of lipids.

The acetyl-CoA from KSHV-enhanced glycolysis leads to upregulated fatty acids synthesis; the ß-oxidation of lipids in peroxisomes is enhanced by short-term KSHV infection; KSHV enhances the phosphorylation of Sphingolipids sphingosine by upregulating the SphK1.

1.1.6 The metabolic reprogramming during KSHV lytic replication

Considering the cellular environments that support KSHV latent and lytic replications are different, the metabolic activities during these two stages could differ. KSHV relies on cellular metabolic machineries for viral replication. Studies regarding the host metabolism during KSHV reactivation are limited. Sanchez et al. reported that glycolysis, glutaminolysis, and FAS are required for KSHV virion production and these metabolic pathways participate in distinct stages of viral life cycle [42]. Glycolysis and glutaminolysis specifically suppress KSHV genome replication while are essential for KSHV early lytic gene expression at transcriptional and

translational levels respectively [42]. In contrast, FAS regulates the egress of KSHV virions without interfering with the genome replication [42]. Furthermore, FAS inhibition notably decreases the infectious KSHV virions in host cells, indicating that FAS might be critical for KSHV virion maturation and assembly [42]. Although these results indicate that there are different requirements for host metabolites during different stages of KSHV lytic replication, one should be careful when interpretting these data since most of the experiments rely on the use of inhibitors that have limited specificity and efficiency. The genetic manipulation of critical metabolic enzymes to reaffirm these data should be considered.

1.1.7 KSHV hijacks metabolic sensors

Although cancer cells are avid to uptake glucose and amino acids, they always encounter the nutrient scarcity because of the imbalance between increased consumption and limited supplies of nutrients. The aberrantly activated growth and survival signaling pathways play a major role in tumorigenesis at least partially by reprogramming the metabolism of cancer cells and allow them to survive in nutrition-stressed conditions. Conversely, the reprogrammed metabolic pathways in cancer also impact the metabolic sensors that finally sustain the uncontrolled proliferation of cancer cells. The most understood metabolite-sensing and signaling pathways are AMPK, sirtuins (SIRTs) and mTOR [43]. Many groups have reported that mTOR is highly activated and is essential for KSHV-induced tumorigenesis [44, 45]. Consistent with these observations, mTORC1 inhibitor rapamycin so far is the most effective therapy for KS tumors clinically [46]. Several KSHV lytic genes including ORFK1, vPK (ORF36), ORF45 and vGPCR (ORF74) are reported to activate mTORC1 signaling pathway, whereas miRNA-K1 and -K4 are the only KSHV latent products reported so far that activate mTORC1 by directly

downregulating the cytosolic arginine sensor for mTORC1 (CASTOR1) [47-51] (**Figure 4**). Normal cells use mTORC1 to sense multiple environmental inputs including oxygen, DNA damage, growth factors, energy and amino acids to maintain metabolic homeostasis [52, 53]. When nutrition is deficient, mTORC1 is inactivated to promote catabolism. Conversely, mTORC1 is activated and anabolism is enhanced if nutrients are surplus. Hence mTORC1 is largely involved in metabolic regulation, including glycolysis, protein synthesis, amino acids, nucleotide synthesis and lipogenesis [54]. As mTORC1 is constitutively activated in KS and PEL tumors, it is hypothesized that the metabolic pathways are likewise reprogrammed regardless of the extracellular nutrition status, although there is no direct evidence to prove it yet.

AMPK is another evolutionarily conserved metabolic sensor and is activated when energy supply is insufficient, such as an increase in the intracellular ratio of AMP/ATP or glucose shortage. Therefore, anabolism is inhibited by AMPK leading to catabolism of glucose and lipids for ATP restoration. As a result, gluconeogenesis is inhibited, glucose uptake is increased and the mitochondrial biogenesis is prompted [55]. Elevated glycolysis coupled with oxidative phosphorylation restores the intracellular ATP level. Additionally, activated AMPK phosphorylates SREBP1c and ACC1/2 to inhibit lipids and cholesterols synthesis and simultaneously enhances lipids oxidation [56]. Of note, AMPK also directly and negatively regulates mTORC1 by activating TSC complex and inhibiting Raptor [57, 58], which greatly expands its role in controlling metabolism. Anders et al. showed that KSHV ORFK1 interacts with and increases AMPK activity under metabolic stressed conditions, which is critical to maintain KSHV-infected cell survival and viral persistence [59] (**Figure 4**). Additionally, Cheng et al. found that although KSHV infection of HUVEC didn't notably affect AMPK activity, AMPK inhibition augments while AMPK activation restricts KSHV lytic replication [60].

Despite tremendous progress made in this field, it is still unknown how AMPK interferes with metabolic pathways and hence sustains the proliferation and survival of KSHV-infected cells.

NAD is a cofactor central to cellular metabolisms and composed of two forms: oxidized and reduced forms, abbreviated for NAD+ and NADH. Catabolism of one glucose requires two molecules of NAD+, producing two NADH as well as two hydrogen ions and two molecules of water. SIRTs, composed of seven members from 1 to 7, are NAD+-dependent type III histone deacetylases (HDACs) that are functionally linked to cellular metabolism and hence regarded as metabolic sensors. Among them SIRT1 is the most well-studied, which has been proven of great importance in cancer because it inhibits glycolysis and stimulates fatty acids [61]. In PEL and KSHV-transformed cells, SIRT1 is significantly upregulated and positively regulates AMPK to sustain cell survival and resist c-PARP induced apoptosis. The KSHV-upregulated SIRT1 is consistent with the inhibited aerobic glycolysis observed in those cells [62, 63]. Whether SIRT1 and glycolysis are indeed causative still needs further investigation. Additionally, SIRT1 epigenetically suppresses RTA such that the inhibition of SIRT1 reactivates KSHV in PEL cells [64]. Consistently, the high concentration of glucose forces the production of hydrogen peroxide (H_2O_2), leading to SIRT1 downregulation and hence KSHV reactivation [65] (**Figure 4**). Whether SIRT1 indirectly regulates KSHV reactivation by modulating host cell metabolic pathways is unknown. Whether the activated SIRT1-AMPK signaling pathway partially arises from the suppressed aerobic glycolysis in KSHV-infected cancer cells and what are the functions of other SIRTs in metabolic regulation in KSHV-associated cancers are of interest.

The notion that KSHV hijacks the metabolic sensors including mTOR, AMPK and SIRT1 is well established. Nevertheless, whether the reprogramming of these sensors accounts for the alterations of host cell metabolism during KSHV latent and lytic infection remains

unclear. Moreover, how KSHV- versus mock-infected cells integrate the signals sensed by mTOR, AMPK and SIRT1 and finally give a differential command is of interest.

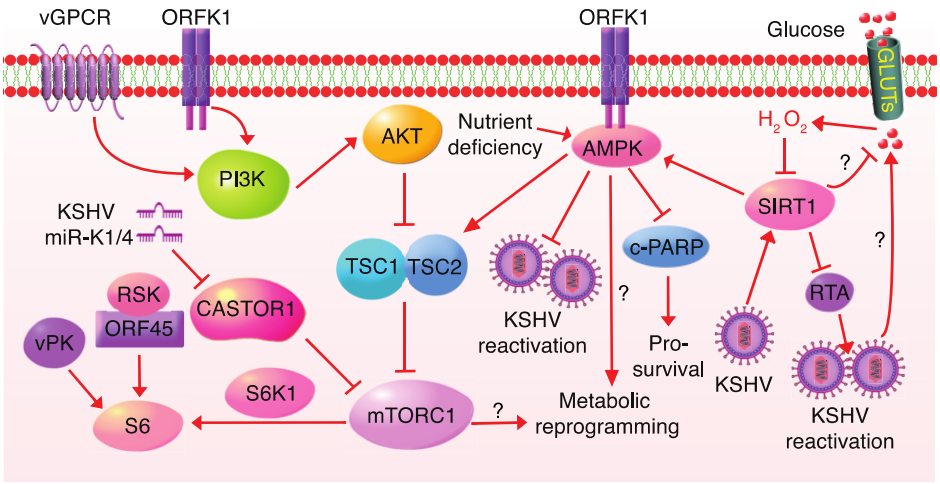

Figure 4: KSHV hijacks cellular metabolic sensors.

KSHV-encoded vGPCR and glycoprotein K1 activate the mTORC1 signaling pathway by PI3K-AKT cascade; KSHV vPK mimics the cellular S6K1 and directly phosphorylates S6, resulting in mTORC1 activation; KSHV miRNA-K1 and -K4 activate mTORC1 by downregulating CASTOR1. KSHV glycoprotein K1 directly interacts with and activates AMPK in nutrients-stressed condition and KSHV mediates AMPK activation by upregulating SIRT1.

1.2 Nutrient regulation of mTORC1

It has been twenty-five years since mTOR was firstly purified and identified as the target of rapamycin [66-68]. Over decades thousands of studies have revealed that mTOR protein kinase is a central regulator of growth in response to environmental cues and is highly conserved across species. It is now widely recognized that mTORC1 activation requires two arms: nutrients- and growth factors-mediated signaling pathways. Whereas the relation of growth factors and mTORC1 is well studied for decades, the link between nutrients and mTORC1 is

ambiguous until the identification of Rag GTPases in 2008 as the core proteins that transduce amino acids' signals [69, 70]. Since then scientists have extensively revisited the role of amino acids in mTORC1 activation, especially leucine and arginine [71]. In recent 10 years, studies from dozens of labs have established the regulatory circuits from amino acids sensing to mTORC1 activation.

1.2.1 mTORC1 and mTORC2 overview

mTOR was simultaneously identified as the target of rapamycin complexed with FKBP12 in 1995 by three groups [66-68]. Years after it was discovered that mTOR acts as a serine/threonine kinase by interacting with multiple proteins to form two distinct complexes, known as mTORC1 and mTORC2. mTORC1 is consisted of DEPTOR, PRAS40, Raptor, mLST8/GßL and mTOR, of which Raptor is the defining component (**Figure 5A**). By contrast, mTORC2 is composed of DEPTOR, mSin1, Protor1/2, Rictor, mLST8 and mTOR, of which Rictor is the defining component [72] (**Figure 5B**).

Diverse signals, including oxygen, growth factors, glucose, DNA damage and amino acids, regulate mTORC1 activation in multiple organisms [72] (**Figure 5C**). mTORC1 integrates these upstream signals to execute multiple functions, including protein synthesis, metabolic reprogramming and autophagy inhibition [72] (**Figure 5C**). In contrast to mTORC1, there are less studies on mTORC2. One striking characteristic of mTORC2 is insensitive to nutrients and the short-term treatment of rapamycin. AKT is the major substrate downstream of mTORC2, which largely accounts for mTORC2-mediated regulation of cell survival and metabolism [73]. Other kinases including PKC, SGK1 and SGK3 are similarly phosphorylated and activated by mTORC2, which is implicated in cytoskeleton remodeling and cell migration [74-78] (**Figure**

5D). Although mTORC2 can be activated by the insulin/PI3K signaling pathway like mTORC1 [79], emerging evidence showed that mTORC2 is independently activated by exercise through the ß-adrenergic receptor-cAMP-PKA signaling axis and phosphatidic acids [80, 81] (**Figure 5D**).

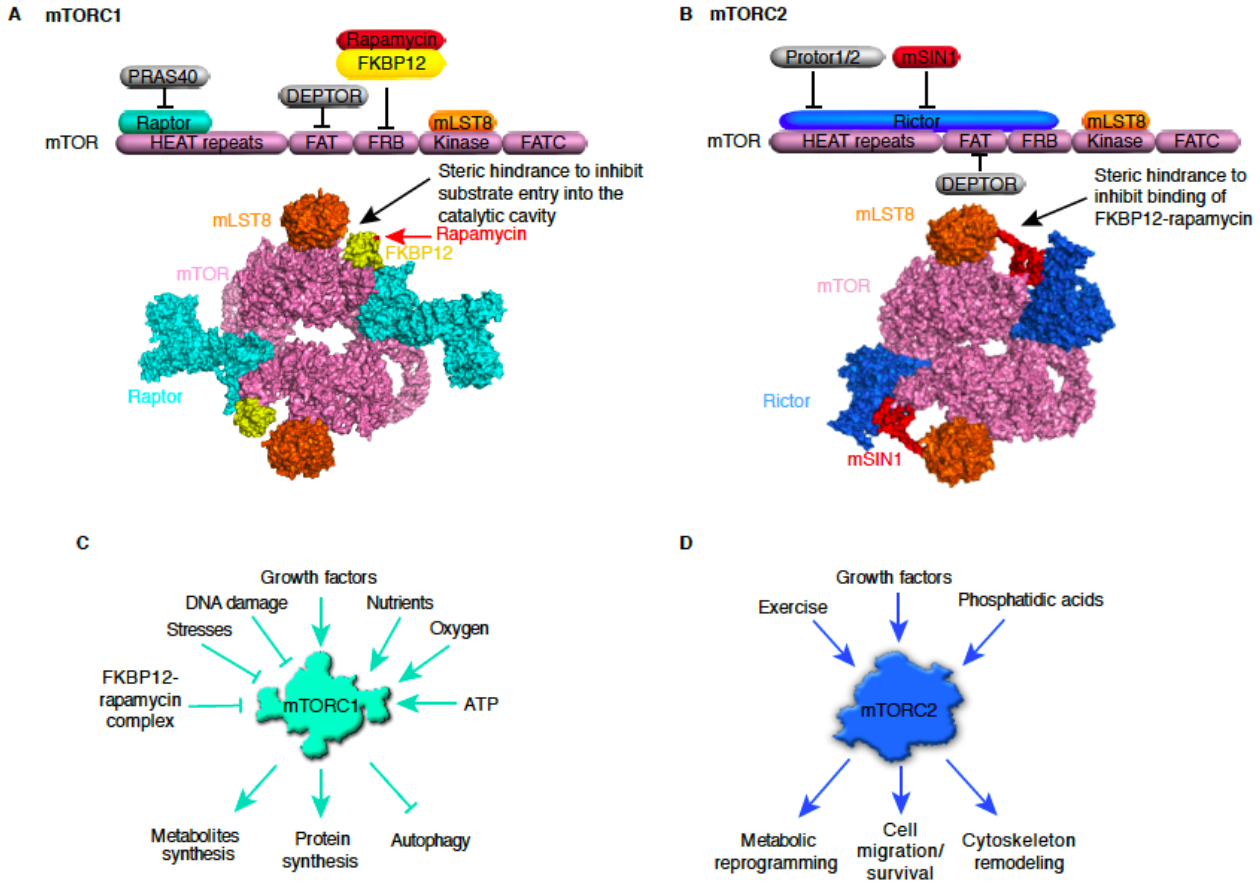

Figure 5: Components and regulators of mTORC1 and 2.

(A) The components and structure of mTORC1 in complex with FKBP12-rapamycin. In the upper panel, the scheme represents the mTORC1 subunits and mTOR kinase domains that is made up by HEAT repeat, FAT, FRB, kinase (catalytic domain), and FATC domains. mTORC1 is composed of DEPTOR, PRAS40, Raptor, mLST8/GßL and mTOR and the interaction sites are depicted. In the lower panel, a crystal structure of mTORC1 combined with FKBP12-rapamycin complex is resolved in 5.9 Aº (PDB: 5FLC). (**B**) The components and structure of mTORC2 are drawed. In the upper panel, the scheme represents the mTOR kinase domains and mTORC1 subunits consisted of DEPTOR, mSin1, Protor1/2, Rictor, mLST8 and mTOR. The interaction sites among these subunits are marked. In the lower panel, an overall structure of human mTORC2 with 4.9 Aº 9 (PDB: 5ZCS) is illustrated. (**C**) mTORC1 responds to growth factors, nutrients, energy, oxygen, DNA damage and other stresses to regulate the synthesis of protein and metabolites as well as inhibit autophagy. **(D)** mTORC2 responds to growth factors, exercise and phosphatidic acids to regulate cell survival, cell migration and reprogram the cellular metabolic pathways and cytoskeleton.

1.2.2 Upstream inputs to mTORC1

The upstream inputs of mTORC1 can be roughly classified into two types: growth factors- and nutrients-dependent signals. Except nutrients, all other signals are transduced by TSC-Rheb cascade. Whereas silencing of TSC2 constitutively activates mTORC1 in cells deprived of growth factors, it cannot block mTORC1 inactivation caused by amino acids deprivation [82]. Currently a "coincidence detector" mechanism is proposed that guarantees mTORC1 activation only when both nutrients and growth factors are copious (**Figure 6A**). In this model, mTORC1 activation is tightly regulated in a cascade fashion that is initiated by the amino acids mediated mTORC1 translocation to lysosomes, followed by growth-factors induced lysosomal Rheb activation of mTOR [69, 83, 84].

1.2.2.1 TSC mediates growth-factor-induced mTORC1 activation

Rheb is a GTPase and the only protein that directly activates mTORC1. Although the crystal structure of mTORC1 in complex with Rheb is resolved, the underpinning mechanism for Rheb activation of mTORC1 is still unclear [85] (**Figure 6B**). It is known that microspherule protein 1 (MCRS1) is required for Rheb interaction with mTORC1 [86]. As a GTP-bound protein, Rheb is activated in a GTP-bound state and inactivated when bound with GDP [87]. A milestone in understanding mTORC1 regulation is the discovery of TSC complex as a core negative regulator of mTORC1 [88, 89]. The TSC complex consists of TSC1, TSC2 and TBC1D7, acting as a GTPase-activating protein (GAP) to inhibit Rheb [90-92]. There are multiple upstream signals transduced to TSC complex, which is integrated and concomitantly regulates mTORC1.

One of the most important inputs regulating the TSC complex is growth factors such as insulin. Food uptake can promote endocrine insulin secretion from islet β cells, and insulin can be distributed throughout the body with the blood circulation and hence systematically regulate cell metabolism. The insulin receptor is located on the cell surface, and the downstream signal is initiated after insulin bound to its receptor, leading to the activation of its effector proteins including ERK1/2, RSK1 and AKT that suppress TSC by direct phosphorylation [93-96]. Ras is a well-studied oncogene and a GTPase, which is regulated by a GTP exchange factor (GEF) called SOS. SOS senses signals from insulin via the adaptor protein Grb2 that boosts the GEF activity of SOS and hence turns Ras-GDP into an activated GTP binding form. Ras mediates TSC phosphorylation and inhibition after a kinase cascade of the Raf-MEK-ERK-RSK [95]. PI3K is another important oncogene that receives signals from insulin via an insulin receptor substrate (IRS). Activated PI3K phosphorylates PIP2 to PIP3 that acts as a second messenger to activate AGC kinases, including AKT, SGK1 and PKCα. AKT disables TSC2 by direct phosphorylation [94]. In addition to the classical insulin signaling pathways, inflammatory signals from tumor necrosis factor (TNF) and developmental signals from Wnt also negatively regulate TSC through IKKβ- and GSK3β-mediated TSC phosphorylation, respectively [97, 98]. Hypoxia can activate the TSC complexes by inducing DNA-damage-inducible transcript 4 (REDD1) and activating AMPK [57, 99-101]. TSC2 is directly phosphorylated and activated by AMPK to inhibit mTORC1 [57]. Alternatively, AMPK directly phosphorylates Raptor, the defining subunit of mTORC1, resulting in 14-3-3 binding and the allosteric inhibition of mTORC1 [58]. Additionally, Zhang et al. reported that upon AMPK activation in a low-energy state, mTORC1 is dragged away from the lysosome due to a mechanical force, resulting in mTORC1 inactivation [102]. DNA damage induces p53 activation and its downstream gene

expression, including DNA damage repair genes like PTEN and Sestrin1/2 [103, 104]. PTEN inactivates mTORC1 by inhibiting the insulin pathway and Sestrin1/2 mediates mTORC1 inactivation through AMPK-dependent TSC activation or a TSC-independent manner described later [105] (**Figure 6A**). Although it is known that TSC complexes accept many upstream signals including insulin, inflammation, Wnt, DNA damage and hypoxia, but how TSC integrates these signals and fine-tunes mTORC1 activity is unclear.

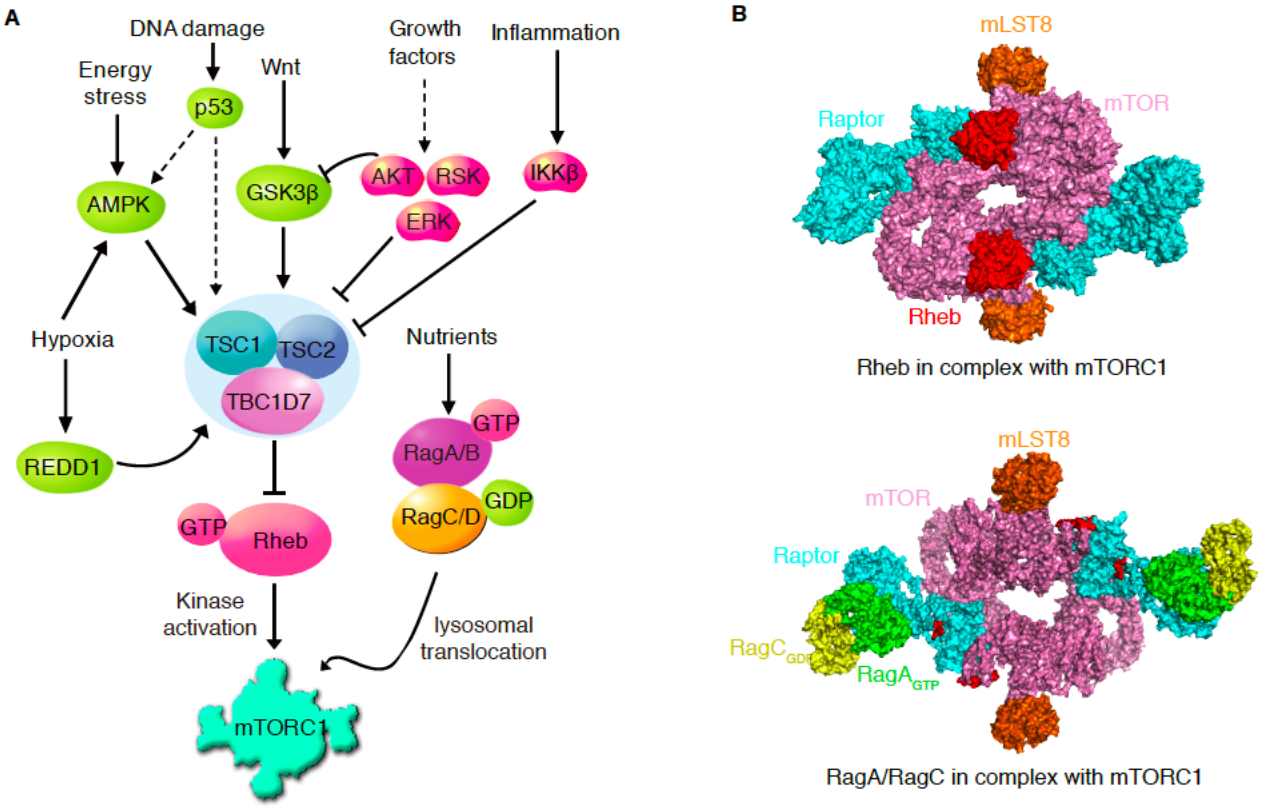

Figure 6: mTORC1 activation by nutrients and growth factors.

(**A**) mTORC1 activation is initiated by Rag GTPases-mediated lysosomal translocation, followed by Rheb-mediated activation of mTORC1. (**B**) The structure of human mTORC1-Rheb complex with a 3.4 Aº (PDB: 6BCU) demonstrates that Rheb rearranges the active sites of mTORC1 to maximize its catalytic activity (top). The structure of human mTORC1-RagA-GTP-RagC-GDP complex with a 5.5 Aº (PDB: 6SB0) illustrates that the active RagA-GTP/RagC-GDP heterodimer preferentially binds the Raptor (green, a protruding claw) of mTORC1.

1.2.2.2 Rag GTPase mediates amino acids induced mTORC1 activation

It was believed for a long time that the amino acids mediated mTORC1 activation relies on TSC-Rheb axis until the TSC2 knockout (TSC2-/-) mice were generated. It was firstly demonstrated that mTORC1 remains sensitive to amino acids in mouse embryonic fibroblasts (MEF) extracted from TSC2-/- mice, suggesting the existence of other mechanisms regulating mTORC1 by sensing amino acids [82, 106]. A breakthrough in encoding the amino acids induced mTORC1 activation is the identification of Rag proteins as the components of mTORC1 pathway [69, 84] (**Figure 6A**). Rag proteins are small GTPases and composed of four members: RagA, B, C and D, of which RagA is like B while RagC is similar to D [107]. Rag subfamily proteins are distinct from other GTPase subfamilies since they work as obligate heterodimers and are functionally redundant. Amino acids control the functionality of Rag heterodimers by modulating their guanine nucleotide binding states. Upon feeding with amino acids, RagA or B is loaded with GTP while RagC or D is in GDP-bound states, forming an active heterodimer by complexing RagA/B-GTP with RagC/D-GDP. Consequently, the active Rag heterodimers preferentially bind to the Raptor of mTORC1 and put mTORC1 on lysosomal surfaces where the mTOR activator Rheb resides, leading to mTORC1 activation [69, 84]. Later a crystal structure of mTORC1 in complex with RagA/C heterodimer further supports this model (**Figure 6B**). Genetic studies showed that constitutively GTP-bound RagB renders mTORC1 hyperactivated and insensitive to amino acids starvation [108]. This is the first evidence demonstrating that amino acids mediated mTORC1 translocation is essential for its activation, suggesting lysosome as the hub for mTORC1 activation. The key step in mediating amino acids activation of mTORC1 is the conversion of GDP-bound RagA or B to GTP-bound states, which can be controlled by either GEF or GAP. The Ragulator, a pentameric complex, consisting of p14, MP1,

p18, HBXIP and C7orf59, is a GEF primarily positively regulating RagC rather than previously regarded RagA to activate mTORC1 [109-111]. It is still unclear which protein of Ragulator complex poses the GEF activity. It is possible that the pentameric complex works as an entirety to affirm its GEF activity as stated by Bar-peled et al [109]. An RNA interference screening revealed that the GEF activity of Ragulator complex is dependent on v-ATPase. v-ATPase senses the lysosomal amino acids to promote the GEF activity of Ragulator towards Rag GTPases [109, 112]. In the absence of amino acids, v-ATPase, Ragulator, and Rag proteins form a super-tight complex on the lysosome and therefore mTORC1 cannot attach to the lysosomal surface and remains inactivated in the cytosol [109, 112]. How v-ATPase exactly affects Ragulator and senses amino acids inside lysosomes is unsure yet. In addition, v-ATPase is critical to maintain the pH gradient of lysosomes, which provides the energy to transport metabolites across the lysosomal membrane [113]. Abu-Remaileh et al showed that the inhibition of v-ATPase decreases the majority of nonessential amino acids (NEAA) efflux from lysosomes, which might be a distinct mechanism to regulate mTORC1 activity [114].

Additionally, by employing the *in vitro* and *in vivo* binding assays for Rag and Raptor, the folliculin complex, composed of folliculin (FLCN) and FLCN-interacting protein 1 and 2 (FNIP1/2), is identified as a GAP towards RagC and D [115, 116]. In response to amino acids stimulation, FLCN accelerates the hydrolysis of RagC/D-bound GTP into GDP, which is required for Rag interaction with and hence activation of mTORC1 [115]. Recently the resolution of structure of FLCN-FNIP2 in complex with Rag GTPases and Ragulator further support the model [117]. GATOR1 complex is another GAP and transmits cytosolic amino acids signals to Rag RagA and B [118]. As a trimer, GATOR1 is composed of DEPDC5, Nprl2 and Nprl3, with Nprl2 of the GAP activity [119]. DEPDC5 mediates the interaction of GATOR1

complex with RagA and B, directly switching their bound GTP to GDP, leading to the dissociation of mTORC1 from lysosomes and consequent mTORC1 inactivation [118]. In cancer cells with GATOR1 complex mutation, mTORC1 is permanently activated and insensitive to amino acids starvation. Additionally, Chen et al found that CUL3-KLHL22 E3 ubiquitin ligases mediates the K48-linked polyubiquitination of DEPDC5 in response to amino acids stimulation, leading to the degradation of DEPDC5 and mTORC1 activation, which promotes tumorigenesis and aging [120]. Another two E3 ubiquitin ligases RNF152 and Skp2 have been found to interact with and ubiquitinate RagA, which increases the interaction of RagA with GATOR1 and consequently inactivates mTORC1 [121, 122]. Mass spectrometry identified a pentameric complex named GATOR2 that consists of MIOS, Seh1L, WDR24, WRD59 and Sec13 and physically interacts with and antagonizes the functions of GATOR1 [118]. Functional studies reveal a bifunctional role of these complexes in regulating mTORC1 in response to amino acids. An epistasis analysis demonstrated that GATOR2 complex positively regulates mTORC1 by acting as a negative regulator upstream of GATOR1 for uncharacterized mechanisms [118]. Currently, the relationship between GATOR1 and GATOR2 is still one of the most hotly pursued areas in mTORC1 field. Later Wolfson et al used a Crispr-Cas9 gene editing technique to tag the endogenous DEPDC5 with flag, followed by the analysis of anti-Flag immunoprecipates, which leads to the identification of KICSTOR complex that comprises KPTN, ITFG2, C12orf66 and SZT2 [123]. KICSTOR is a negative regulator of mTORC1 as cells depleted of KICSTOR have constitutively activated mTORC1 and are insensitive to amino acids starvation [123, 124] (**Figure 7**). Mechanistically KICSTOR acts as a scaffold protein to anchor GATOR1 complex on lysosomes where GATOR1 interacts with and inactivates its substrate Rag GTPases, leading to mTORC1 suppression. This mechanism is also important for mTORC1

inactivation during fasting, which is indispensable process for the maintenance of cellular homeostasis. However, whether KICSTOR has additional functions besides anchoring GATOR1 on lysosomes is still elusive.

1.2.3 Amino acids sensors

In 1995, Luiken et al reported that amino acids, particularly leucine and arginine, activate S6K in hepatocytes in a rapamycin-sensitive manner [125], which was generalized to other cell types by Hara et al [71]. However, how cells perceive amino acids and transduce the signal to mTORC1 is unclear until the recent discoveries of amino acids sensors. There are several properties to be an amino acid sensor. Firstly, it can directly bind to amino acids in physiological conditions. Secondly, the binding of amino acids can result in transduction of signal and activation of mTORC1. Sensors for leucine, arginine and S-adenosylmethionine (SAM) have been recently reported.

1.2.3.1 Cytosolic leucine sensors: SESN2

Studies about the relation between leucine and mTORC1 are relatively complex. Nicklin et al demonstrated in 2009 that the import of extracellular leucine into cells is essential for mTORC1 activation and highly depends on the intracellular level of glutamine [126]. When pre-loaded with glutamine, cells can act as a motivator to induce a synergistically bi-directional transporting: the export of glutamine and the import of leucine. By contrast, cells deprived of glutamine are unable to pump leucine into the cells, causing mTORC1 inactivation, which suggests a critical role of leucine and glutamine in mTORC1 activation [126].

Sestrin1/2/3 (SESNs) are evolutionarily conserved proteins and induced by stresses, including DNA damage, hypoxia and oxidative stress. SESNs were previously reported to negatively regulate mTORC1 by interfering with the AMPK-TSC axis [105]. Additionally, SESN2 enhances AMPK expression in breast cancer and indirectly promotes LKB1-mediated AMPK phosphorylation and activation in the ischemic heart, leading to mTORC1 inactivation [127, 128]. Later several studies demonstrated that SESNs can inhibit mTORC1 in the absence of AMPK or TSC2. All these studies stated that SESNs, particularly SESN2, are negative regulators of mTORC1 by controlling the subcellular location of mTORC1 in response to amino acids, specifically leucine. However, two distinct mechanisms are described. Chantranupong et al, Kim et al and Parmigiani et al reported that SESNs, particularly SESN2, interact with GATOR2 rather than GATOR1 complex in an amino-acid dependent way [129-131]. With amino acids deprivation, the GATOR2-SESN2 interaction is dramatically strengthened whereas amino acids repletion largely abolishes the binding of SESN2 to GATOR2. It also showed that SESN2 overexpression neither affects GATOR2 interaction with GATOR1 nor the GAP activity of GATOR1 towards Rag A/B [129, 130]. Kim et al showed that the ectopic expression of SESN2 indeed releases GATOR1 from GATOR2. Therefore the dissociated GATOR1 complex inactivates mTORC1 by converting the RagA/B-GTP into -GDP states [131]. In striking contrast to these findings that emphasized the effects of SESN2 on GATOR complexes, Peng et al found that all three SESNs directly interact with RagA/B-RagC/D heterodimers, and act as a guanine nucleotide dissociation inhibitors (GDIs) specifically for RagA and B for unknown reasons [132]. The overexpression of SESNs suppresses the amino acids induced guanine nucleotide exchange of RagA or B, resulting in a stably GDP-bound RagA or B and mTORC1 inactivation. Loss of SESNs renders mTORC1 activation and insensitive to amino acids depletion [132]. SESNs share

a conserved GDI motif and mutation of three key amino acids in SESN2 GDI motif switches RagA/B-GDP to -GTP states and hence constitutively activates mTORC1 independent of amino acids [132]. Additionally, Peng et al showed a partial co-localization of Rags with SESN2 in lysosomes, which is not observed by Kim et al and Chantranupong et al [132]. What causes the inconsistency is unknown.

Wolfson et al later identified SESN2 negatively regulates mTORC1 by functioning as a cytosolic leucine sensor [133]. SESN2 potently sequesters GATOR2 complex upon leucine starvation, whereas the SESN2-GATOR2 interaction is disrupted with leucine stimulation [133]. A SESN2 mutant (S190W) with significantly decreased binding capacity to GATOR2 constitutively inactivates mTORC1, whereas two SESN2 mutants (L261A and E451A) that are unable to bind to leucine desensitize cells to leucine-induced mTORC1 activation [133]. Therefore, a prerequisite of leucine-mediated mTORC1 activation is leucine bound to SENS2. Simultaneously Wolfson et al resolved the crystal structure of human SESN2 in complex with leucine, revealing at atomic level how leucine is sensed by SESN2 and thereby activates mTORC1 [134]. Despite these insights, there are still some debates regarding whether SESN2 is an absolute leucine sensor. Firstly, how leucine dissociates SESN2 from GATOR2 remains unsolved [135]. Considering the small size of leucine, the steric hindrance is probably less likely. Secondly, although leucine almost completely disrupts the SESN2-GATOR2 interaction, methionine and isoleucine have similar effects, indicating that there are some nonspecificities existed in SESN2 sensing of leucine [133]. Thirdly, yeast TOR is leucine-sensitive, however there are no SESNs homologs found in yeast [136]. All these results suggest the existence of other leucine sensors.

1.2.3.2 Arginine sensors

1.2.3.2.1 Lysosomal arginine sensor: SLC38A9 and TM4SF5

Zoncu et al described that the export of amino acids from lysosomes interrupts mTORC1-Rag interaction and suppresses amino acids induced mTORC1 activation both *in vivo* and *in vitro,* strongly suggesting that amino acids sensing begins inside the lysosomes [112]. Since then scientists started to seek for proteins that interplay with known mTORC1 components and contain transmembrane domains. SLC38A9 is the first protein found to play an important role in transducing lysosomal amino acids signals outside. SLC38A9 is a member of the amino-acid transporter family that contains multiple transmembrane domains and is persistently localized on lysosomes [137]. A mass spectrometry identified the interaction of the isoform 1 of SLC38A9 with RagB and Ragulator complex and co-immunoprecipitation experiments further confirmed their interaction on lysosomes [138, 139]. A screening assay employing the alanine mutagenesis identifies several key residues of SLC38A9 critical for Ragulator binding [138]. Functionally, silencing of SLC38A9 abolishes amino acids induced mTORC1 activation, whereas SLC38A9 overexpression renders cells insensitive to amino acids deprivation and constitutively activated in mTORC1, suggesting that SLC38A9 is an amino acid sensor and positively regulates mTORC1 [138]. The reconstitution of SLC38A9 into liposomes *in vitro* allows the direct tracing of the radiolabeled amino acids, which demonstrates that SLC38A9 seems to have a nonspecific profile of substrates binding. A competition assay with different amino acids further proved that SLC38A9 probably has the highest affinity to arginine [138]. A genetic study showing that 1140 μM arginine and 100 μM leucine overcomes SLC38A9 knockout-induced mTORC1 inactivation,

which might support that SLC38A9 has a more specific binding to arginine [138]. However, the affinity of SLC38A9 to arginine is still low as the dissociation constant Km is around 39 mM [138]. Additionally, by applying quantitative methods, Shen et al discovered that SLC38A9 poses a noncanonical GEF activity towards RagA and triggers GDP dissociation from RagA upon arginine stimulation, partially accounting for arginine and SLC38A9 activation of mTORC1 [111]. Moreover, Wyant et al reported that SLC38A9 exports several lysosomal essential amino acids preferentially leucine in an arginine-dependent manner to activate mTORC1 [140]. Additionally, SLC38A9 can function independent of arginine sensing and amino acids transporting. In this regard, SLC38A9, particularly its conserved cholesterol-responsive motifs, senses the increases of cholesterol inside lysosomes to mediate cholesterol activation of mTORC1 [141]. However, whether SLC38A9 directly binds cholesterol is unknown and this study has not separated arginine from cholesterol sensing, making it difficult to state that SLC38A9 acts as a cholesterol sensor to regulate mTORC1.

A recent study by Jung et al identified transmembrane 4 six family member 5 (TM4SF5) as a new lysosomal arginine sensor that senses arginine at physiological level to activate mTORC1 [142]. TM4SF5 is highly glycosylated and contains four transmembrane domains, which can be located on membrane-associated organelles [142, 143]. Intriguingly TM4SF5 interacts with both mTORC1 and mTORC2 but unable to bind Rag GTPases. Although the functional importance of TM4SF5 in complex with mTORC2 is unknown, TM4SF5 silencing abolishes both arginine- and leucine-induced mTORC1 activation [142]. Consistent with the characteristics of previously described amino acids sensors, the TM4SF5-mTORC1 complex is disassembled by amino acids, specifically by arginine. Strikingly different from the persistent lysosomal localization of SLC38A9 regardless of arginine status, arginine activates mTORC1 by

directly regulating TM4SF5 localization, with TM4SF5 translocating to lysosomes in arginine replete conditions and residing in plasma membrane with arginine depletion [142]. Interestingly, the authors also found that the intracellular localization of TM4SF5 is sensitive to temperature. Whereas TM4SF5 localizes in cell membrane in 37 ºC, an increasing portion of TM4SF5 moving onto lysosomes in 4 ºC. Whether other environmental stresses similarly modulate mTORC1 activity by controlling TM4SF5 localization are unknown. Further TM4SF5 constitutively interacts with SLC38A9, which is not regulated by amino acids [142]. Whereas SLC38A9 binding cannot interfere with TM4SF5-mTORC1 interaction, SLC38A9 deletion indeed suppresses TM4SF5-mediated mTORC1 activation upon arginine stimulation [142], probably because the functions of TM4SF5 require the arginine efflux by SLC38A9. The *in vitro* experiments proved that there is a direct binding of TM4SF5 with leucine with a Km ~37.9 μM and the further structural analysis of TM4SF5 identified a docking motif for arginine [142]. Considering the concentration of lysosomal arginine is approximately 120 μM in HEK293T cells [144], TM4SF5 is speculated to be functional at physiological conditions by interplaying with arginine, indicating a promising role of TM4SF5 in cancer progression by modulating mTORC1 [142].

1.2.3.2.2 Cytosolic arginine sensor: CASTOR1

Cytosolic arginine sensor for mTORC1 (CASTOR1) and CASTOR2 were characterized proteins in 2016. They have high sequence homology [145]. CASTOR1 is composed of four ACT domains that are involved in amino acids binding and display the sequence similarity to the ACT domains of bacteria and to prokaryotic aspartate kinases. Whereas CASTOR1 functions as

a homodimer or heterodimer with CASTOR2, which bind to arginine to sequester GATOR2 complex, CASTOR2 homodimer fails to bind arginine and constitutively interacts with GATOR2 complex [145]. Co-immunoprecipitation experiments showed that the CASTOR2 homodimer has the highest affinity to GATOR2 complex, with CASTOR1-CASTOR2 heterodimer stronger than CASTOR1 homodimer [145]. Similar to SESN2, the binding of CASTOR1 rather than CASTOR2 with GATOR2 is strengthened upon arginine withdrawal, leading to mTORC1 inactivation [145]. Consistent with this notion, arginine rather than any other fifteen tested non-essential amino acids specifically disrupts the purified CASTOR1-GATOR2 complex *in vitro*, which recapitulates the effects of total amino acids. Further experiments demonstrated that CASTOR1 directly binds to arginine *in vitro* with a Km ~35 μM, which is comparable to lysosomal arginine sensor TM4SF5 [145]. Moreover, the amino acids induced mTORC1 activation subsides with the overexpression of CASTOR1 or CASTOR2, mimicking the effect of a dominant negative Rag GTPases heterodimer. Whereas knockdown of CASTOR1 or CASTOR2 in HEK293T cells enhances amino acids mediated mTORC1 activation, introduction of a CASTOR1 mutant lacking arginine binding ability renders cells insensitive to arginine and constitutively inactive in mTORC1 although the interaction with GATOR2 complex remains unaltered, suggesting arginine binding is the prerequisite for CASTOR1 in regulating mTORC1 [145]. Of note, CASTOR1 silencing in a SLC38A9 knockout cells reduces arginine-induced activation of mTORC1, suggesting a parallel effect of SLC38A9 and CASTOR1 in sensing arginine to regulate mTORC1 [145]. The structure of CASTOR1 bound to arginine further deciphers the mechanism and provides the structural basis of arginine sensed by CASTOR1 [146]. The monomeric mutants of CASTOR1(Y207S and I202E) weaken the GATOR2 as well as the arginine binding and hence are disabled to suppress mTORC1 [146].

Conversely, Mutations of any one of two key residues of CASTOR1 in arginine binding pocket (S111A and D304A) significantly enhance GATOR2 recruitment while decrease arginine binding, leading to mTORC1 inactivation even in the presence of arginine [146]. Further analysis by Gai et al suggests a possible mechanism by which arginine enables the dissociation of CASTOR1 from GATOR2 complex [147, 148]. It is proposed that arginine binding stabilizes the interface of ACT2 and ACT4 in CASTOR1, which alters the position and exposure of CASTOR1 residues required for GATOR2 interaction [147, 148]. All these data suggest a conformational change of CASTOR1 following arginine binding. However, Zhou et al reported that the crystal structures of CASTOR1 in arginine-bound and ligand-free states are almost identical [149]. Hence, Zhou et al proposed that arginine might serve as a linker between CASTOR1 ACT2 and ACT4 domains, which probably favors CASTOR1 in a conformation free from GATOR2 complex [149]. What causes the discrepancy and how GATOR2 complex is dissociated from CASTOR1 by arginine are debatable. Recently, an arginine analogue is created, featuring in binding with CASTOR1 with a similar affinity as natural arginine and without disrupting the CASTOR1-GATOR2 interaction, which results in constitutive mTORC1 inactivation [150]. Whether this small molecule can be used as an effective mTORC1 inhibitor clinically need further investigation.

Considering the important role of CASTOR1 and CASTOR2 in modulating mTORC1 activity and the high frequency of mTORC1 dysregulated in cancers, it's not surprising that CASTORs might be involved in tumorigenesis. By applying an KSHV-transformed cell system, our lab has discovered that KSHV suppressed both CASTOR1 and CASTOR2 expression to activate mTORC1 pathway [151]. Either CASTOR1 or CASTOR2 overexpression dramatically suppresses cell proliferation and colony formation in softagar of KSHV-transformed cells by

attenuating mTORC1 activation, recapitulating the phenotype of mTOR inhibition [151]. Mechanistically, KSHV-encoded miRNA (miR)-K4-5p and likely -K1-5p directly targeted CASTOR1 for degradation, leading to mTORC1 activation. CASTOR1 or CASTOR2 overexpression, and mTOR inhibitors abolish mTORC1 activation and growth transformation induced by pre-miR-K1 and -K4 [151]. Our results provide the scientific basis for targeting mTORC1 for KSHV-associated cancers. Besides, Zhou et al observed that CASTOR1 is notably decreased in lung adenocarcinoma compared to its normal lung epithelial cells [152]. The ectopic expression of CASTOR1 inhibits mTORC1 and leads to a significant suppression of proliferation, migration, and invasion of lung adenocarcinoma cells [152]. Our extensive analysis of TCGA datasets found that a lower CASTOR1 expression level was correlated with overall poor survival in pan-cancer analyses. In details, at least ten types of cancer showed the same trend, implying a likely critical role of CASTOR1 in tumor suppression. We also found that AKT1 directly binds to and phosphorylates CASTOR1 at S14, which enhances its interaction with E3 ubiquitin ligase RNF167 and therefore promotes CASTOR1 ubiquitination and degradation. More importantly, CASTOR1 overexpression inhibits while CASTOR1 silencing accelerates breast cancer growth *in vivo* by suppressing mTORC1, suggesting that CASTOR1 might be a tumor suppressor for breast cancer, which could potentially be used as a biomarker. These results illustrate a mechanism by which CASTOR1 is suppressed in cancer and reveal a novel therapeutic target for RNF167-positive and CASTOR1-negative cancer.

1.2.3.3 S-adenosylmethionine sensor: SAMTOR

S-adenosylmethionine (SAM) is the methyl donor and largely involved in DNA and RNA methylation, which is highly dysregulated in cancer. SAM sensor upstream of mTORC1 (SAMTOR) is an uncharacterized protein and negatively regulates mTORC1 by acting as a

sensor for SAM with a different mechanism from SESN2 and CASTOR1. Instead of sequestering GATOR2, SAMTOR coimmunoprecipates with GATOR1 only in the presence of KICSTOR [153] and inactivates mTORC1 by displacing it from lysosomes in a dose-dependent manner [153]. Consistently SAMTOR knockout renders cells insensitive to SAM deprivation and constitutively activated in mTORC1 by positioning mTORC1 on lysosomes [153]. An epistasis experiment demonstrated that SAMTOR is upstream of Rag GTPases and requires both GATOR1 and KICSTOR to be functional. Additionally, the equilibrium binding assay further illustrated that SAMTOR1 is a direct SAM binding protein with a dissociation constant ~7 μM. Intriguingly SAMTOR1 can also bind to the demethylated form of SAM (SAH) with similar affinity. Consistently, SAM and SAH rather than other amino acids disassemble the purified SAMTOR from the GASTOR1-KISTOR complex both *in vitro* and *in vivo* [153]. SAMTOR mutants lacking the SAM binding ability constantly interact with KICSTOR-GATOR1 complex independent of SAM, indicating that SAMTOR is indeed a SAM sensor to transduce methionine sufficiency to mTORC1 [153]. It seems that SAMTOR potentiates the effects of GATOR1 to inhibit mTORC1, how it exactly works is still unknown. What are the functions of KICSTOR in mediating SAMTOR regulation of GATOR1 by is likewise mysterious. A better understanding of all these might be benefited by a crystallography of SAMTOR in complex with SAM as well as the GATOR1-KICSTOR complex.

1.2.3.4 Glutamine sensors: present or absent?

Glutamine is a particularly preferred amino acid by cancer cells due to its fundamental functions in controlling cell growth and metabolism, but how exactly it is perceived and regulates mTORC1 is poorly defined. The sensing of glutamine seems to be very complicated. One on hand, glutamine can be used as a driving force to pump amino acids into cells to

indirectly regulate mTORC1 pathway [126]. Alternatively, the intracellular glutamine can be catabolized to α-ketoglutarate (α-KG) with the catalysis of glutaminase (GLS) and glutamate dehydrogenase (GDH). The α-KG produced from glutamine appears to directly activate mTORC1. Although the specific mechanism is unclear, an increase in α-KG through enhanced glutaminolysis or direct supplementation dramatically activates mTORC1, which might explain why mTORC1 inactivation by glutamine deprivation requires prolonged treatment compared to 50 min deprivation of either leucine or arginine [154]. Mechanistically, Duran et al observed an increased GTP loading into RagB after cells incubated with glutamine, which is abolished by the silencing of glutaminolytic enzymes GLS or GDH, suggesting that glutaminolysis is essential for this process [154]. The active RagB-GTP subsequently recruits mTORC1 to lysosomes for Rheb-mediated activation.

By contrast, Jewell et al stated a Rag-independent mechanism by which glutamine mediates mTORC1 activation [155]. It was observed that cells with knock out of Rag A/B remained partially responsive to amino acids as the deletion of RagA and RagB did not completely block amino acids induced mTORC1 activation. A screening of twenty standard amino acids revealed that only glutamine displayed similar kinetics in activating mTORC1 in RagA/B wild-type and knockout cells [155]. Moreover, glutamine rather than leucine induces mTORC1 translocating to lysosomes in the absence of RagA and RagB, which requires both v-ATPase and ADP ribosylation factor-Arf1 (Arf1) [155] (**Figure 7**). All these studies suggest that glutamine displays a Rag-independent regulation of mTORC1, which is strikingly different from other amino acids. Despite tremendous advances in connecting glutamine with mTORC1, the underpinning mechanism is still undefined. It is still possible that glutamine or α-KG sensors exist.

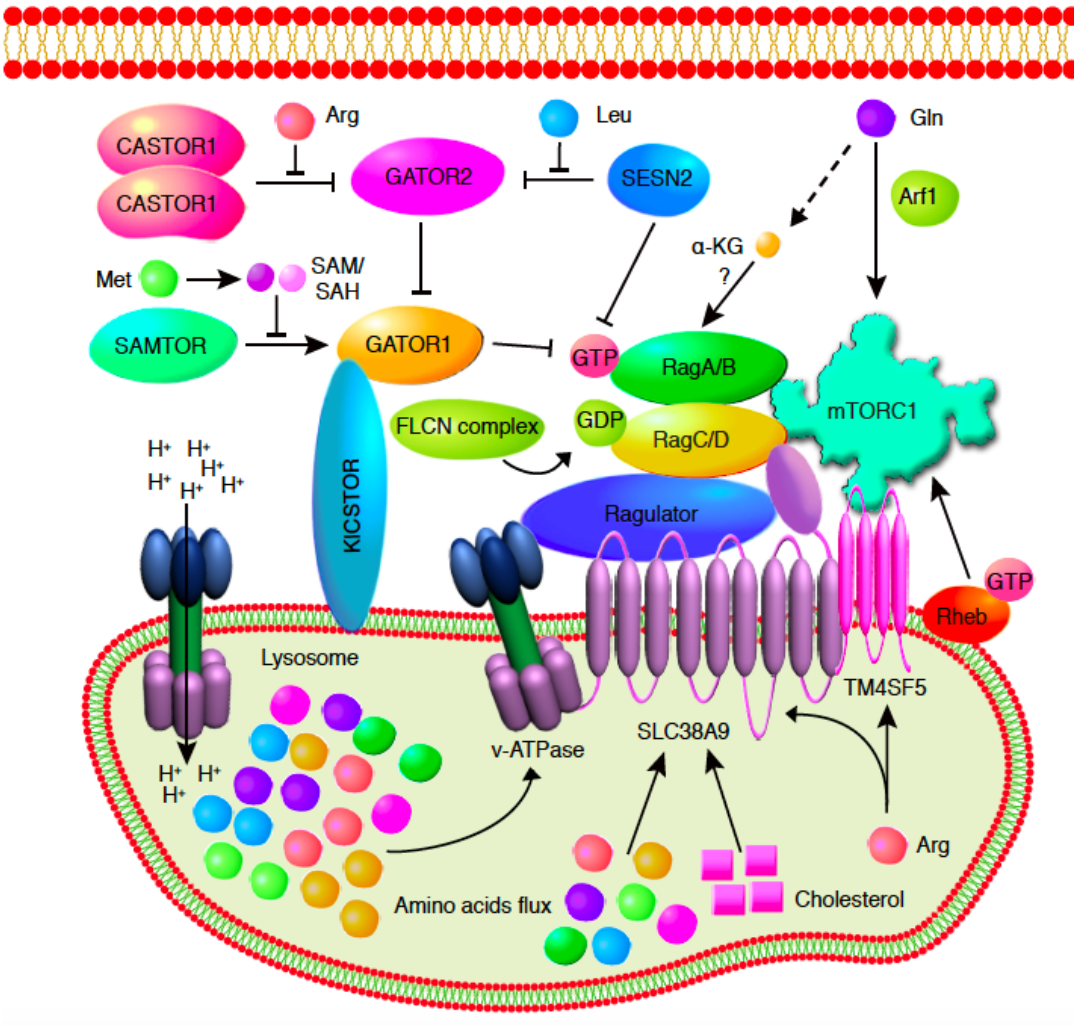

Figure 7: Amino acids dependent mTORC1 activation.

The Rag GTPases mediate mTORC1 activation by amino acids. Rag GTPases are essential for mTORC1 anchoring on lysosomal surface for Rheb activation. SESN2 and CASTOR1 are cytosolic whereas SLC38A9 and TM4SF5 are lysosomal leucine and arginine sensors respectively, all of which govern mTORC1 activation by interplaying with amino acids and GATOR2 complex. SAMTOR is a cytosolic sensor for SAM and SAH, which regulates mTORC1 by interacting with GATOR1 complex. GATOR1 complex is a GAP for RagA and RagB, which is negatively regulated by GATOR2 complex. v-ATPase is a positive regulator of mTORC1 by controlling lysosomal proton gradient, amino acids efflux and the GEF of Ragulator towards Rag GTPases. KICSTOR complex is essential for anchoring GATOR1 complex on lysosomes. FLCN complex is a GAP towards RagC and RagD to positively regulate mTORC1.

1.2.4 mTORC1 signaling in cancer and aging

New components and upstream/downstream regulators of mTORC1 pathway continue to be revealed. New information of mTORC1 signaling pathway is updated daily even after its discovery for twenty-five years. At the same time, the complex regulatory circuits between the mTOR pathway and diseases are constantly being illustrated. In particular, mTOR is linked to tumorigenesis, aging and aging-related diseases.

1.2.4.1 mTORC1 signaling in cancer

mTORC1 is hyperactivated in cancer at least partially due to mutations of its own components and upstream regulators of mTORC1. Growth factors-mediated signaling pathway is one of the most typical. Also some tumor suppressors negatively regulating mTORC1 such as p53, PTEN, TSC1, TSC2, TBC1D7 and LKB1 are normally silenced in cancer [57, 156, 157]. Rheb is an essential activator of mTORC1 and its somatic doublets have been reported in brain, leading to mTORC1 activation [158]. Additionally, the GATOR1 complex has genomic deletion in glioblastoma and RagC has mutations in follicular cancer and Birt-Hogg-Dubé syndrome. Besides, mTOR is also mutated in multiple types of cancer [159]. All these together account for the recurrent mTORC1 activation in cancer [118, 160, 161].

Rapamycin is shown to inhibit cell proliferation in various species by preferentially inducing G1 phase arrest. Although a very early study demonstrated the rapamycin-mediated inhibition of protein synthesis in yeasts, it was only widely accepted until the identification of eukaryotic 4EBP1 and S6K as the downstream effectors of mTORC1 [162, 163]. 4EBP1 extensively participates in mRNA translation initiation and S6K directly phosphorylates the ribosomal protein S6 to promote the protein synthesis, which links mTORC1 to metabolism and

cell growth besides the well-characterized cell proliferation [164, 165]. Furthermore mTORC1 and S6K directly enhance the transcription of rRNA and hence ribosomal biogenesis by increasing the activity of several RNA polymerase-related proteins including MAF1, TIF1a and UBF [166-169]. Genetic studies further supported that as the deletion of TOR alleles in yeast, fruit fly and mice reduces body sizes, mimicking the effect of rapamycin on protein synthesis and cell growth [170-172]. Further characterizations of knockout mice of other mTORC1 components such as Raptor and mSLT8 position mTORC1 an undoubted regulator of growth in mammalians, which is extremely essential for the early development of mice [173, 174].

In addition to the positive role in protein synthesis, mTOR also negatively regulates lysosome formation and autophagy by phosphorylating transcription factor TFEB and the components of the autophagy initiation complex [175] (**Figure 8**). TFEB is the master gene controlling the autophagy by regulating the transcription of multiple genes involved in the formation of autophagosome and lysosomes as well as the fusion of autophagosome and lysosome, which promotes the catabolism in nutrition-deficient conditions and hence maintains cellular homeostasis [176, 177]. The phosphorylation of TFEB by mTORC1 disables its functions as a transactivator, as the phosphorylated TFEB is sequestered by 14-3-3 in the cytoplasm [178, 179]. ULK1 is a fundamental enzyme involved in early steps of the autophagosome biogenesis [180] and mTORC1 decreases the kinase activity of ULK1 by direct phosphorylation [181]. Additionally, mTORC1 directly phosphorylates some core proteins involved in autophagy including ATG13, ATG14, NRFB2 and UVRAG to inhibit autophagy [182-185] (**Figure 8**). The role of autophagy before and after tumor development is likely different. Before tumorigenesis, autophagy provides the energy source under nutrient-deficient conditions by decomposing the damaged and aged cellular components, which decreases

cytopathy and carcinogenesis. After tumorigenesis, autophagy plays a critical role in enhancing tumor development and the direct inhibition of autophagy has a notable effect on antagonizing tumors [186]. For example, germline deletion of LKB1 results in hyperactivated mTORC1 and autophagy is causally inhibited, leading to a variety of malignant tumor types [187].

The rapid proliferation is one of the hallmarks of cancer, which requires the high supplies of energy and macromolecules such as lipids, nucleotides, amino acids. It is now well-established that cancer cells have rewired glycolysis that is closely tied to *de novo* fatty acids and nucleotides synthesis. mTORC1 is able to reprogram these metabolic pathways to sustain cancer cell proliferation and growth [54]. The hyperactivated mTORC1 in cancer normally enhances the expression of Myc and HIF1α that drives the expression of glucose transport 1(GLUT1) and several other glycolytic enzymes including phosphoglucoisomerase, phosphofructokinase, hexokinase 2 and enolase to promote the aerobic glycolysis [54, 188] (**Figure 8**). The mTORC1-induced Myc also stimulates the influx of pentose phosphate pathway (PPP) from glycolysis by upregulating pyrophosphate synthase 2 (PRPS2), which consequently increases the purine synthesis [189]. Alternatively mTORC1 activates the transcription factor AFT4 such that its downstream target the mitochondrial methylene-tetrahydrofolate dehydrogenase 2 (MTHFD2) is increased, leading to upregulated purine synthesis [190]. Further mTORC1 effector S6K1 directly phosphorylates the aspartate transcarbamylase and dihydroorotase (CAD) to drive pyrimidine synthesis [191, 192]. SREBP family proteins (SREBP1 and SREBP2) are key enzymes involved in the *de novo* fatty acids synthesis and mTORC1 enhances their activities by directly phosphorylating its inhibitor LIPIN1 [193-196]. Alternatively S6K increases the stability and splicing of FASN, ACLY and SCD1 transcripts through phosphorylation and hence

activation of SRPK2 [197] (**Figure 8)**. All these observations account for upregulated lipogenesis in cancer.

Overall, mTORC1 is activated in cancer due to genetic changes or constitutively activated upstream pathways, enhancing the protein synthesis and reprograming the autophagy and cellular metabolic pathways to support cancer cell growth and proliferation [57] (**Figure 8**) .

1.2.4.2 mTORC1 signaling in aging or aging-related diseases

With aging, the metabolic rate is slowing down, the immune system is weakening, and the risk of infection is increasing. In the aging process, the efficiency of our body to clean up harmful substances is decreasing, leading to the accumulation of metabolic wastes, followed by related geriatric diseases. The internal and external factors together accelerate aging and cause aging-related diseases. The relationship between mTORC1 and aging is increasingly revealed. Genetic deletion of mTORC1 components or pharmacologically targeting mTORC1 can significantly extend lifespan, a phenomenon that has been demonstrated in yeast, nematodes, fruit flies, and mice [72]. In addition, it is also illustrated that animals tend to rejuvenate their activity while extend their lifespan, indicating that both lifespan and healthy span are prolonged simultaneously. Rapamycin and metformin are two drugs that have been tested clinically in antagonizing aging by inhibiting mTORC1. Early biochemical experiments demonstrated that rapamycin in complex with FKBP12 immunophillin directly binds to mTOR protein and hence suppresses its functionalities [66-68]. Yip et al uncovered a crystal structure of mTORC1 before and after rapamycin-FKBP12 binding, and therefore proposed a mechanism by which the mTORC1 is dissembled by rapamycin stepwise [198]. By contrast, the molecular mechanism by which metformin inhibits mTORC1 seems to be confounded, and experiments in mammalians have demonstrated that metformin inhibits mTORC1 through both Rag- and Rheb-dependent

manners [199, 200]. In agreement with mTORC1 inhibition, both rapamycin and metformin have proved to prolong the lifespan of nematodes and increase their movement independent of the insulin signaling pathway [200, 201].

The risk of senile diseases significantly increases with aging. Typical examples are neurodegenerative diseases, such as Parkinson, Huntington, Alzheimer diseases. A characteristic of these diseases is the accumulation of toxic proteins inside cells, which is hardly eliminated and eventually leads to cell death. Since nerve cells are not regenerative, cell death will result in a continuous decrease in the total number of neurons, and the functions of brain are gradually lost. Autophagy and proteasome-dependent pathways are the primary tools to remove misfolded and excessive proteins in cells, which effectively prevent the accumulation of toxic proteins. As one of the most fundamental negative regulator of autophagy, mTORC1 plays a critical role in neurodegenerative diseases. Autophagy inhibition is very common in neurodegenerative diseases and silencing of ATG5 or ATG7, two important proteins involved in autophagy in the mouse central nervous system, causes the accumulation of ubiquitinated proteins, resulting in neurodegenerative diseases in mice [202]. Many people have reported that autophagy is resumed and the neurodegenerative syndromes are relieved if neurodegenerative mice are treated with rapamycin [203]. Additionally, mTORC1 regulates cap-dependent and -independent translation of mRNA by directly phosphorylating S6K and 4EBP1. Several studies support that the general decrease in mRNA translation prevents the accumulation of proteotoxic and oxidative stresses such that the suppression of mTORC1 retards aging [72, 204]. Further the caloric restriction (CR) is shown to extend the lifespan and delay the onset of aging across a myriad of species [205-207]. As mTORC1 is a key responder to nutrients and growth factors, the effects of CR are thought to

be mediated by mTORC1 inhibition (**Figure 8**). Although the link between mTORC1 and aging is well-established, the exact mechanisms are far from clear.

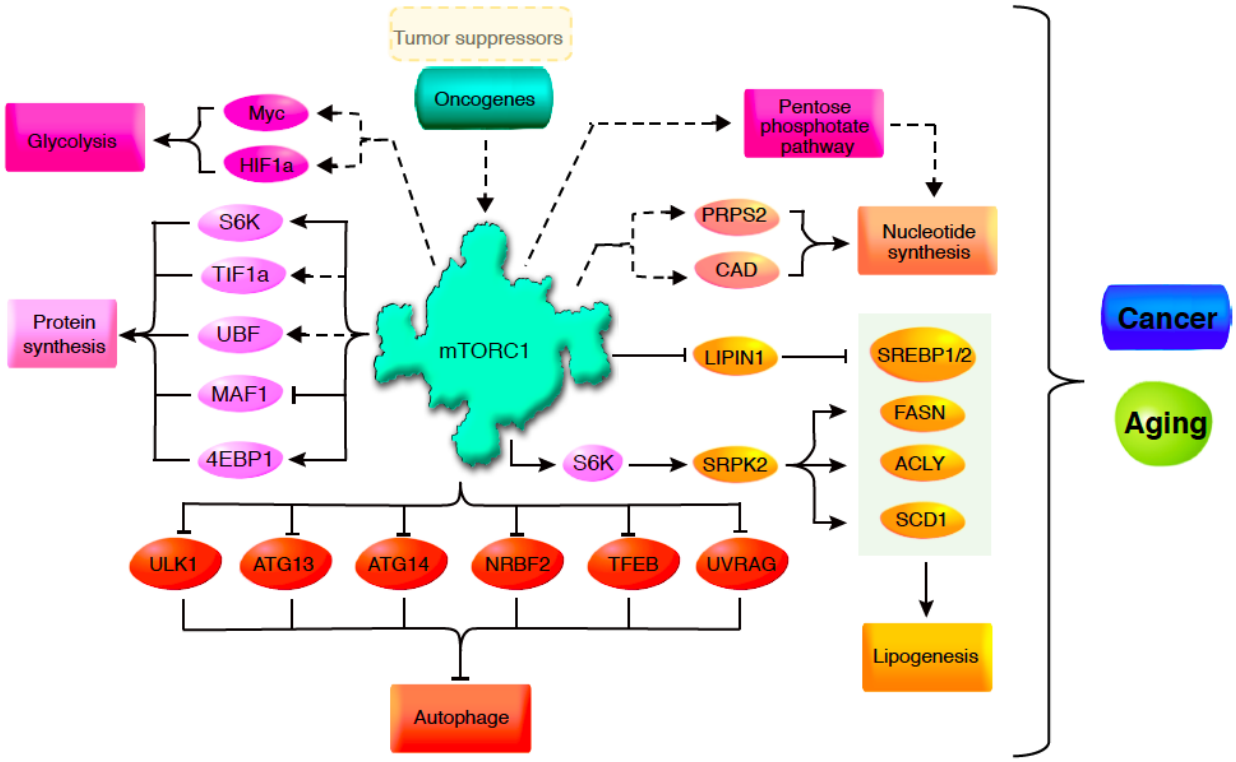

Figure 8: mTORC1 promotes cancer and aging.

mTORC1 accelerates tumorigenesis, aging and aging-related diseases by suppressing autophagy and promoting the overall protein synthesis and metabolic rewiring.

2.0 Oncogenic KSHV upregulates argininosuccinate synthase 1, a rate-limiting enzyme of the citrulline-nitric oxide cycle, to activate the STAT3 pathway and promote cellular transformation

Preface:

The text and figures in this chapter are taken from my previous publication, "**Li T**, Zhu Y, Cheng F, Lu C, Jung JU, Gao S-J. Oncogenic KSHV upregulates argininosuccinate synthase 1, a rate-limiting enzyme of the citrulline-nitric oxide cycle, to activate STAT3 pathway and promote growth transformation. **Journal of Virology, 2019**, 93: e01599-18", under the journal's copyright permission.

Cancer cells are required to rewire existing metabolic pathways to support their abnormal proliferation. We have previously shown that, unlike glucose-addicted cancers, KSHV-transformed cells depend on glutamine rather than glucose for energy production and synthesis of amino acids and nucleotides. High-level consumption of glutamine by cells requires tight regulation and is often coupled with the citrulline-NO cycle. We have found that KSHV infection accelerates the nitrogen efflux by upregulating ASS1, a key enzyme in the citrulline-NO cycle. KSHV upregulation of ASS1 requires viral miRNAs. Knockdown of ASS1 suppresses cell proliferation, abolishes colony formation in soft agar, and decreases NO generation of KSHV-transformed cells, which is mimicked by knockdown iNOS. Furthermore, by maintaining intracellular NO level, ASS1 mediates KSHV activation of the STAT3 pathway, which is essential for KSHV-induced abnormal cell proliferation and transformation (**Figure 9**). These results illustrate a novel mechanism by which an oncogenic virus hijacks a key metabolic

pathway to promote cellular transformation and reveal a potential novel therapeutic target for KSHV-induced malignancies.

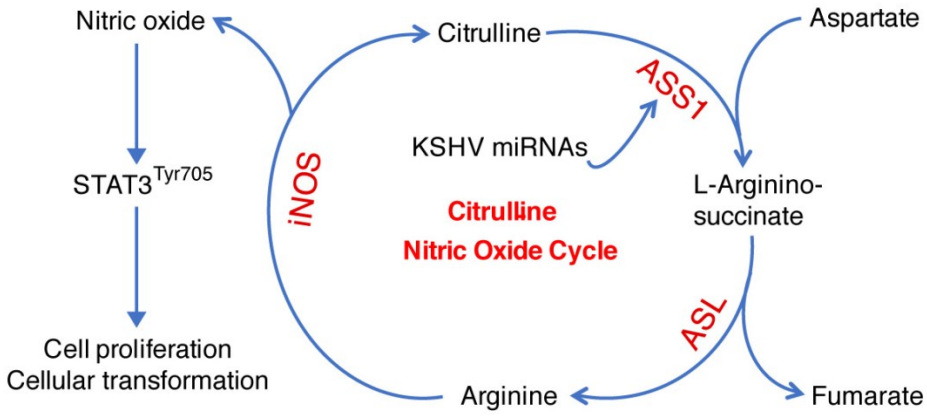

Figure 9: A model illustrated that KSHV miRNA cluster upregulate ASS1 to promote cell transformation by regulating NO generation and thereby STAT3 activation.

2.1 ASS1 is upregulated in KSHV-infected and -transformed cells

We have previously shown that KSHV-transformed cells depend on glutamine for anabolic proliferation [35]. Because active glutamine consumption requires tight regulation of the metabolic pathway, we hypothesized that KSHV-transformed cells would have active citrulline-NO cycle. ASS1 has a critical role in the citrulline-NO cycle and is upregulated in several types of human cancers by an unknown mechanism [208]. Thus, we examined ASS1 expression in KSHV-infected and -transformed cells and found that the expression of ASS1 transcript was elevated by 108-fold in KMM cells compared to MM cells (**Figure 10A**). To confirm the upregulation of ASS1 in KMM cells at the protein level, we tested several ASS1 antibodies. However, none of them worked except one, which detected the ASS1 band and an additional lower band. Using MM and KMM cells with and without overexpression of ASS1, we

confirmed that the top band was indeed the ASS1 protein (**Supplementary Figure 1**). As expected, the expression level of ASS1 protein was much higher in KMM than MM cells (**Figure 10A**). We further examined ASS1 expression in other types of KSHV-infected cells. KSHV infection of iSLK cells derived from renal carcinoma upregulated ASS1 expression at both transcript and protein levels albeit to a lesser extent, which was possibly due to the relative high expression level of ASS1 in the uninfected iSLK cells (**Figure 10B**). Primary effusion lymphoma (PEL) is an aggressive B-cell non-Hodgkin's lymphoma associated with KSHV infection [12]. Several KSHV-infected PEL cell lines including BCBL1, BC3 and BCP1 expressed higher levels of ASS1 with an increase of transcript ranging from 1.8 to 7.0-fold compared to BJAB, an EBV- and KSHV-negative Burkitt's lymphoma cell line. Interestingly, KSHV infection of BJAB increased the expression of ASS1 transcript by 11.5 fold (**Figure 10C**). These results were further confirmed at the protein level (**Figure 10C**). Hence, latent KSHV infection upregulated ASS1 expression in different cell types. However, the extent of upregulation varied according to individual types of cells.

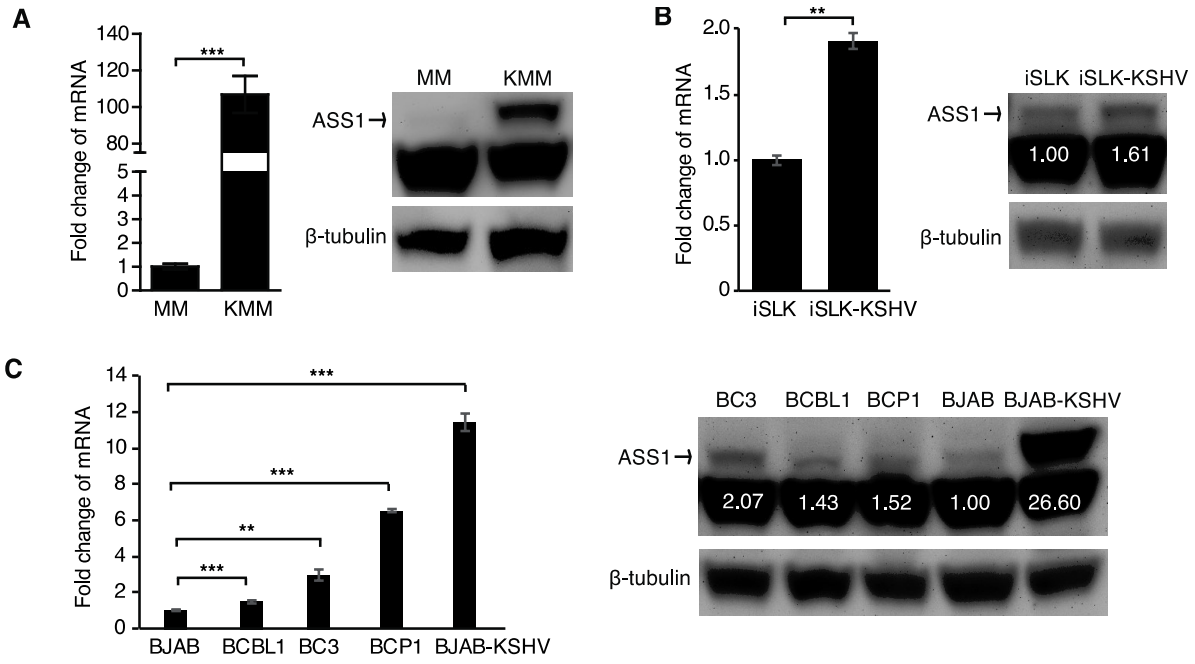

Figure 10: ASS1 is upregulated in KSHV latently infected cells.

(A) Induction of ASS1 in KSHV-transformed cells. RT-qPCR and Western-blot results showed that the expression of ASS1 was induced in both mRNA and protein levels in KSHV-transformed cells, compared to untransformed MM cells. **(B-C)** Upregulation of ASS1 in KSHV-infected iSLK cells and in PEL cells. Western-blotting detection of ASS1 protein levels in PEL cell lines BCBL1, BC3 and BCP1, in uninfected and KSHV-infected BJAB cells, and in uninfected and KSHV-infected iSLK cells. **(D-E)** Analysis of ASS1 expression in cells infected by different recombinant virus including wild-type KSHV (KMM), and mutants with a deletion of a cluster of 10 precursor miRNA (ΔmiRs), vFLIP (ΔvFLIP) or vCyclin (ΔvCyclin) by Western-blot and RT-qPCR, respectively. **(F-G)** Western-blot and qPCR to detect ASS1 expression in MM cells and ΔmiRs cells overexpressed with KSHV miRNA cluster or MM cells transduced with the empty vector pITA (MM+pITA) as the control. **(H)** Western-blot to detect ASS1 expression in ΔmiRs cells overexpressed with single miRNAs. Mock: MM, WT: KMM. The top band in the western blot for ASS1 is specific as verified by ASS1 overexpression done in MM and KMM cells (Sup Fig 1A). Three independent experiments were repeated and results were shown as mean ± SEM. Data were analyzed by Student's t-test; ** for $P < 0.01$; and *** for $P < 0.001$.

2.2 Multiple KSHV-encoded miRNAs upregulate ASS1 expression

Most KSHV-transformed cells are latently infected by KSHV and mainly express four viral latent products: LANA, vCyclin, vFLIP and a cluster of 12 pre-miRNAs [209]. To identify which viral product is responsible for ASS1 upregulation in KMM cells, we examined MM cells latently infected by a KSHV mutant with a deletion of either vFLIP, vCyclin or a cluster of 10 of the 12 pre-miRNAs (miR-K1-9 and 11), named ΔvFLIP, ΔvCyclin and ΔmiRs, respectively [210-213]. We were not able to obtain MM cells latently infected by the KSHV mutant with LANA deleted or mutated because of LANA's essential role in viral genome persistence [214, 215]. Deletion of vFLIP or vCyclin had minimal effect on ASS1 expression (**Figure 11A** and **B**). In contrast, deletion of the miRNA cluster completely abolished ASS1 expression at both transcript and protein levels (**Figure 11A** and **B**). Expression of the miRNA cluster in ΔmiRs cells partially rescued ASS1 expression (**Figure 11C** and **D**). Interestingly, expression of the miRNA cluster in MM cells was sufficient to upregulate ASS1 expression, though to a lesser extent, compared to KMM cells (**Figure 11C** and **D**). These results indicated that KSHV miRNAs were required for KSHV-induced upregulation of ASS1. However, other KSHV genes might also contribute to the maximal induction of ASS1 expression. To identify the individual miRNA(s) that might mediate KSHV-induced ASS1 upregulation, we examined ASS1 expression in ΔmiRs cells expressing individual miRNAs (miR-K1-12) [216, 217]. Western-blotting results showed that numerous miRNAs including K2, K6, K7, K8, K9, K10, K11 and K12 partially upregulated ASS1 expression in KMM cells (**Figure 11E**).

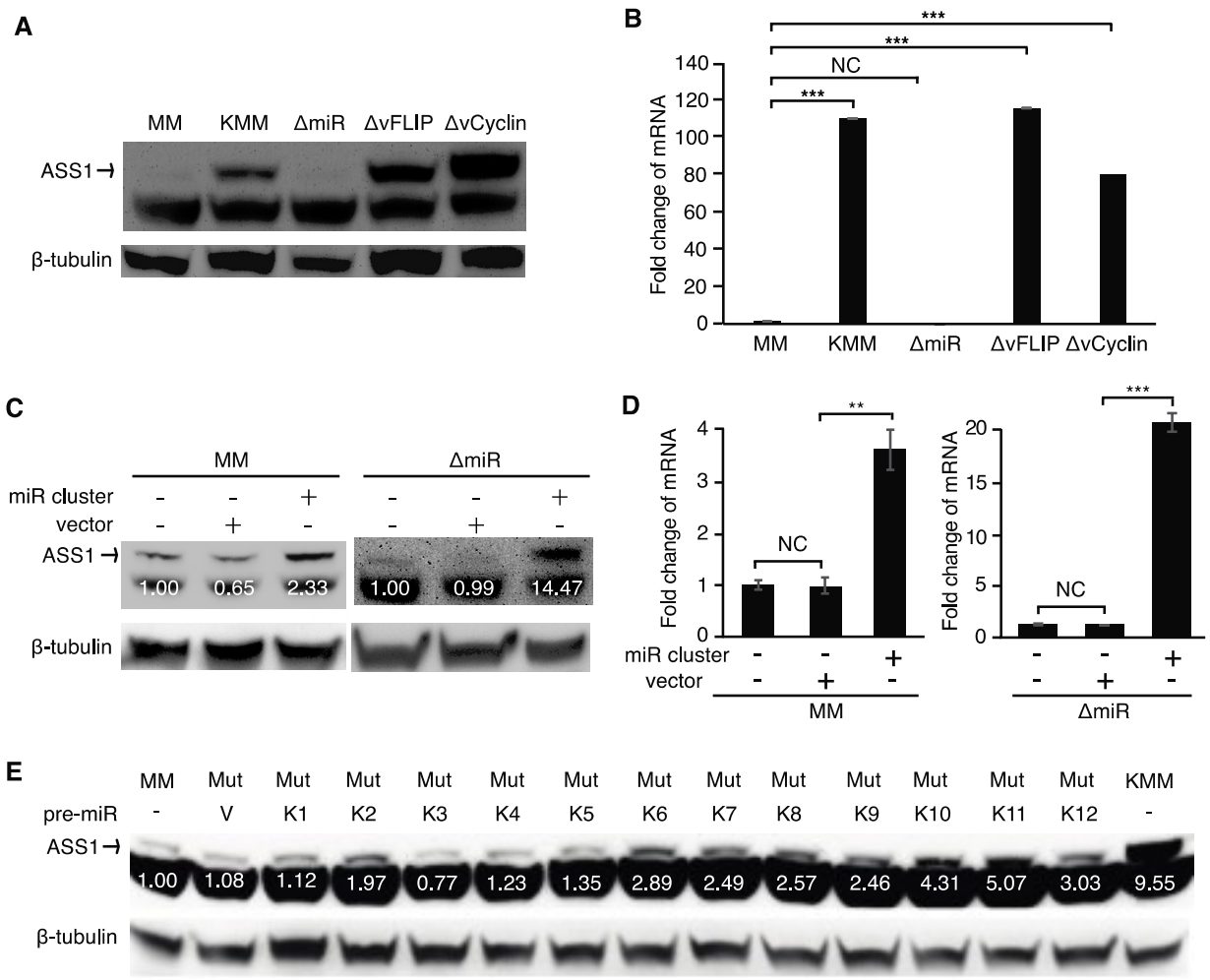

Figure 11: Multiple of KSHV-encoded miRNAs upregulates ASS1.

(A and **B)** Analysis of ASS1 expression in cells infected by different recombinant virus including wild-type KSHV (KMM), and mutants with a deletion of a cluster of 10 precursor miRNA (ΔmiRs), vFLIP (ΔvFLIP) or vCyclin (ΔvCyclin) by Western-blot and RT-qPCR, respectively. **(C** and **D)** Western-blot and qPCR to detect ASS1 expression in MM cells and ΔmiRs cells overexpressed with KSHV miRNA cluster or MM cells transduced with the empty vector pITA (MM+pITA) as the control. **(E)** Western-blot to detect ASS1 expression in ΔmiRs cells overexpressed with single miRNAs. Mock: MM, WT: KMM. The top band in the western blot for ASS1 is specific as verified by ASS1 overexpression done in MM and KMM cells (Sup Fig 1A). Three independent experiments were repeated and results were shown as mean ± SEM; Data were analyzed by Student's t-test; ** for $P < 0.01$, and *** for $P < 0.001$.

2.3 Suppression of ASS1 inhibits KSHV-induced cell proliferation and cellular transformation

To explore the role of ASS1 in KSHV-transformed cells, we used three different short hairpin RNAs (shRNAs) to knock down ASS1. The shRNAs achieved approximately 80% knock down efficiencies at the RNA level, which were confirmed at the protein level (**Figure 12A** and **B**). Knock down of ASS1 reduced cell proliferation by 55-85% in KMM cells but only have marginal effects on MM cells (**Figure 12C**). Knockdown of ASS1 also significantly reduced the efficiencies of colony formation of KMM cells in softagar assay as shown by the reduced sizes and numbers of colonies (**Figure 12D**). As expected, MM cells with and without ASS1 knock down failed to form any colonies in softagar assay (**Figure 12D**). Taken together, these results demonstrated that ASS1 was essential for KSHV-induced cell proliferation and cellular transformation.

To further investigate how ASS1 might regulate KSHV-induced cell proliferation and cellular transformation, we examined cell cycle progression and apoptosis. ASS1 knockdown with 3 shRNAs induced cell cycle arrest in KMM cells by increasing G1 phase cells from 50.6% to 55.3-70.5%, and decreasing S phase cells from 36.5% to 10.4-20.9% (**Figure 12E**). As for MM cells, the G1 phase cells were increased from 51.1% to 57.9-69.7% while the S phase cells were decreased from 35.5% to 7.3-27.2% (**Figure 12E**). ASS1 knockdown also significantly increased the numbers of dead cells from 5.3% to 15.4-52.7% in KMM cells and from 9.1% to 16-27.3% in MM cells (**Figure 12F**). Overall, ASS1 knockdown suppressed the proliferation of KSHV-transformed cells by inducing both cell cycle arrest and apoptosis while there was less effect on untransformed cells.

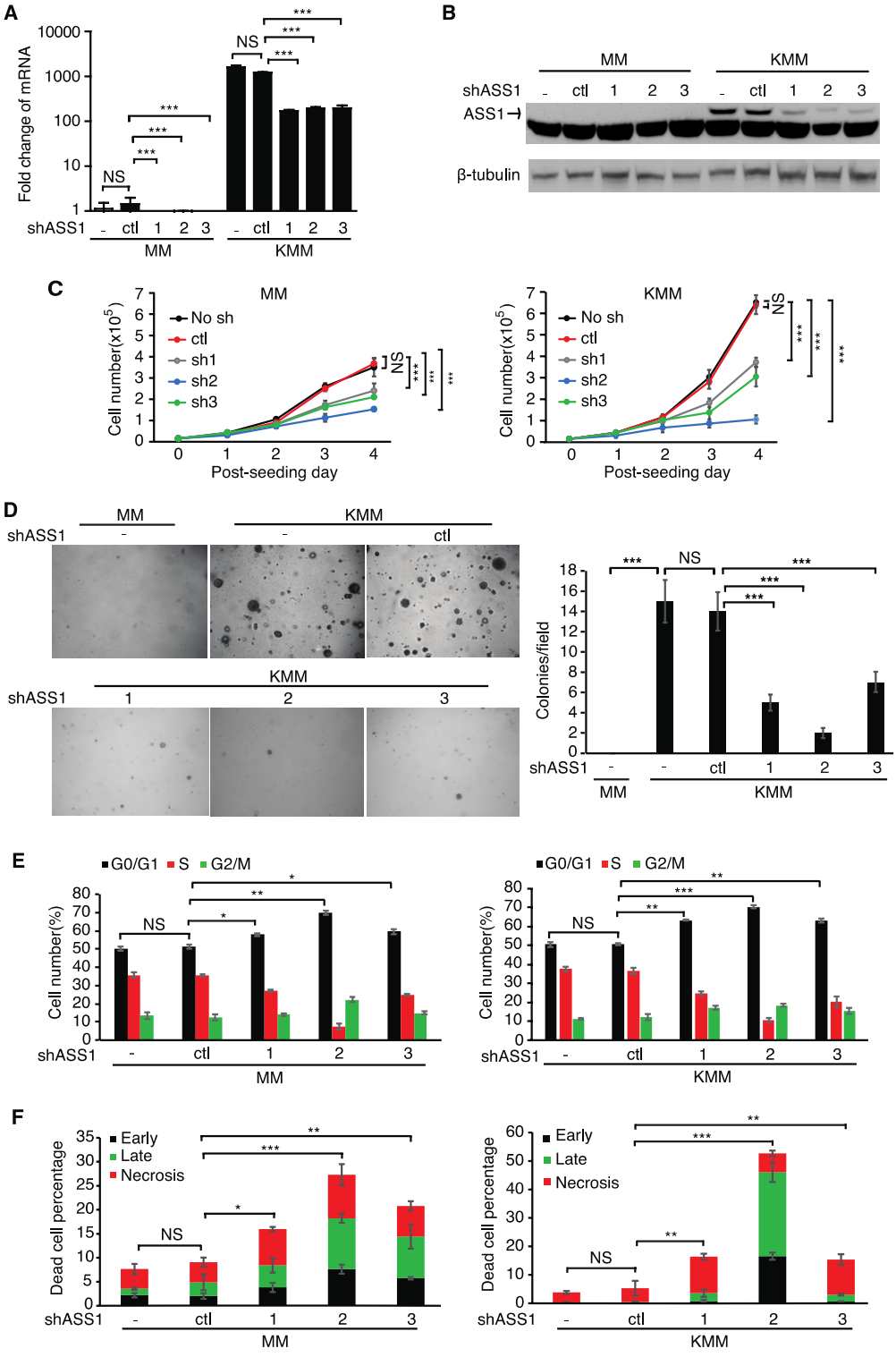

Figure 12: ASS1 knockdown inhibits cell proliferation and formation of colonies in soft agar, and induces apoptosis.

(A and **B)** Analysis of ASS1 expression in MM and KMM cells upon ASS1 knockdown by RT-qPCR (**A**) and Western-blot (**B**). respectively. (**C)** ASS1 knockdown inhibits cell proliferation in MM and KMM cells. Cells were seeded in 6-well plates. In the following day cells were infected with scrambled control(ctl) and three ASS1 shRNAs (1, 2 and 3). 24h after transduction, cells were split and re-seeded at $1.5x10^4$ cells/well in 24-well plates and counted daily. (**D)** ASS1 knockdown inhibited colony formation of KMM cells in soft agar. $2x10^4$ KMM cells with ASS1 knockdown were at day 2 post-infection with ASS1 shRNA lentiviruses were suspended in 1ml 0.3% top agar and plated onto one well of 0.5% base agar in 6 well plate and maintained for three weeks. Representative pictures at 40x magnification were shown. Colonies with diameter >50μm were quantified in each field and the results were graphed in the right panel. (**E** and **F)** ASS1 knockdown caused G1 cell cycle arrest (**E**) and induced apoptosis (**F**) in both MM and KMM cells. Cell cycle was analyzed by FACS 48h after ASS1 shRNA transduction. Apoptotic cells were detected by Annexin V staining 72h after ASS1 shRNA transduction. Three independent experiments were repeated and results were shown as mean ± SEM; Data were analyzed by Student's t-test; * for $P < 0.01$, ** for $P < 0.01$, and *** for $P < 0.001$.

2.4 Inhibition of iNOS induces cell cycle arrest and apoptosis of KSHV-transformed cells

ASS1 is a metabolic enzyme involved in the citrulline-NO cycle, arginine metabolism and NO synthesis [218-220]. To delineate the mechanism by which ASS1 regulates KSHV-induced cell proliferation, we complemented medium with various ASS1 downstream metabolites to determine which of them could rescue the effect of ASS1 knockdown. Altogether, we tested polyamines, arginine, glutamine, asparagine, fumarate, proline, α-ketoglutarate and their different combinations but none of them showed any rescue effect on KMM cells with ASS1 knockdown (data not shown). Another metabolite related to ASS1 is NO. However, due to the short half-life of commercially available NO donors, we could not perform the NO rescue experiments.

Alternatively, if ASS1 impact the proliferation of KSHV-transformed cells by regulating NO production, knocking down the enzymes that catalyze NO production should induce a phenotype similar to the effect of ASS1 knockdown. There are three different NOS in mammalian cells: iNOS, nNOS, eNOS [221, 222]. We first examined the expression levels of these three NOSs in KMM cells. Surprisingly, KSHV infection had no effect on the expression of nNOS, and only increased the expression of eNOS by 2 fold (**Figure 13A**). In contrast, KSHV infection increased the expression of iNOS by 7-fold, suggesting that iNOS might play a role in KSHV-transformed cells (**Figure 13A**). We then performed knock down of iNOS to examine its role in KSHV-induced cellular transformation (**Figure 13B** and **C**). Knock down of iNOS suppressed the cell proliferation of both MM and KMM cells (**Figure 13D**). Inhibition of iNOS with a chemical inhibitor L-NAME reduced cell proliferation of both MM and KMM cells in a dose-dependent manner (**Supplementary Figure 2**). Knock down of iNOS significantly inhibited the colony formation efficiencies of KMM cells in softagar assay (**Figure 13E**). Upon iNOS knockdown, the percentage of G1 phase cells was increased from 51.9% to 61-73.1% and from 48.1% to 70.1-72.5% in MM and KMM cells, respectively. Accordingly, the percentage of S phase cells was reduced from 31.35% to 9.5-12.9% and from 35.6% to 8.6-9.7% in both MM and KMM cells, respectively (**Figure 13F**). The results of apoptotic assay showed that the dead cells were increased from 11.0% to 33.0-40.0% in MM cells, and from 6.23% to 24.3-37.3% in KMM cells (**Figure 13G**). Taken together, these data showed that iNOS knockdown gave phenotypes similar to ASS1 knockdown, indicating that ASS1 and iNOS might function through the same downstream effector, NO.

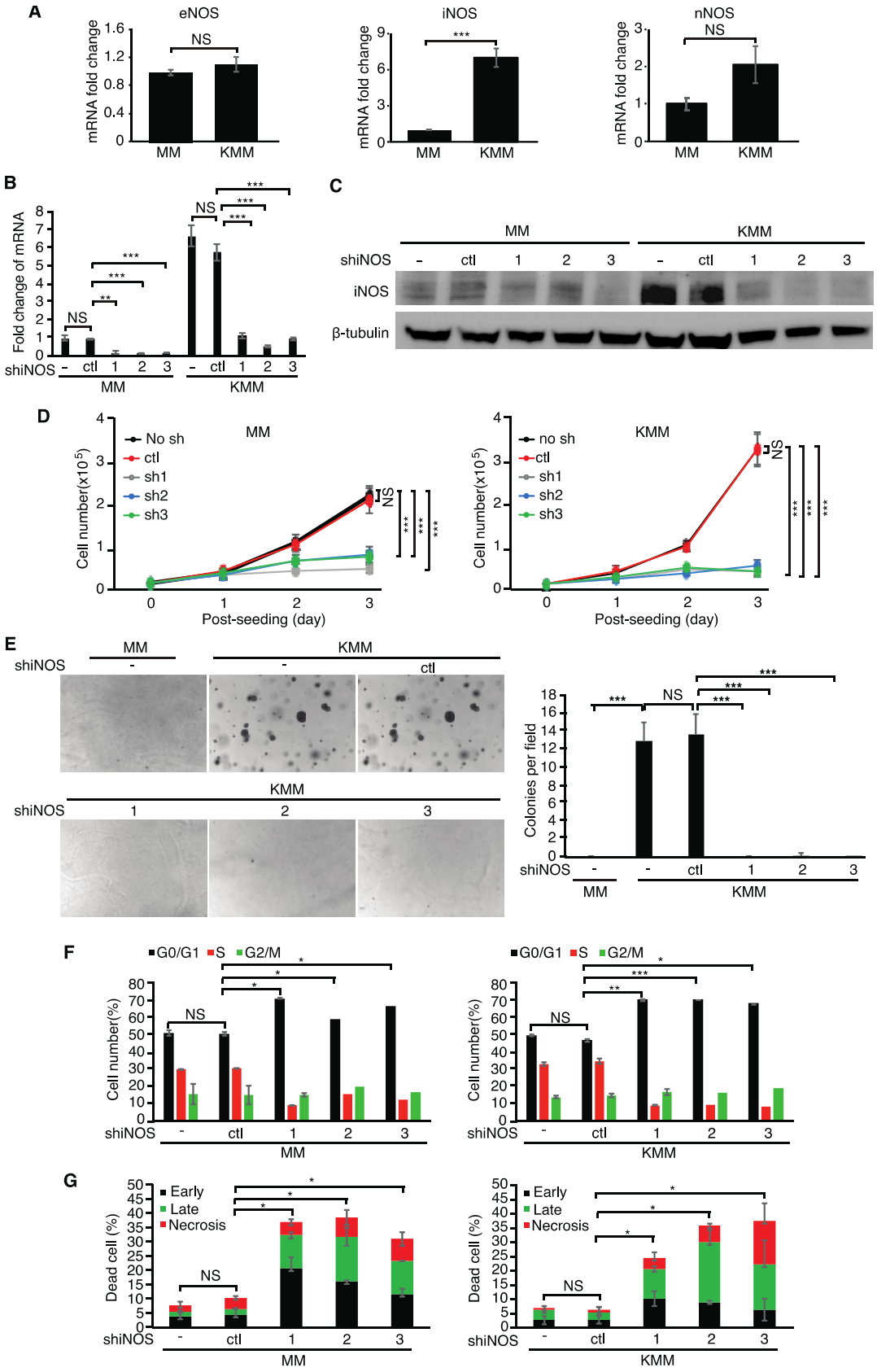
A
eNOS
iNOS
nNOS
mRNA fold change
NS
***
MM
KMM
B
Fold change of mRNA
shiNOS
ctl
MM
KMM
C
MM
KMM
shiNOS
iNOS
β-tubulin
D
No sh
ctl
sh1
sh2
sh3
Cell number(x10^5)
Post-seeding (day)
E
shiNOS
ctl
Colonies per field
F
G0/G1
S
G2/M
Cell number(%)
G
Early
Late
Necrosis
Dead cell (%)

Figure 13: iNOS knockdown suppresses the cell proliferation, colony formation in soft agar and induces apoptosis.

(A) RT-qPCR results showed that only iNOS expression is elevated in KMM cells, whereas the expressions of eNOS and nNOS is similar in MM and KMM cells. **(B-C)** Analysis of iNOS expression in MM and KMM cells upon ASS1 knockdown by RT-qPCR (B) and Western-blot (C). (**D)** iNOS knockdown inhibits cell proliferation in MM and KMM cells. $2x10^4$ cells were seeded in 24-well plates. In the following day, cells were infected with either a scrambled control (ctl) or three iNOS shRNAs (1, 2 and 3) and were counted daily. (**E)** iNOS knockdown inhibited the colony formation of KMM cells in soft agar. Soft agar was performed as described in Fig 2D. Representative pictures at 40x magnification were shown. Colonies with diameter >50 were quantified in each field and the results were graphed in the right panel. (**F-G)** iNOS knockdown reduced induced G1 cell cycle arrest (F) and apoptosis (G) in both MM and KMM cells. Cell cycle analysis of wild-type and ASS1 knockdown cultures of MM and KMM cells was performed by FACS after 48h iNOS shRNA transduction. Apoptotic cells were detected by Annexin V staining 72 h after iNOS shRNA transduction. Three independent experiments were repeated and results were shown as mean ± SEM; Data were analyzed by Student's t-test; * for $P < 0.05$, ** for $P < 0.01$, and *** for $P < 0.001$.

2.5 Knockdown of ASS1 or iNOS reduced the intracellular NO level

ASS1 is the rate-limiting enzyme for de novo arginine synthesis, providing essential substrate for NO production [218-220]. The reduced expression of ASS1 or iNOS decreased NO production despite of excessive extracellular arginine supply [223-225]. To evaluate the role of ASS1 and iNOS in NO production in KSHV-transformed cells, endogenous NO level was measured in MM and KMM cells with or without knock down of ASS1 or iNOS using DAR 4M AM (DAR), which is a cell permeable diaminorhodamine-based dye emitting red fluorescent upon reacting with NO in the presence of ROS [226-228] (**Supplementary Figure 3A**). Since the presence of ROS is a prerequisite for DAR to emit fluorescence when reacting with NO, we

first compared the ROS between MM and KMM cells. Surprisingly, MM cells had much higher intracellular ROS level than that of KMM cells (**Supplementary Figure 3B**). However, treatment with S-nitroso-N-acetyl-D, L-penicillamine (SNAP), a known NO donor, had no effect on endogenous ROS in both MM and KMM cells (**Supplementary Figure 3C**), indicating that DAR could be used as a reliable sensor for endogenous NO detection after ASS1 knockdown and SNAP is an effective NO donor in these cells. Knock down of either ASS1 or iNOS led to dramatic decrease in the intracellular NO production (**Figure 14A-D**) whereas had no effects on ROS generation (**Supplementary Figure 4**) in both MM and KMM cells. L-NAME inhibits the generation of NO by inhibiting iNOS function but not iNOS expression [229]. Treatment with L-NAME inhibited NO production (**Supplementary Figure 5A** and **B**), which was consistent with its inhibitory effect on cell proliferation (**Supplementary Figure 2**). Collectively, our results demonstrated that ASS1 and iNOS were necessary for endogenous NO generation, which was essential for the proliferation of KSHV-transformed cells.

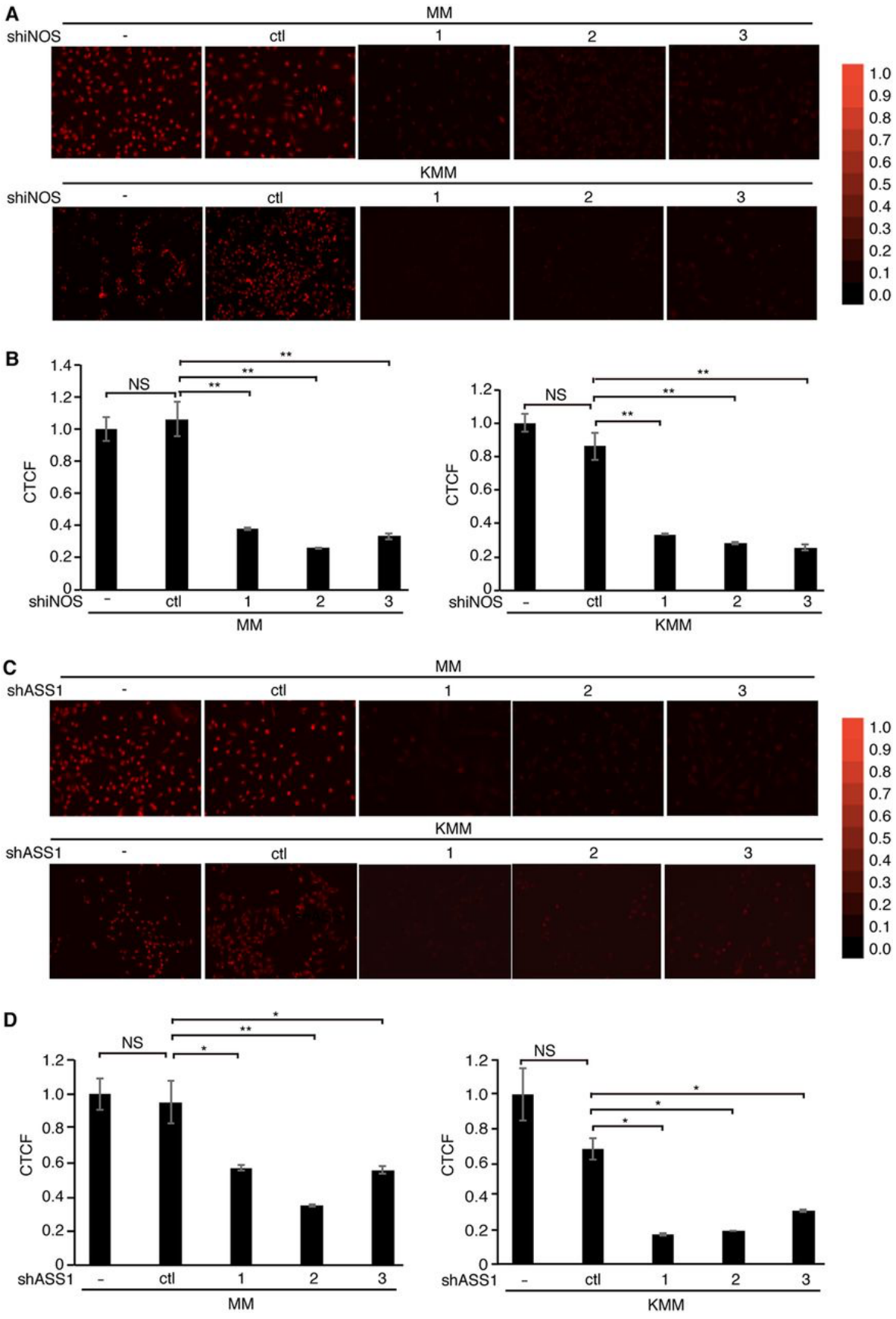
A
MM
shiNOS
-
ctl
1
2
3
KMM
1.0
0.9
0.8
0.7
0.6
0.5
0.4
0.3
0.2
0.1
0.0
B
CTCF
NS
**
shiNOS
MM
KMM
C
shASS1
D
*

Figure 14: ASS1 or iNOS silencing reduces the intracellular production of NO.

(A and **C)** MM and KMM cells were seeded in 6-well plates. In the following day, cells were infected either with scrambled control (ctl), three iNOS shRNAs (1, 2 and 3) or three ASS1 shRNAs (1, 2 and 3). 24h after transduction, cells were split and re-seeded at $1.5x10^4$ cells/well in 24 well-plates. Two days post-reseeding, the cells were stained with DAR for 1h in cell culture incubator. Then, MM and KMM cells were washed with PBS for four times for 5 minutes per time in shaker in room temperature. Representative images were captured at 20x magnification using fluorescent microscope in the top. **(B** and **D)** The images were quantitated by image J and were shown in the bottom. CTCF represented the corrected total cell fluorescence by imageJ. Three independent experiments were repeated and results were shown as mean ± SEM; Data were analyzed by Student's t-test; * for $P < 0.05$, and ** for $P < 0.01$.

2.6 NO produced through the ASS1-iNOS cycle activates STAT3 to promote the proliferation of KSHV-transformed cells

ASS1 expression has been reported to correlate with STAT3 protein expression in human gastric cancer cells by an unknown mechanism [230]. We observed a marginal increase of STAT3 protein expression in KMM cells compared to MM cells (**Figure 15A**). STAT3 plays a crucial role in promoting tumor progression, and thus is a favorable target for cancer therapy [231, 232]. In latent KSHV-infected and transformed cells, it has been shown that STAT3 is activated with increased phosphorylation at Tyr705 through the activation of alternative complement and TLR4 pathways, and that STAT3 activation is essential for the survival of KSHV-transformed cells [233, 234]. Since NO has been shown to activate STAT3 in ovarian cancer cells [235], we hypothesized that STAT3 might be a potential common downstream target of NO, ASS1 and iNOS. Knock down ASS1 reduced the phosphorylation of STAT3 (Tyr705) in

KMM cells, suggesting that STAT3 was regulated by ASS1 in KSHV-transformed cells (**Figure 15A**).

To determine if NO mediated ASS1-induced STAT3 activation, we searched a method to increase intracellular NO level. SNAP is a known NO donor. To determine whether SNAP could be used as a reliable NO donor, we treated MM and KMM cells with SNAP and then measured NO by fluorescence live cell imaging following treatment with DAR. As expected, stronger fluorescent DAR was observed in the SNAP-treated cells than untreated cells (**Figure 15B** and **C**). Finally, we examined if NO mediated ASS1-induced STAT3 activation. We treated MM and KMM cells with SNAP after ASS1 knockdown and then examined STAT3 phosphorylation. As expected, SNAP partially rescued the decreased phosphorylation of STAT3 caused by ASS1 knockdown, which implied that NO mediated STAT3 activation in KSHV-transformed cells (**Figure 15D**). However, SNAP failed to rescue the reduced cell proliferation rate caused by ASS1 knock down which was possibly due to its short half-life of four hours. Taken together, these results indicated that STAT3 activation in KSHV-transformed cells was at least partially dependent on ASS1-mediated NO production.

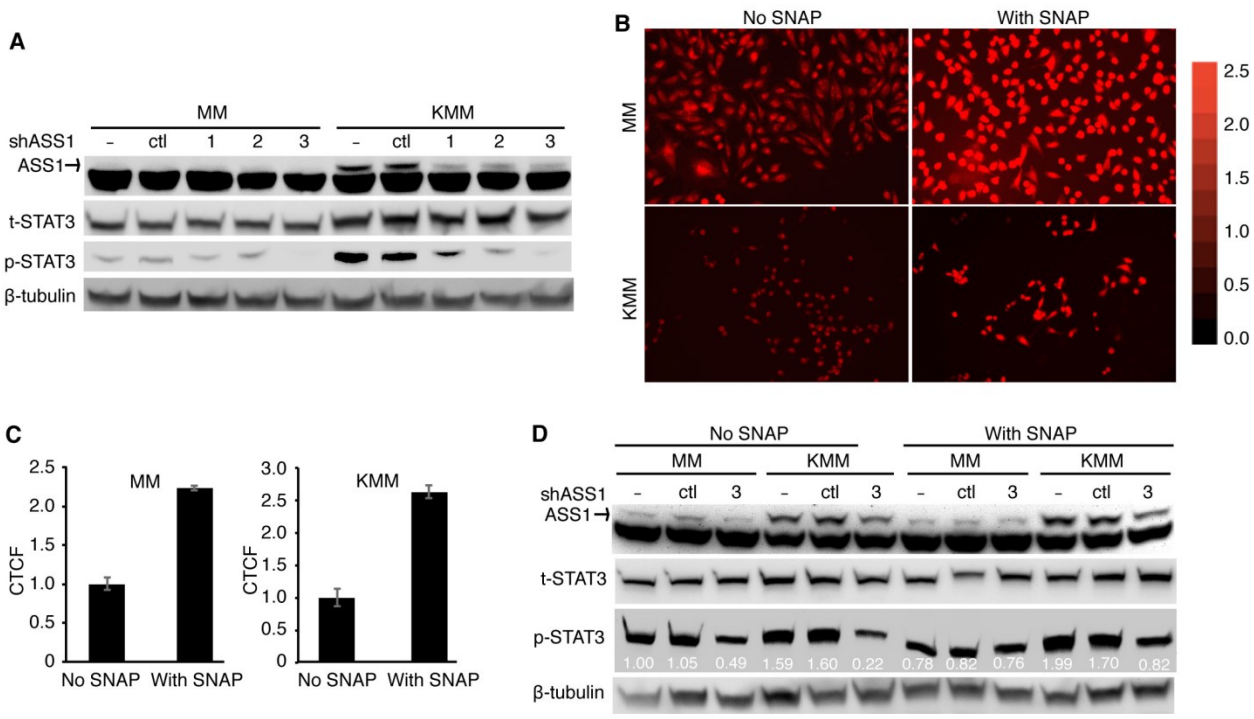

Figure 15: ASS1 or iNOS knockdown inactivates STAT3, which is rescued by SNAP.

(A and **B)** Reduced ASS1 or iNOS expression inhibits STAT3 tyrosine phosphorylation or activation. MM and KMM cells were transduced with either scrambled control (ctl), three ASS1 respectively, lysed at day 2 post-transduction, and then were examined for the expression of phosphorylated STAT3 (Y705) by Western-blot. **(B)** MM and KMM cells were seeded at $1.5x10^4$ cells/well in 24 well plates. In the following day, MM and KMM cells were treated with 0.5mM SNAP for 1h followed by DAR staining for another 1h in cell culture incubator. Then, MM and KMM cells were washed with PBS for four times for 5 minutes per time in shaker in room temperature. Representative images were captured at 20x magnification using fluorescent microscope. **(C)** The images were quantitated by image J. CTCF represented the corrected total cell fluorescence by imageJ. **(D)** NO donor SNAP reverted the inhibitory effect on the expression of phosphorylated STAT3 induced ASS1 knockdown. MM and KMM cells were transduced with either scrambled control (ctl) or three ASS1 shRNA (1,2,3) lentivirus. Two-day post infection of ASS1 shRNA lentivirus, MM and KMM cells were treated with 0.5mM SNAP for half hour, and the expression of phosphorylated STAT3 was checked by Western-blot.

2.7 Glucose metabolism does not regulate ASS1 and intracellular NO and vice versa

We have previously shown that KSHV inhibits aerobic glycolysis to promote cell survival in KSHV-transformed cells by downregulating the expression levels of GLUT1 and GLUT3. Our results so far showed the importance of ASS1 upregulation and the citrulline-NO cycle in KSHV-transformed cells. Thus, we further examined the role of ASS1 in the expression of GLUT1 and GLUT3 in KSHV-transformed cells. Knockdown of ASS1, which also led to a reduced level of intracellular NO (**Figure 14C** and **D**), did not alter the levels of GLUT1 and GLUT3 (**Supplementary Figure 6A**). Overexpression of ASS1 also did not alter the levels of GLUT1 and GLUT3 (**Supplementary Figure 6**B). Hence, it is unlikely that ASS1 and the citrulline-NO cycle regulate the expression of GLUT1 and GLUT3 and glucose metabolism. Similarly, glucose deprivation, which increases glutamine uptake [213], did not alter ASS1 expression and intracellular NO levels (**Supplementary Figure 6C** and **D**). Therefore, glucose metabolism does not regulate ASS1 expression and the citrulline-NO cycle.

2.8 Discussion

We have previously shown that KSHV suppresses glucose uptake and aerobic glycolysis but upregulates glutamine metabolism to promote cell survival and proliferation in KSHV-transformed cells [35, 213]. In this report, we have demonstrated that KSHV regulates ASS1 to maintain NO production, which is essential for the survival and proliferation of KSHV-transformed cells. ASS1 knockdown significantly reduced intracellular NO levels and knockdown of iNOS gave a phenotype similar to that of ASS1 knockdown. Additionally, ASS1

silencing decreased STAT3 activation, which was partially rescued by NO. Taken together, these results reveal a novel mechanism by which an oncogenic virus rewires the metabolic pathways to support the proliferation and survival of KSHV-transformed cells by sustaining NO generation and STAT3 activation.

ASS1 is a rate-limiting enzyme in the citrulline-NO cycle, arginine synthesis and NO production [218, 224, 236]. Previous studies have shown that ASS1 is upregulated in several types of cancer but the role of ASS1 in cancer as well as the molecular basis mediating ASS1 upregulation remains unclear [208, 230, 237, 238]. In KSHV-transformed cells, we found that numerous KSHV-encoded miRNAs were required for ASS1 upregulation (**Figure 11**). Significantly, we showed that ASS1 was required for the proliferation and colony formation in softagar of KSHV-transformed cells (**Figure 12**). These findings are consistent with the results of another study showing that inhibition of ASS1 results in decreased proliferation and tumorigenicity of colorectal cancer [239]. Interestingly, ASS1 is reported to be downregulated in several types of cancer cells, leading to the increased dependence of tumor cells on exogenous arginine, and hence enhanced sensitivity to arginine deprivation [240, 241]. However, the significance of ASS1 loss in cancer is currently unclear.

By far, the only known function of ASS1 is to recycle citrulline to synthesize argininosuccinate that is further converted into arginine by ASL to provide the substrate for NO production. Although the extracellular arginine concentration is much higher than the reported Km of arginine for iNOS, NO generation still depends on the availability of intracellular arginine in multiple cell lines [224, 236, 242, 243]. Results of a previous microarray study showed that ASS1 upregulation was positively correlated with NO production, suggesting a possible role of ASS1 in NO generation [244]. Our results demonstrated that the ASS1 was required for NO

generation in KSHV-transformed cells. Suppressing either ASS1 or iNOS expression significantly reduced NO concentration in vitro (**Figure 14**). Interestingly, we did not detect a higher concentration of NO in KMM cells than MM cells despite of higher expression of both ASS1 and iNOS in KMM cells (**Supplementary Figure 3A and B**) [228]. We speculate that higher level of ASS1 and citrulline-NO cycle are required for maintaining the intracellular NO level, which is essential for sustaining the proliferation of KSHV-transformed cells. Indeed, knockdown of iNOS reduced the intracellular NO level as well as cell proliferation (**Figure 13** and **Figure 14**), indicating that the normal flow of the NO-citrulline cycle carried out by iNOS and ASS1 is indispensable for the proliferation of KSHV-transformed cells. Paradoxically, overexpression of ASS1 did not further increase the intracellular NO level (results not shown) suggesting that ASS1 needs to cooperate with other components of the citrulline-NO cycle. As excess NO level might be toxic to the cells [221, 222], maintaining the homeostasis of NO could maximize the survival of KSHV transformed cells.

NO is a multifunctional regulator implicated in diverse physiological and pathological processes [245-247]. A known NO donor SNAP can both activate and inactivate STAT3 [229, 235, 248], but there is no report that has linked ASS1 to STAT3 activation. Our results showed that STAT3 was inactivated following ASS1 knockdown, which was partially rescued by SNAP (**Figure 15**). These results linked ASS1 to STAT3 activation, which was mediated by NO. Our previous studies have shown that STAT3 activation is essential for the survival and proliferation of KSHV-transformed cells [234]. Hence, the effect of ASS1 knockdown on reduced KSHV-induced proliferation and cellular transformed was likely due to the inactivation of STAT3, resulting from the decreased intracellular NO level. Our results, for the first time, demonstrated that STAT3 activation was closely regulated by ASS1 and NO, and hence the citrulline-NO

cycle. Further mechanistic studies are required to delineate the mechanism by which NO mediates STAT3 activation.

Interestingly, we did not find a role of ASS1 or the citrulline-NO cycle in regulating the expression of GLUT1 and GLUT3 even though they are downregulated in KSHV-transformed cells [35]. Glucose deprivation also did not alter ASS1 expression and intracellular NO levels. These results are expected, as the glutamine pathway is not reprogrammed in MM cells, while KMM cells are already reprogrammed by KSHV to utilize glutamine with or without glucose deprivation [213]. Hence, these are the distinct properties of MM and KMM cells that define their primary and transformed features, respectively.

In summary, we have shown that KSHV miRNAs upregulate ASS1 in KSHV-transformed cells, resulting in enhanced cell proliferation and cellular transformation by regulating NO-mediated STAT3 activation. These findings might also be relevant in other types of cancer that have dysregulated ASS1 expression.

3.0 Kaposi's sarcoma-associated herpesvirus miRNAs suppress CASTOR1-mediated mTORC1 activation and tumorigenesis

Preface:

The text and figures in this chapter are taken from my previous publication, "**Li T**, Ju EG, Gao S-J. Suppression of mTORC1 inhibitor CASTOR1 by oncogenic KSHV-encoded miRNAs promotes cell proliferation and growth transformation. **Journal of Clinical Investigation, 2019**, 130: 3310-3323", under the journal's copyright permission.

CASTOR1 and CASTOR2 inhibit mTORC1 upon arginine deprivation. mTORC1 regulates cell proliferation, survival and metabolism, and is often dysregulated in cancers, indicating that cancer cells may regulate CASTOR1/2 to control mTORC1 signaling and promote tumorigenesis. mTORC1 is the most effective therapeutic target of Kaposi sarcoma, caused by infection of KSHV. Hence, KSHV-induced cellular transformation is a suitable model for investigating mTORC1 regulation in cancer cells. Currently, the mechanism of KSHV activation of mTORC1 in KSHV-induced cancers remains unclear. We showed that KSHV suppressed CASTOR1/2 expression to activate mTORC1 pathway. CASTOR1 or CASTOR2 overexpression, and mTOR inhibitors abolished cell proliferation and colony formation in softagar of KSHV-transformed cells by attenuating mTORC1 activation. Furthermore, KSHV-encoded miRNA (miR)-K4-5p and likely -K1-5p directly targeted CASTOR1 to inhibit its expression. Knockdown of miR-K1-5p and -K4-5p restored CASTOR1 expression and thereby attenuated mTORC1 activation. CASTOR1 or CASTOR2 overexpression, and mTOR inhibitors abolished activation of mTORC1 and growth transformation induced by pre-miR-K1 and -K4

(Figure 16). Our results defined the mechanism of KSHV activation of mTORC1 pathway and established the scientific basis of targeting this pathway for treating KSHV-associated cancers.

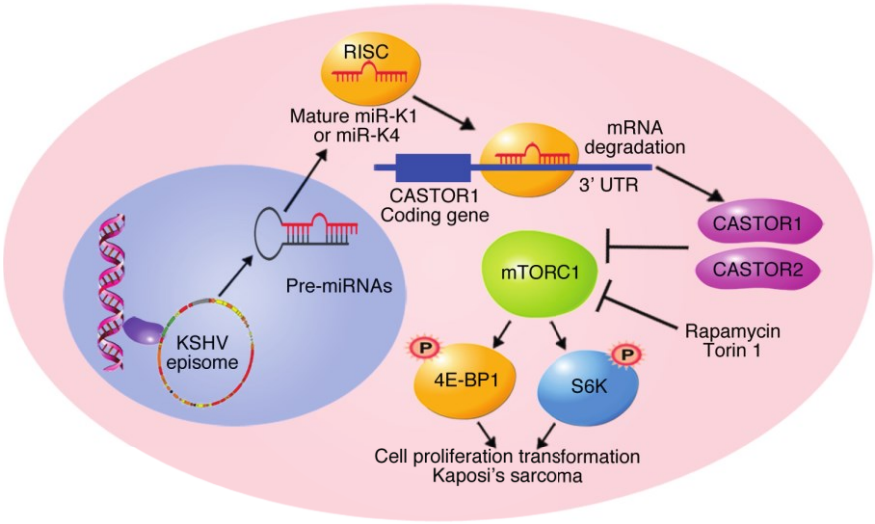

Figure 16: Schematic illustration of KSHV miR-K4-5p and possibly -K1-5p direct suppression of CASTOR1, leading to activation of mTORC1 pathway, enhanced cell proliferation and cellular transformation.

3.1 KSHV-transformed cells are sensitive to mTORC1 inhibition

Rapamycin, a potent inhibitor for mTORC1, is the most effective therapy for KS patients, indicating the importance of mTORC1 in KS tumors [249, 250]. We examined the activation of mTORC1 pathway in KMM cells, and detected the activation of two canonical downstream effectors of mTORC1 S6K and 4EBP1 in KMM cells as shown by their higher phosphorylated levels with S6K at Thr389 (pS6K) and 4EBP1 at Ser65 (p4EBP1), respectively, compared to the primary MM cells (**Figure 17A**). Thus, the mTORC1 pathway was activated in the KSHV-transformed cells.

We then determined whether KSHV-transformed cells were sensitive to mTOR inhibition by treating them with mTOR inhibitors rapamycin and Torin1. Both mTOR inhibitors effectively decreased the levels of pS6K and p4EBP1 in KSHV-transformed cells (**Figure 17B**). Furthermore, inhibition of mTORC1 significantly reduced the proliferation and efficiency of colony formation in softagar of KSHV-transformed cells (**Figure 17C** and **D**). The mTOR inhibitors also reduced the proliferation of MM cells but the inhibitory effect was much weaker than on KMM cells (**Figure 17C**), indicating that KSHV-transformed cells were more addicted to mTORC1 pathway. Furthermore, Torin1 and rapamycin induced cell cycle arrest but no significant apoptosis in both MM and KMM cells (**Figure 17E** and **F**). These results indicate that the status of the mTOR pathway and the response to mTOR inhibitors of KMM cells resemble those observed in KS tumors in the clinics [249-251]. Therefore, the KMM model can be used to delineate the mechanism of KSHV-induced activation of mTORC1 pathway.

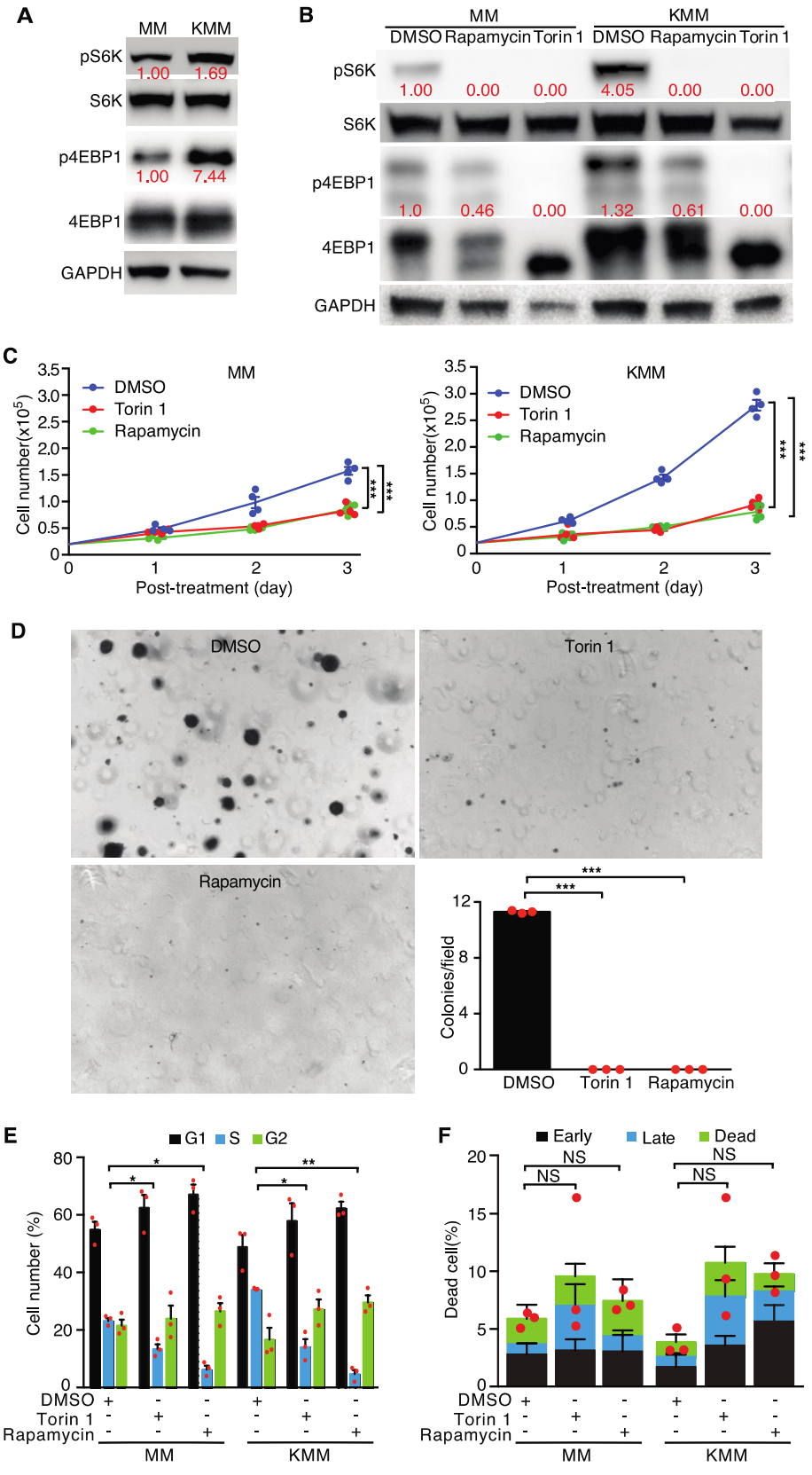
A
MM
KMM
pS6K
1.00
1.69
S6K
p4EBP1
1.00
7.44
4EBP1
GAPDH
B
MM
KMM
DMSO
Rapamycin
Torin 1
DMSO
Rapamycin
Torin 1
pS6K
1.00
0.00
0.00
4.05
0.00
0.00
S6K
p4EBP1
1.0
0.46
0.00
1.32
0.61
0.00
4EBP1
GAPDH
C
MM
DMSO
Torin 1
Rapamycin
Cell number(x10^5)
Post-treatment (day)
***
***
KMM
DMSO
Torin 1
Rapamycin
Cell number(x10^5)
Post-treatment (day)
***
***
D
DMSO
Torin 1
Rapamycin
***
***
Colonies/field
DMSO
Torin 1
Rapamycin
E
G1
S
G2
Cell number (%)
DMSO
Torin 1
Rapamycin
MM
KMM
F
Early
Late
Dead
NS
NS
NS
NS
Dead cell(%)
DMSO
Torin 1
Rapamycin
MM
KMM

Figure 17: KSHV-transformed cells have activated mTORC1 pathway and are sensitive to mTOR inhibitors. (**A**) mTORC1 is activated in KSHV-transformed cells. Cells were analyzed for phospho-4EBP1 at Ser65 (p4EBP1) and phospho-S6K at Thr389 (pS6K). Three independent experiments were repeated with similar results, and results of one representative experiment were shown. (**B**) Rapamycin and Torin1 inhibit mTORC1 activation in KSHV-transformed cells. Cells were treated with DMSO, 100 nm rapamycin or 50 nm Torin1 for 16 h and analyzed for mTORC1 activation. Three independent experiments were repeated with similar results, and results of one representative experiment were shown. The same set of samples were run in different gels but with the same loading calibration. (**C**) Rapamycin and Torin1 significantly inhibit cell proliferation of KSHV-transformed cells. Cells were treated with DMSO, 100 nM rapamycin or 50 nM Torin1, and cell numbers were counted daily. Three independent experiments were repeated with similar results, and results from one representative experiment with four biological repeats were shown as mean ± SEM. (**D**) Rapamycin and Torin1 significantly inhibit colony formation of KMM cells in softagar. KMM cells treated with DMSO, 200 nM Rapamycin or 100 nM Torin1 were examined for colony formation in softagar. Representative pictures at 4x objective were shown. Colonies with diameter >50 μm were quantified (right bottom panel). Three independent experiments were repeated and results were shown as mean ± SEM. (**E** and **F**) Rapamycin and Torin1 induce cell cycle arrest but no significant apoptosis in MM and KMM cells. Cells were treated with DMSO, 100 nM rapamycin or 50 nM Torin1 for 24 h, and analyzed for cell cycle progression (**E**) or apoptosis (**F**). Three independent experiments were repeated and results were shown as mean ± SEM. Data were analyzed by one-way ANOVA followed by Tukey post-hoc test if $P < 0.05$. Statistically significant differences are indicated as NS for no significance; * for $P < 0.05$ and *** for $P < 0.001$.

3.2 KSHV latent infection activates mTORC1 by downregulating CASTOR1/2

Previous studies have shown that CASTORs are negative regulators of mTORC1 pathway upon arginine deprivation [145, 146, 148]. We examined whether CASTORs might be downregulated in KSHV-transformed cells. Compared to MM cells, CASTOR1 and CASTOR2 transcripts were downregulated by 10- and 2.5-fold in KMM cells, respectively (**Figure 18A** and

B). To confirm these results, we examined telomerase-immortalized human umbilical vein endothelial cells (TIVE) latently infected by KSHV (KTIVE). Compared to the uninfected TIVE cells, CASTOR1 and CASTOR2 transcripts were downregulated in KTIVE by 30- and 4-fold, respectively (**Figure 18A** and **B**). These results were further confirmed at the protein levels (**Figure 18C**). Hence, latent KSHV infection downregulated the expression of CASTOR1 and CASTOR2. Because TIVE cells were already immortalized before KSHV infection, we chose to focus on MM cells.

To determine whether KSHV-induced downregulation of CASTOR1 or CASTOR2 was the cause of mTORC1 activation, we overexpressed CASTOR1 or CASTOR2 in KMM cells. Overexpression of either CASTOR1 or CASTOR2 was sufficient to reduce the levels of pS6K1 and p4EBP1 in KMM cells (**Figure 18D**). Interestingly, the levels of pS6K1 were also reduced in MM cells following overexpression of either CASTOR1 or CASTOR2 (**Figure 18D**), confirming the essential roles of CASTORs in regulating mTORC1 function in normal cells. Together, these results indicate that CASTORs mediate KSHV activation of mTORC1 in KSHV-transformed cells.

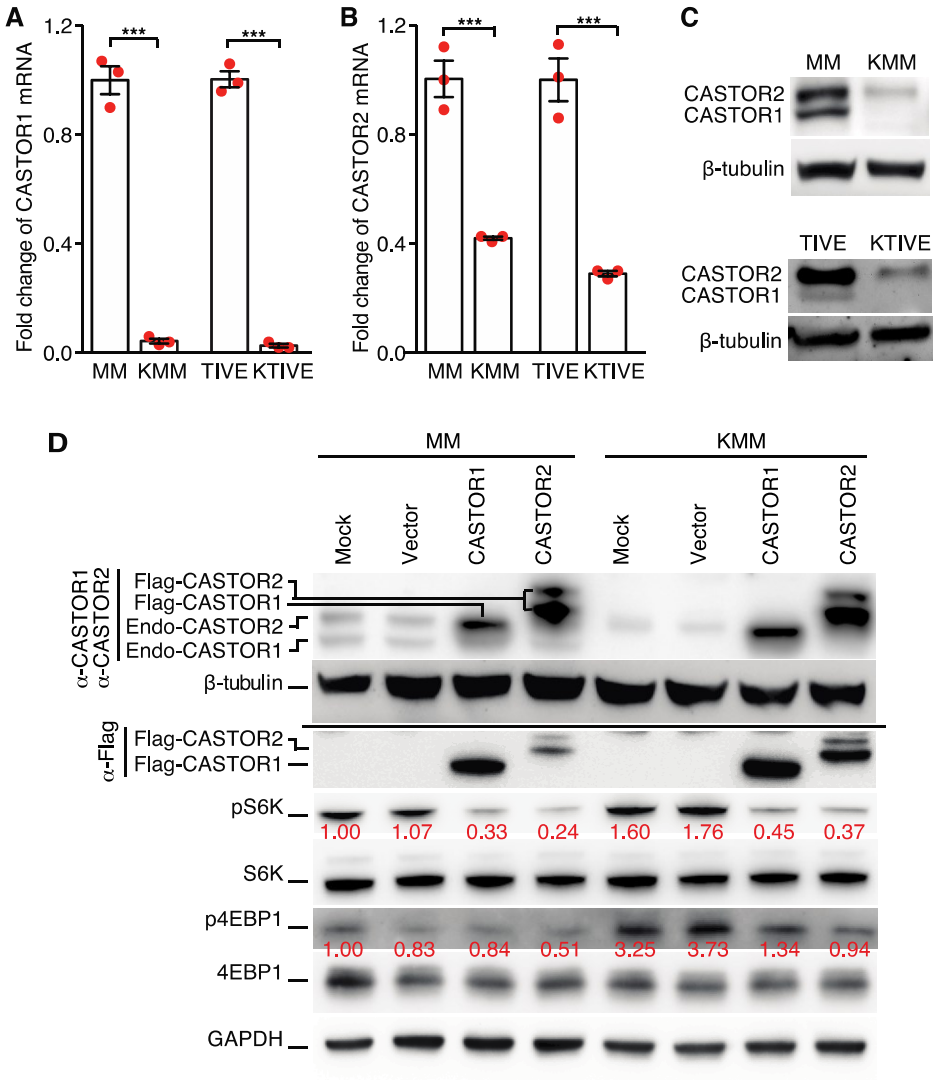

Figure 18: Latent KSHV infection activates mTORC1 by downregulating CASTOR1/2.

(**A-C**) Latent KSHV infection downregulates CASTOR1/2 examined at mRNA level by RT-qPCR (**A** and **B**), and at protein level by Western-blotting (**C**). Three independent experiments were repeated with similar results and results from one representative experiment were shown. mRNA results from three biological repeats were shown as mean ± SEM (**A** and **B**). For Western-blotting (**C**), the same set of samples were run in different gels but with the same loading calibration. (**D**) Overexpression of CASTOR1 or CASTOR2 suppresses mTORC1 activation. Western-blotting analysis of CASTOR1 and CASTOR2 proteins with an anti-Flag antibody and an antibody that detected endogenous CASTOR1 and CASTOR2 proteins, and mTORC1 downstream effectors pS6K and p4EBP1 in untransduced MM and KMM cells, and MM and KMM cells transduced with Vector control, CASTOR1 or CASTOR2. Three independent experiments were repeated with similar results and results from one representative

experiment were shown. P-value was calculated using unpaired Student's t-test (two tailed). Statistically significant differences are shown as *** for $P < 0.001$.

3.3 KSHV-encoded miR-K1 and -K4 mediate KSHV activation of mTORC1 by inhibiting CASTOR1 expression

We focused on identifying the mechanism of KSHV downregulation of CASTOR1 since the extent of its downregulation was much more robust than that of CASTOR2. During KSHV latency, only few viral products are expressed, including vFLIP, vCyclin, LANA and a cluster of 12 pre-miRNAs. To identify the viral product(s) that downregulate(s) CASTOR1, we examined CASTOR1 expression in MM, KMM ΔvFLIP, ΔvCyclin, and ΔmiR cells and found either deletion of vFLIP or miRNA cluster restored CASTOR1 expression to almost the same level as the uninfected MM cells while deletion of vCyclin had no effect (**Figure 19A** and **B**). These results indicated that both the miRNA cluster and vFLIP were required for suppressing CASTOR1 expression. To confirm these results, we examined mTORC1 activation in these mutant cells. Whereas deletion of the miRNA cluster significantly attenuated mTORC1 pathway shown by the decreased pS6K and p4EBP1 levels, deletion of neither vFLIP nor vCyclin had any effect on mTORC1 activation (**Figure 19C**). These contradictory results between CASTOR1 expression and mTORC1 activation in ΔvFLIP mutant cells suggested that alternative mechanism in addition to CASTOR1 expression might be involved in vFLIP regulation of mTORC1 activation. Since the miRNA cluster mutant exhibited the most consistent results of CASTOR1 expression and mTORC1 activation, we subsequently focused on the miRNA cluster.

Previous studies have shown that KSHV miRNAs are highly expressed in KS tumors, and are required for KSHV-induced tumorigenesis [211, 213, 252, 253]. Deletion of the miRNA cluster abolished KSHV-induced cellular transformation and tumorigenesis [211]. However, expression of numerous individual KSHV pre-miRNAs was sufficient to restore KSHV-induced cellular transformation and tumorigenesis with pre-miR-K1, -K4 and -K11 giving the strongest oncogenic effects [211]. These cells, termed ΔmiR-pre-K1, -K4 and -K11, formed large colonies in softagar and induced tumors in nude mice as efficiently as the WT KMM cells. We examined CASTOR1 expression in ΔmiR cells expressing individual KSHV pre-miRNAs. Among all the pre-miRNAs examined, expression of either pre-miR-K1 or -K4 alone in ΔmiR cells significantly inhibited the expression of CASTOR1 transcript (**Figure 19D**), which was confirmed at the protein level (**Figure 19E**). In agreement with these results, we observed higher pS6K1 and p4EBP1 levels in both ΔmiR-pre-K1 and -K4 cells than ΔmiR cells, indicating activation of mTORC1 by pre-miR-K1 and -K4 (**Figure 19F**).

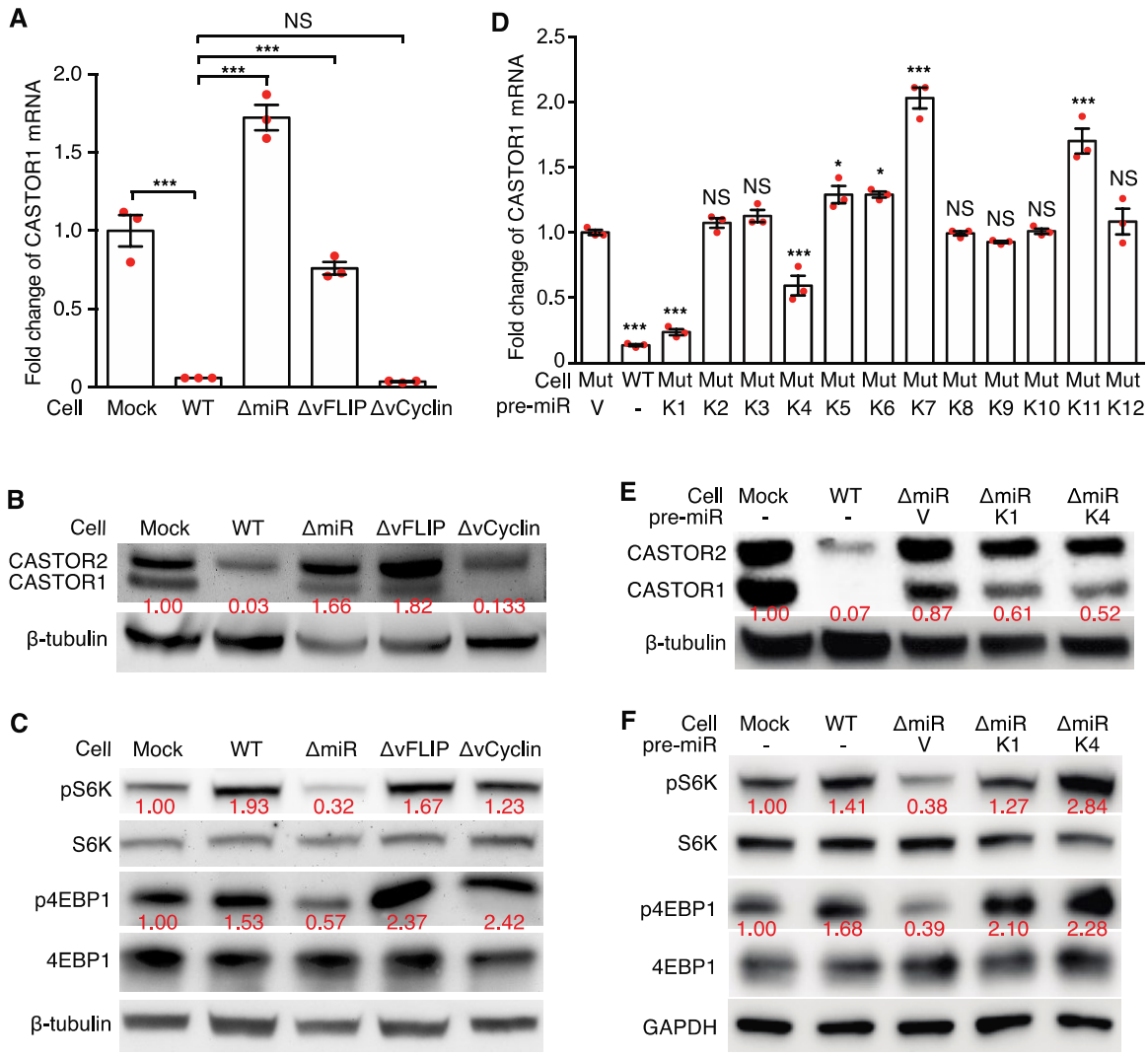

Figure 19: Pre-miR-K1 and -K4 mediate KSHV downregulation of CASTOR1 and activation of mTORC1.

(**A** and **B**) The miRNA cluster and vFLIP mediate KSHV downregulation of CASTOR1. Analysis of CASTOR1 mRNA level by RT-qPCR (**A**) and protein level by Western-blotting (**B**) in Mock (MM), WT (KMM), ΔvFLIP, ΔvCyclin and ΔmiR cells, respectively. Three independent experiments were repeated with similar results and results from one representative experiment were shown. mRNA results from three biological repeats were shown as mean ± SEM (**B**). (**C**) The miRNA cluster mediate KSHV activation of mTORC1 pathway. Analysis of mTORC1 downstream effectors pS6K and p4EBP1 in Mock, WT, ΔvFLIP, ΔvCyclin and ΔmiR cells by Western-blotting. Three independent experiments were repeated with similar results, and results from one representative experiment were shown. The same set of samples were run in different gels but with the same loading calibration. (**D-E**) Pre-miR-K1 and -K4 mediate KSHV downregulation of CASTOR1. Analysis of CASTOR1 mRNA level (**D**) and

protein level (**E**) in WT cells, and ΔmiR cells complemented with Vector control or individual KSHV pre-miRNAs. Three independent experiments were repeated with similar results, and results from one representative experiment were shown. mRNA results from three biological repeats were shown as mean ± SEM (**D**). (**F**) Pre-miR-K1 and -K4 mediate mTORC1 activation. Analysis of mTORC1 downstream effectors pS6K and p4EBP1 in Mock and WT cells, and ΔmiR cells complemented with Vector control (V), or pre-miR-K1 or -K4 by Western-blotting. Three independent experiments were repeated with similar results, and results from one representative experiment were shown. Data were analyzed by one-way ANOVA followed by Tukey post-hoc test if P <0.05. Statistically significant differences are shown as NS for no significance; * for $P < 0.05$ and *** for $P < 0.001$.

To confirm the above results, we first performed knockdown of miR-K1-5p and -K4-5p, derived from pre-miR-K1 and -K4, using different doses of locked nucleic acid (LNA)-based suppressors (**Figure 20A** and **B**). Knockdown of miR-K1-5p and -K4-5p significantly increased CASTOR1 expression in a dose-dependent manner at both mRNA and protein levels in KMM but not MM cells (**Figure 20C-E**). Additionally, simultaneous knockdown of both miR-K1-5p and -K4-5p in KMM cells additively increased CASTOR1 expression (**Figure 20C** and **E**), indicating that both miRNAs worked synergistically to suppress CASTOR1 expression. Furthermore, knockdown of either miR-K1-5p or -K4-5p suppressed mTORC1 activation as shown by the decreased pS6K and p4EBP1 levels (**Figure 20F** and **G**). These results indicate that both miR-K1-5p and -K4-5p activate mTORC1 by inhibiting CASTOR1 expression.

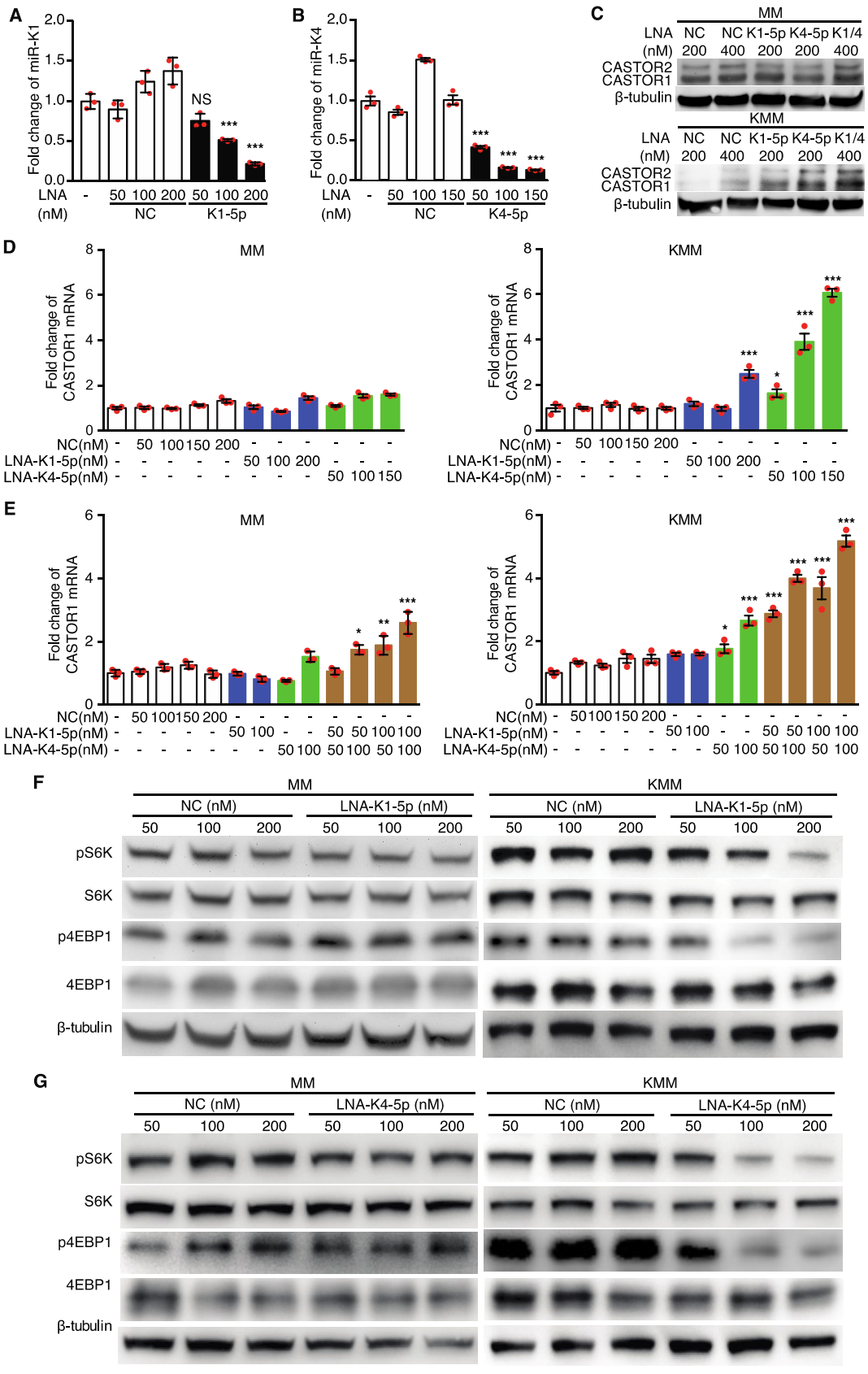
A
Fold change of miR-K1
LNA
(nM)
NC
K1-5p
NS
B
Fold change of miR-K4
K4-5p
C
MM
KMM
CASTOR2
CASTOR1
β-tubulin
D
Fold change of CASTOR1 mRNA
NC(nM)
LNA-K1-5p(nM)
LNA-K4-5p(nM)
E
F
pS6K
S6K
p4EBP1
4EBP1
G

Figure 20: KSHV miR-K1-5p and -K4-5p inhibit CASTOR1 expression and activate mTORC1.

(**A** and **B**) miRNA suppressors reduce level of miR-K1-5p (**A**) or -K4-5p (**B**) in KSHV-transformed cells, respectively. RT-qPCR examination of miR-K1-5p (**A**) or -K4-5p (**B**) in untransfected cells, or KMM cells transfected with locked nucleic acid (LNA)-based scrambled control (NC), miRNA suppressor LNA-K1-5p (**A**) or LNA-K4-5p (**B**), respectively. Three independent experiments were repeated with similar results, and results from one representative experiment with three biological repeats were shown as mean ± SEM. (**C** and **D**) Knockdown of either miR-K1-5p or -K4-5p increases CASTOR1 expression in KMM but not MM cells. Untransfected cells, or cells transfected with different concentrations of LNA-based NC, LNA-K1-5p or LNA-K4-5p were examined for CASTOR1 protein level (**C**) and mRNA level (**D**), respectively. Three independent experiments were repeated with similar results, and results from one representative experiment were shown. mRNA results from three biological repeats were shown as mean ± SEM (**D**). (**E**) Knockdown of miR-K1-5p and -K4-5p additively increases CASTOR1 mRNA level. Untransfected cells, or cells transfected with different concentrations of LNA-based NC, LNA-K1-5p, LNA-K4-5p, or LNA-K1-5p and LNA-K4-5p were examined for CASTOR1 mRNA expression. Three independent experiments were repeated with similar results, and results from one representative experiment with three biological repeats were shown as mean ± SEM. (**F** and **G**) Knockdown of miR-K1-5p (**F**) or -K4-5p (**G**) inhibits mTORC1 activation in KMM cells but not MM cells. Cells transfected with LNA-based NC, or LNA-K1-5p (**F**) or LNA-K4-5p (**G**) were examined for pS6K and p4EBP1 by Western-blotting. Three independent experiments were repeated with similar results, and results from one representative experiment were shown. For the Western-blotting of KMM cells in panel **G**, the same set of samples were run in different gels but with the same loading calibration. Data were analyzed by one-way ANOVA followed by Tukey post-hoc test if $P < 0.05$. Statistically significant differences are shown as NS for no significance; * for $P < 0.05$, ** for $P < 0.01$ and *** for $P < 0.001$.

3.4 CASTOR1 is directly targeted by miR-K4-5p and possibly miR-K1-5p

miRNAs induce degradation of transcripts or inhibit translation of proteins by directly binding to their target genes. To explore whether CASTOR1 is a direct target of miR-K1-5p and

-K4-5p, we cloned the full length 3'UTR of CASTOR1 into the pGL3-Control plasmid downstream of the luciferase gene (named as pGL3-CASTOR1 3'UTR). We detected pGL3-CASTOR1 3'UTR luciferase reporter activity in MM, KMM and ΔmiR mutant cells. However, the activity was significantly reduced in KMM cells compared to MM and ΔmiR mutant cells (**Figure 21A**), indicating that KSHV-encoded miRNAs might directly target CASTOR1 3'UTR. Accordingly, knockdown of either miR-K1-5p or -K4-5p in KMM cells significantly increased the luciferase reporter activity (**Figure 21B**), whereas expression of either pre-miR-K1 or -K4 decreased CASTOR1 3'UTR but not the pGL3-Control construct reporter activity in 293T cells (**Figure 21C**). Further deletion analysis identified a 35 bp and a 26 bp fragments in CASTOR1 3'UTR that were targeted by miR-K1-5p and -K4-5p, respectively. Overexpression of pre-miR-K1 significantly reduced the luciferase activity of a reporter containing the 35 bp fragment in 293T cells (**Figure 21D**). Similarly, overexpression of pre-miR-K4 significantly reduced the luciferase activity of a reporter containing the 26 bp fragment in 293T cells (**Figure 21E**). Bioinformatics analysis identified a putative miR-K1-5p binding site in the 35 bp fragment (**Figure 21F**) and a putative miR-K4-5p binding site in the 26 bp fragment (**Figure 21G**), respectively. However, we were not able to confirm the miR-K1-5p binding site by mutagenesis analysis (results not shown). It is entirely possible that miR-K1-5p might indirectly regulate the expression of CASTOR1. In contrast, mutation of the putative miR-K4-5p binding site in the 26 bp fragment abolished the inhibitory effect of miR-K4-5p on the CASTOR1 3'UTR reporter in 293T cells (**Figure 21H**), thus confirming that miR-K4-5p bound to this site to suppress CASTOR1 expression. Nevertheless, the identified miR-K4-5p seed sequence is non-canonical. This mechanism of action has been reported for miRNAs, including KSHV miRNAs [217, 254].

Collectively, these results indicate that CASTOR1 is a direct target of KSHV-encoded miR-K4-5p, and possibly an indirect target of miR-K1-5p.

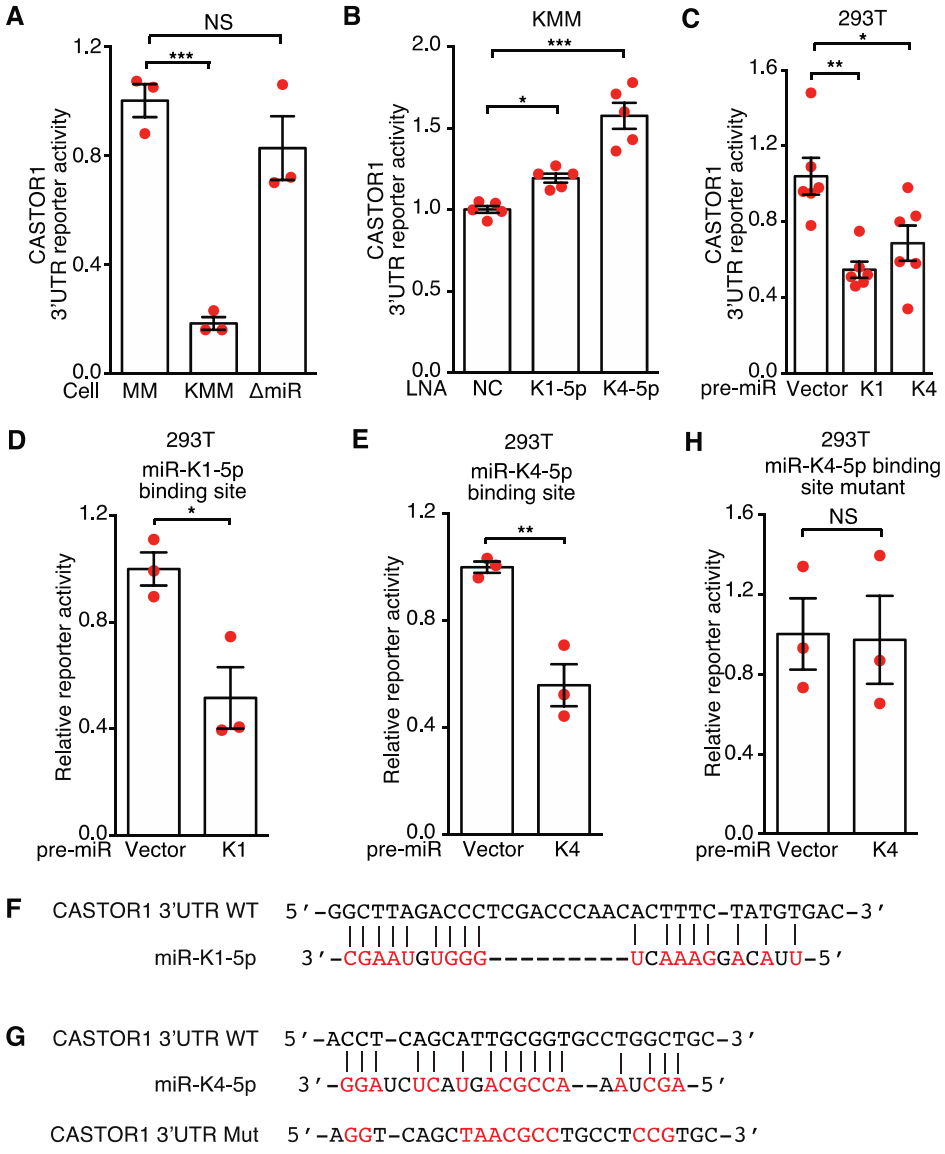

Figure 21: CASTOR1 transcript is directly targeted by miR-K4-5p and probably -K1-5p.

(**A**) Deletion of miRNA cluster relieves KSHV suppression of CASTOR1 3'UTR. Reporter activity was examined in Mock (MM), WT (KMM) and ΔmiR cells transfected with pGL3-CASTOR1 3'UTR and pRL-TK expressing renilla luciferase for normalization. (**B**) Knockdown of miR-K1-5p or -K4-5p increases CASTOR1 3'UTR activity in KMM cells. Cells transfected with pGL3-CASTOR1 3'UTR and miRNA suppressor LNA-K1-5p, LNA-K4-5p or scrambled control (NC) were examined. (**C**) Pre-miR-K1 or -K4 inhibits CASTOR1 3'UTR. 293T cells were transfected with pGL3-CASTOR1 3'UTR and pre-miR-K1 or -K4 plasmid, or Vector control, and reporter activity was examined. (**D**) Pre-miR-K1 suppresses a reporter containing a 35 bp fragment from CASTOR1 3'UTR. 293T cells were transfected with a reporter containing a 35 bp fragment from CASTOR1 3'UTR and pre-miR-K1 plasmid

or Vector control, and the reporter activity was examined. (**E)** Pre-miR-K1 suppresses a reporter containing a 26 bp fragment from CASTOR1 3'UTR. 293T cells were transfected with a reporter containing a 35 bp fragment from CASTOR1 3'UTR and pre-miR-K4 plasmid or Vector control, and the reporter activity was examined. (**F**) Putative targeting sequence of miR-K1-5p in CASTOR1 3'UTR. (**G**) Putative targeting sequence of miR-K4-5p in CASTOR1 3'UTR and mutagenesis of the putative binding site. (**H**) Mutation of miR-K4-5p binding site in CASTOR1 3'UTR fragment abolishes reporter suppression by miR-K4-5p. 293T cells were transfected with mutated reporter plasmid and pre-miR-K4 plasmid or Vector control, and the reporter activity was examined. All experiments were independently repeated three times with similar results, and results from one representative experiment with at least three biological repeats were shown as mean ± SEM. Data with two groups were analyzed by two-tailed Student's t-test. Data with more than two groups were analyzed by one-way ANOVA followed by Tukey post-hoc test if P <0.05. Statistically significant differences are shown as NS for no significance; * for $P < 0.05$, ** for $P < 0.01$ and *** for $P < 0.001$.

3.5 CASTOR1/2 inhibits KSHV-induced cell proliferation and growth transformation

mTORC1 is dysregulated in diverse types of cancer and it is a prime target in cancer therapy [255]. Since CASTOR1/2 are downregulated and negatively regulate mTORC1 in KSHV-transformed cells, they might restrict the proliferation and growth transformation of KSHV-transformed cells. We infected MM and KMM cells with a lentivirus expressing flag-tagged CASTOR1 or CASTOR2 at different multiplicity of infection (MOIs) (**Figure 22A**). As expected, we observed significant inhibitory effects on the proliferation of KMM cells in a dose-dependent manner in response to transduction of CASTORs, with CASTOR1 exerting a higher inhibitory efficiency than CASTOR2 (**Figure 22B**). At MOI of 2, 4 and 6, CASTOR1 reduced cell proliferation by 24%, 67% and 80%, respectively, while CASTOR2 reduced cell proliferation by 21%, 32% and 59%, respectively (**Figure 22B**). In contrast, transduction of

either CASTOR1 or CASTOR2 only had marginal suppressive effect on the proliferation of MM cells (**Figure 22B**). Furthermore, transduction of either CASTOR1 or CASTOR2 at MOI of 2 was sufficient to significantly reduce the efficiency of colony formation in softagar while at MOI of 4 or 6 almost completely abolished colony formation in softagar of KSHV-transformed cells (**Figure 22C**). In agreement with these results, both CASTOR1 and CASTOR2 induced cell cycle arrest of KMM cells but had more marginal effect on cell cycle progression of MM cells (**Figure 22D**). Transduction of either CASTOR1 or CASTOR2 also weakly increased the number of apoptotic or dead cells in KMM but not MM cells (**Figure 22E**). Taken together, we conclude that CASTOR1/2 are suppressive genes for growth transformation of KSHV-transformed cells and that their downregulation by KSHV is critical for maintaining the growth transformation of these cells.

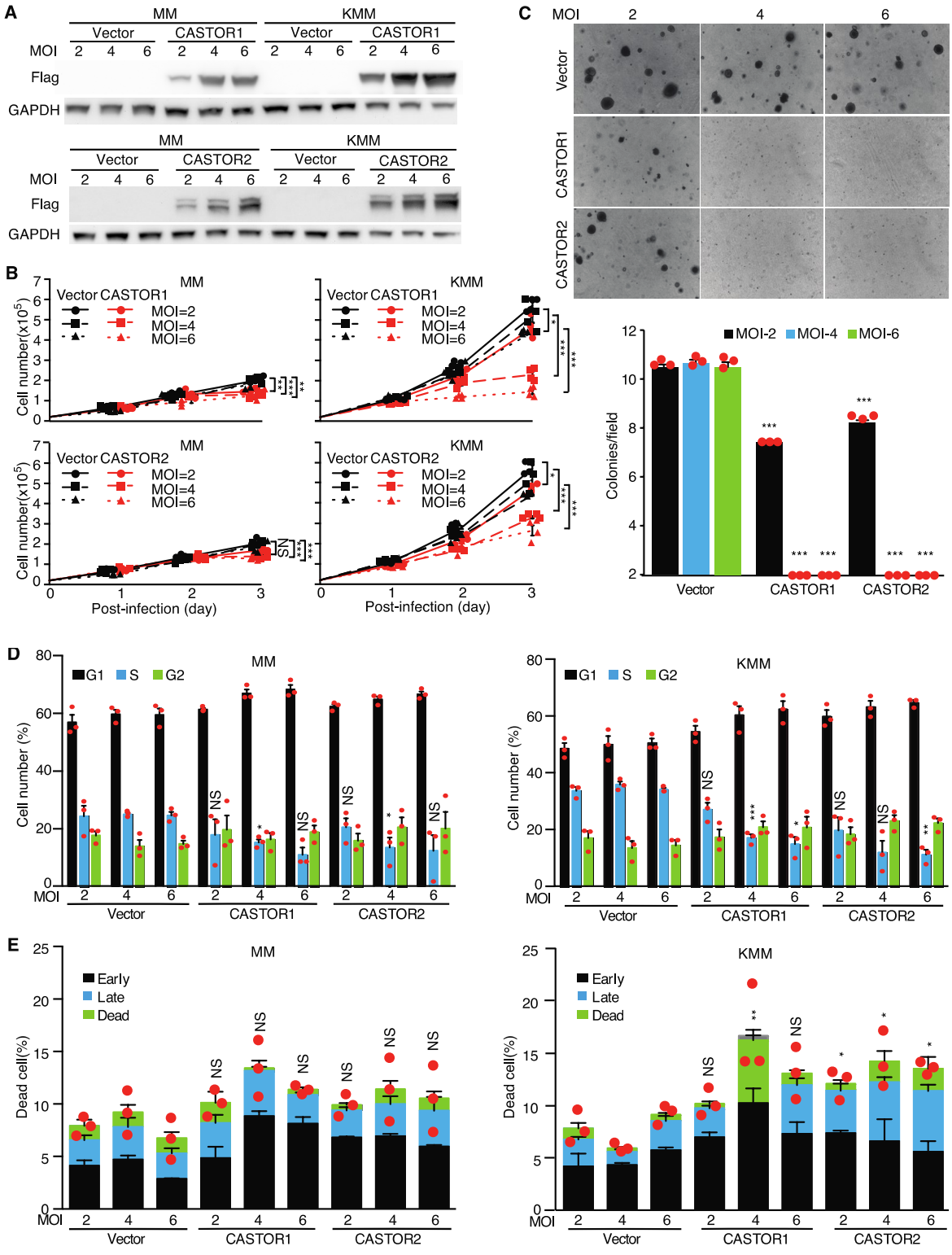

Figure 22: CASTOR1 and CASTOR2 inhibit cell proliferation and cellular transformation of KSHV-transformed cells.

(**A**) Dose-dependent expression of CASTOR1 and CASTOR2 in MM and KMM cells. Western-blotting analysis of CASTOR1 and CASTOR2 in MM and KMM cells transduced with increasing doses of lentiviruses of CASTOR1, CASTOR2 or Vector control at 2, 4 or 6 MOIs. Three independent experiments were repeated with similar results, and results from one representative experiment were shown. (**B** and **C**) Overexpression of either CASTOR1 or CASTOR2 impaired the proliferation and cellular transformation of KMM but not MM cells. MM and KMM cells transduced with different MOIs of lentiviruses of CASTOR1, CASTOR2 or Vector control as described in **A** were examined for cell proliferation (**B**) and colony formation in softagar (**C**). Three independent experiments were repeated with similar results, and results from one representative experiment with four biological repeats (**B**) or three combined experiments (**C**) were shown as mean ± SEM. (**D** and **E**) Overexpression of either CASTOR1 or CASTOR2 induces cell cycle arrest in KMM cells but has weak effect on MM cells, and weak apoptosis in KMM but not MM cells. MM and KMM cells transduced with increasing doses of lentiviruses of CASTOR1, CASTOR2 or a Vector control at 2, 4 or 6 MOIs for 48 h were examined for cell cycle progression (**D**) or apoptosis (**E**). Three independent experiments were repeated with similar results, and results from one representative experiment with three biological repeats were shown as mean ± SEM. Data were analyzed by one-way ANOVA followed by Tukey post-hoc test if P <0.05. Statistically significant differences are shown as NS for no significance; * for $P < 0.05$, ** for $P < 0.01$ and *** for $P < 0.001$.

3.6 CASTOR1/2 override KSHV pre-miR-K1 and -K4-induced cell proliferation and growth transformation

We have previously reported that KSHV pre-miR-K1 and -K4 are essential for KSHV-induced growth transformation [211]. Whereas deletion of the miRNA cluster abolished KSHV-induced growth transformation and tumorigenesis, complementation of ΔmiR mutant cells with either pre-miR-K1 or -K4 was sufficient for restoring KSHV-induced growth transformation and tumorigenesis [211]. To determine whether activation of the mTORC1 pathway by targeting CASTORs was essential for the pro-oncogenic effects of pre-miR-K1 and -K4, we infected pre-

miR-K1 or -K4 complemented ΔmiR cells with a lentivirus expressing either CASTOR1 or CASTOR2 at different MOIs (**Figure 23A-C**). While complementation of ΔmiR mutant cells with either pre-miR-K1 or -K4 was sufficient for activating the mTORC1 pathway, transduction of either CASTOR1 or CASTOR2 suppressed the activation of mTORC1 pathway (**Figure 23A-C**). In agreement with the suppression of mTORC1 pathway, both CASTOR1 and CASTOR2 inhibited cell proliferation induced by pre-miR-K1 or -K4 (**Figure 23D**). Furthermore, transduction of either CASTOR1 or CASTOR2 induced cell cycle arrest (**Figure 23E**), and weakly increased the numbers of apoptotic and dead cells in pre-miR-K1 and -K4 complemented ΔmiR cells (**Figure 23F**). Collectively, these results demonstrate that CASTOR1/2 antagonize the oncogenic effects of pre-miR-K1 and -K4, and that targeting CASTOR1 by both miR-K1-5p and -K4-5p is essential for the pro-oncogenic functions of these two viral miRNAs, which are essential for KSHV-induced growth transformation.

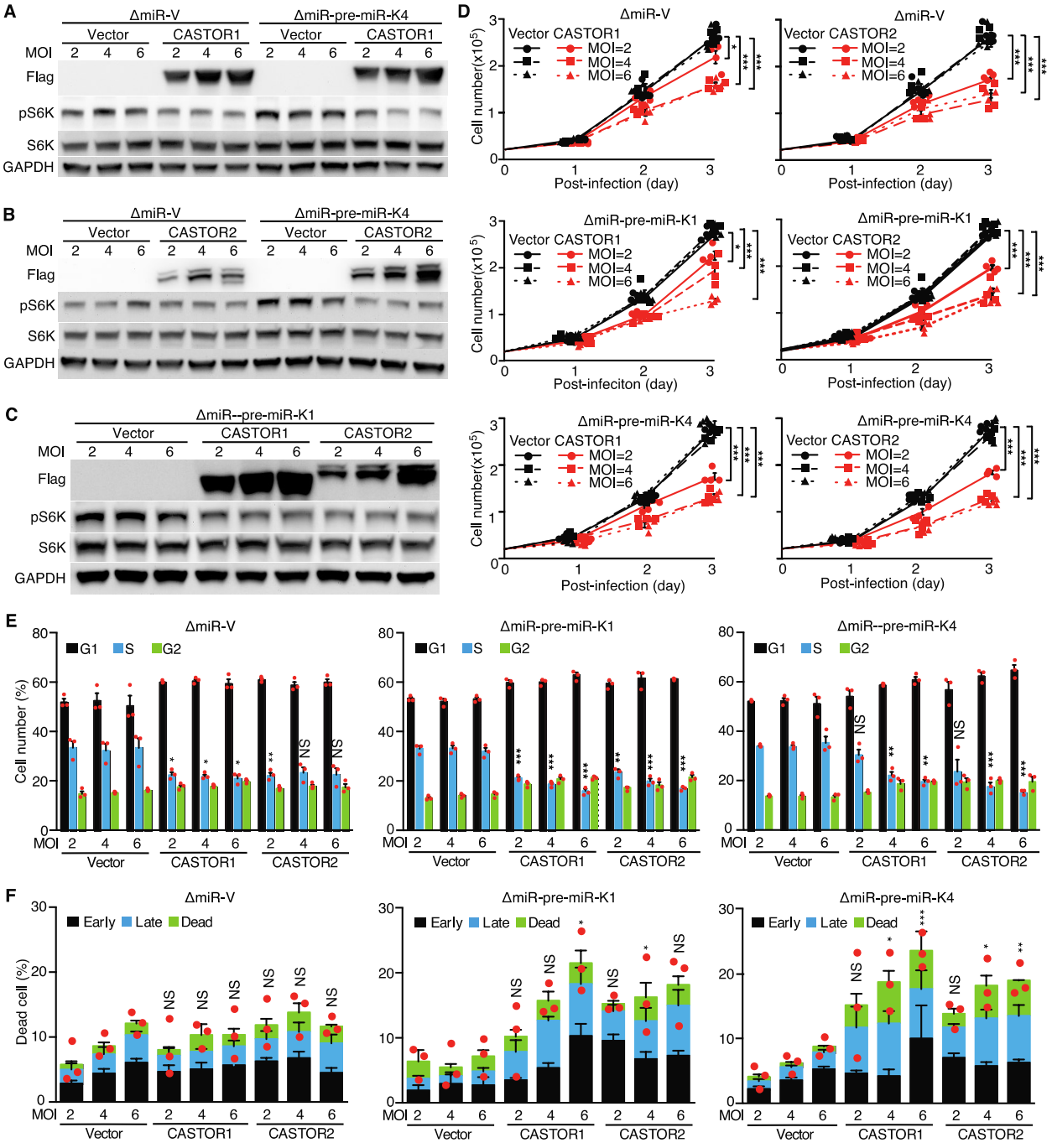

Figure 23: CASTOR1 and CASTOR2 inhibit pre-miR-K1 and -K4-induced cell proliferation.

(**A-C**) CASTOR1 and CASTOR2 inhibit pre-miR-K1 and -K4-induced mTORC1 activation. ΔmiR cells stably expressing Vector control (ΔmiR-V), or pre-miR-K4 (ΔmiR-pre-K4 in **A** and **B**) or pre-miR-K1 (ΔmiR-pre-K1 in **C**) were transduced with increasing lentiviruses of CASTOR1, CASTOR2 or Vector control at 2, 4 or 6 MOIs for 48 h, and examined for mTORC1 downstream effectors pS6K and p4EBP1 by Western-blotting. Three independent

experiments were repeated with similar results, and results from one representative experiment were shown. (**D**) CASTOR1 and CASTOR2 inhibit pre-miR-K4 and -K4-induced cell proliferation. ΔmiR cells stably expressing a Vector control (ΔmiR-V), pre-miR-K4 (ΔmiR-pre-K4) or pre-miR-K1 (ΔmiR-pre-K1) were transduced with increasing doses of lentiviruses of CASTOR1, CASTOR2 or Vector control at 2, 4 or 6 MOIs for 48 h and examined for cell proliferation, Three independent experiments were repeated with similar results, and results from one representative experiment with four biological repeats were shown as mean ± SEM. (**E** and **F**) CASTOR1 and CASTOR2 inhibit pre-miR-K4 and -K4-induced cell cycle progression and induce weak apoptosis. ΔmiR cells stably expressing Vector control (ΔmiR-V), pre-miR-K4 (ΔmiR-pre-K4) or pre-miR-K1 (ΔmiR-pre-K1) were transduced with increasing doses of lentiviruses of CASTOR1, CASTOR2 or Vector control at 2, 4 or 6 MOIs for 48 h and examined for cell cycle progression (**E**) and apoptosis (**F**). Three independent experiments were repeated with similar results, and results from one representative experiment with three biological repeats were shown as mean ± SEM. Data were analyzed by one-way ANOVA followed by Tukey post-hoc test if $P < 0.05$. Statistically significant differences are shown as NS for no significance; * for $P < 0.05$, ** for $P < 0.01$ and *** for $P < 0.001$.

3.7 mTOR inhibitors suppress KSHV pre-miR-K1 and -K4-induced cell proliferation and growth transformation

Since our results showed that CASTOR1/2 inhibited growth transformation induced by pre-miR-K1 and -K4 by suppressing mTORC1 pathway, we further investigated whether mTOR inhibitors rapamycin and Torin1 could mimic the effects of CASTORs. Both rapamycin and Torin1 efficiently inhibited the activation of mTORC1 induced by pre-miR-K1 or -K4 alone in ΔmiR cells complemented with pre-miR-K1 or -K4 as shown by the decreased pS6K and p4EBP1 levels (**Figure 24A**). Consistent with mTORC1 inhibition, rapamycin and Torin1 significantly reduced pre-miR-K1 and -K4-induced cell proliferation (**Figure 24B**). Furthermore, mTOR inhibitors induced cell cycle arrest in Vector as well as pre-miR-K1 and -K4

complemented ΔmiR cells (**Figure 24C**). Both mTOR inhibitors increased the numbers of apoptotic and dead cells in pre-miR-K1 and -K4 complemented ΔmiR cells. However, only Torin1 but not rapamycin increased the numbers of apoptotic and dead cells in Vector complemented ΔmiR cells (**Figure 24D**). Together, these results confirmed that pre-miR-K1 and -K4-induced cell proliferation could be reversed by mTORC1 inhibition.

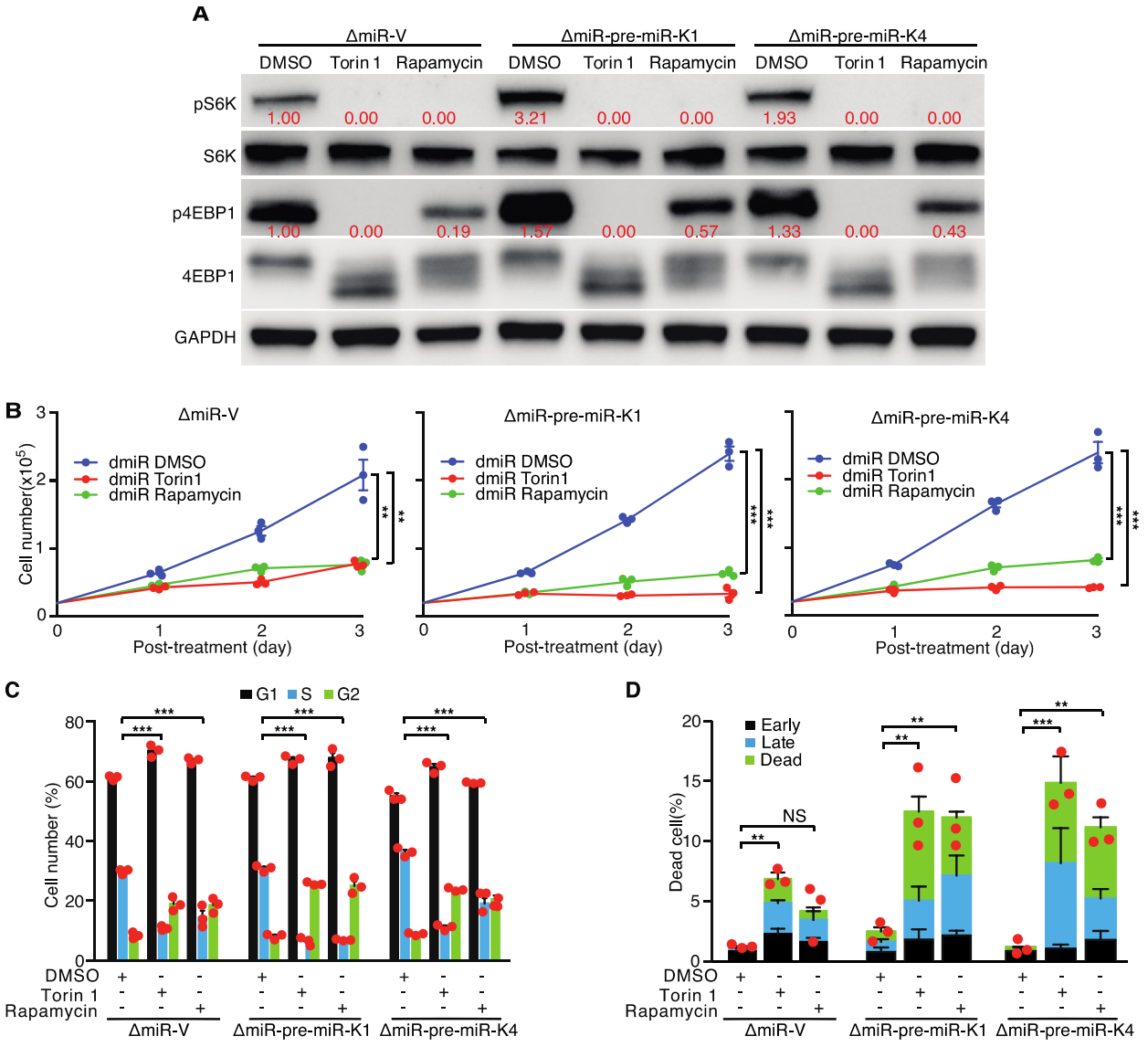

Figure 24: mTOR inhibitors suppress pre-miR-K1 and -K4-induced cell proliferation.

(**A**) mTOR inhibitors rapamycin and Torin1 inhibit mTORC1 activation in ΔmiR-V, ΔmiR-pre-miR-K1 and ΔmiR-pre-miR-K4 cells. Cells were treated with DMSO, 200 nM rapamycin or 50 nM Torin1 for 4 h and analyzed for mTORC1 activation by examining downstream effectors pS6K and p4EBP1 by Western-blotting. Results from one experiment were shown. (**B**) Rapamycin and Torin1 significantly inhibit pre-miR-K4 and -K4-induced cell proliferation. ΔmiR cells stably expressing Vector control (ΔmiR-V), pre-miR-K4 (ΔmiR-pre-K4) or pre-miR-K1 (ΔmiR-pre-K1) were treated with DMSO, 100 nM rapamycin or 50 nM Torin1, and cell numbers were counted daily. Three independent experiments were repeated with similar results, and results from one representative experiment with three biological repeats were shown as mean ± SEM. (**C** and **D**) Rapamycin and Torin1 inhibit pre-miR-K4 and

-K4-induced cell cycle progression and induce apoptosis. ΔmiR cells stably expressing Vector control (ΔmiR-V), pre-miR-K4 (ΔmiR-pre-K4) or pre-miR-K1 (ΔmiR-pre-K1) were treated with DMSO, 100 nM rapamycin or 50 nM Torin1 for 24 h, and analyzed for cell cycle progression (**C**) or apoptosis (**D**). Three independent experiments were repeated with similar results, and results from one representative experiment with three biological repeats were shown as mean ± SEM. Data were analyzed by one-way ANOVA followed by Tukey post-hoc test if P <0.05. Statistically significant differences are shown as NS for no significance; ** for $P < 0.01$ and *** for $P < 0.001$.

3.8 Discussion

While mTORC1 complex is well conserved from prokaryotes to eukaryotes, it is hyperactivated and functions as a downstream effector of many oncogenic signaling pathways such as PI3K/AKT and MAPK pathways in diverse types of human cancer [255]. Up to 95.7% of KS tumors had strong staining for pS6K indicating robust mTORC1 activation in these tumors [251]. Numerous reports have shown that mTOR inhibitor rapamycin or similar inhibitors is the most effective and tolerable therapeutic agent for KSHV-induced cancers [46, 256]. Consistent with the results of clinical studies, we have shown that mTOR inhibitors are effective in inhibiting the proliferation and cellular transformation of KSHV-transformed cells, and have minimal toxicity in normal cells (**Figure 17C** and **D**). Previou studies have identified several KSHV genes including vGPCR, vPK, ORF-K1 and ORF45 that activate mTORC1 [47, 49, 257, 258]. However, all of them are viral lytic genes, which are barely expressed during KSHV latency and KS tumors. Since most KS tumor cells are latently infected by KSHV [4], the activation of mTOR pathway is likely mediated by KSHV latent products. Hence, the underlying mechanism of mTOR pathway activation in KS and PEL remains unclear.

Numerous proteins such as Sestrin1/2, SLC39A9 and SMATOR are found to negatively regulate mTORC1 activation in response to nutrition status [259]. CASTOR1/2 are newly discovered suppressors of mTORC1 but their roles in cancer cells remain unclear [145, 146, 148]. In this study, we report, for the first time, that CASTOR1 has a suppressive role in cell proliferation and cellular transformation. We show that KSHV-encoded miR-K4-5p and possibly miR-K1-5p activate mTORC1 by directly targeting CASTOR1, which facilitates KSHV-induced cell proliferation and cellular transformation.

CASTOR1 was originally described as an arginine sensor because it regulates mTORC1 activity in response to arginine concentration [145, 146, 148]. Because tumor microenvironment is often deprived of nutrition including arginine, CASTOR1 is expected to be active in tumor cells. Hence, we speculate that tumor cells are expected to evolve specific mechanism to inhibit CASTOR1 in order to facilitate anabolic proliferation. In this study, we have observed that overexpression of either CASTOR1 or 2 dramatically inhibits the mTORC1 pathway even in replete medium, leading to decreased cell proliferation in KSHV-transformed cells. These results suggest that either the intracellular arginine concentration of KSHV-transformed cells is below the threshold required to interrupt the CASTOR1-GATOR2 interaction, or there is an alternative mechanism by which CASTOR1 regulates the mTORC1 pathway. In fact, high level of CASTOR1 could overcome the suppressive effect of arginine on CASTOR1 [145]. These findings demonstrate CASTOR proteins as negative regulators of KSHV-induced proliferation and growth transformation. Whether CASTOR1 is a tumor suppressor in other types of cancer requires further investigations.

KSHV miRNAs are highly expressed during latency and in KS tumors, implicating their essential roles in the development of KS [252, 253]. Indeed, KSHV miRNAs target numerous

growth and survival pathways to promote cell growth and cellular transformation [14]. We have previously shown that KSHV pre-miR-K1, -K4 and -K11 have essential roles in KSHV-induced cellular transformation and tumorigenesis [211]. miR-K1-5p and miR-K11, an orthologue of cellular oncogenic miR-155, enhance cell survival and viral latency by directly targeting IκBα to activate the NF-κB pathway, and repressing Fos and BACH1, respectively [211, 217, 260]. However, the role of miR-K4-5p in KSHV-induced transformation remains unknown. Our results showed that miR-K4-5p and possibly -K1-5p directly target CASTOR1 to inhibit its expression, leading to mTORC1 activation, and KSHV-induced cell proliferation and cellular transformation (**Figure 16**). These results reveal a novel mechanism by which KSHV hijacks the mTORC1 pathway to promote tumorigenesis, and hence provide the scientific basis for using mTOR inhibitors for the treatment of KS patients.

We have shown that overexpression of CASTORs and treatment with mTOR inhibitors induced cell cycle arrest and, in some cases, weak apoptosis in KMM cells, and pre-miR-K1 and -K4 complemented ΔmiR cells, indicating that CASTORs and mTORC1 pathway regulate both cell proliferation and survival in these cells. While overexpression of CASTORs and treatment with mTOR inhibitors also induced cell cycle arrest in MM cells and Vector complemented ΔmiR cells, there was minimal effect on cell survival in these cells. These results indicate that KSHV miRNAs target other oncogenic and survival pathways in addition to the mTORC1 pathway, which are in agreement with the reported functions of KSHV miRNAs [14].

4.0 RNF167 activates mTORC1 and promotes tumorigenesis by targeting CASTOR1 for ubiquitination and degradation

Preface:

All figures and text in this chapter are unpublished data.

mTORC1, frequently dysregulated in human cancer, is a central controller of cell proliferation, and primarily responds to growth factors and nutrients [52, 72]. Arginine mediated-mTORC1 activation depends on arginine binding to CASTOR1 to release the GATOR2 complex, the core positive regulator of mTORC1 [118, 145-147, 261]. However, high level of CASTOR1 protein overrides arginine-mediated mTORC1 activation [145]. Furthermore, *de novo* arginine synthesis pathway is silenced in most types of cancer rendering cancer cells addicted to extracellular arginine, which is often restricted in tumor microenvironment [238, 262, 263]. Hence, an alternative mechanism regulating CASTOR1 expression exists for controlling cell proliferation and mTORC1 activation in cancer. By investigating the mechanism of KSHV induction of cellular transformation, we have previously reported that viral miRNAs target CASTOR1 to activate mTORC1 [151]. Here we report a novel cellular mechanism regulating CASTOR1 expression. Specifically, we identify E3 ubiquitin ligase RNF167 that promotes K29-linked polyubiquitination and degradation of CASTOR1. Additionally, AKT binds to and phosphorylates CASTOR1 at S14 to enhance its ubiquitination and degradation by significantly increasing RNF167 binding to CASTOR1. Significantly, RNF167-mediated CASTOR1 degradation activates mTORC1 independent of arginine and promotes breast cancer progression. These results illustrate RNF167 as a key regulator of mTORC1, which could serve as a novel therapeutic target in diseases associated with dysregulated mTORC1 activation (**Figure 25**).

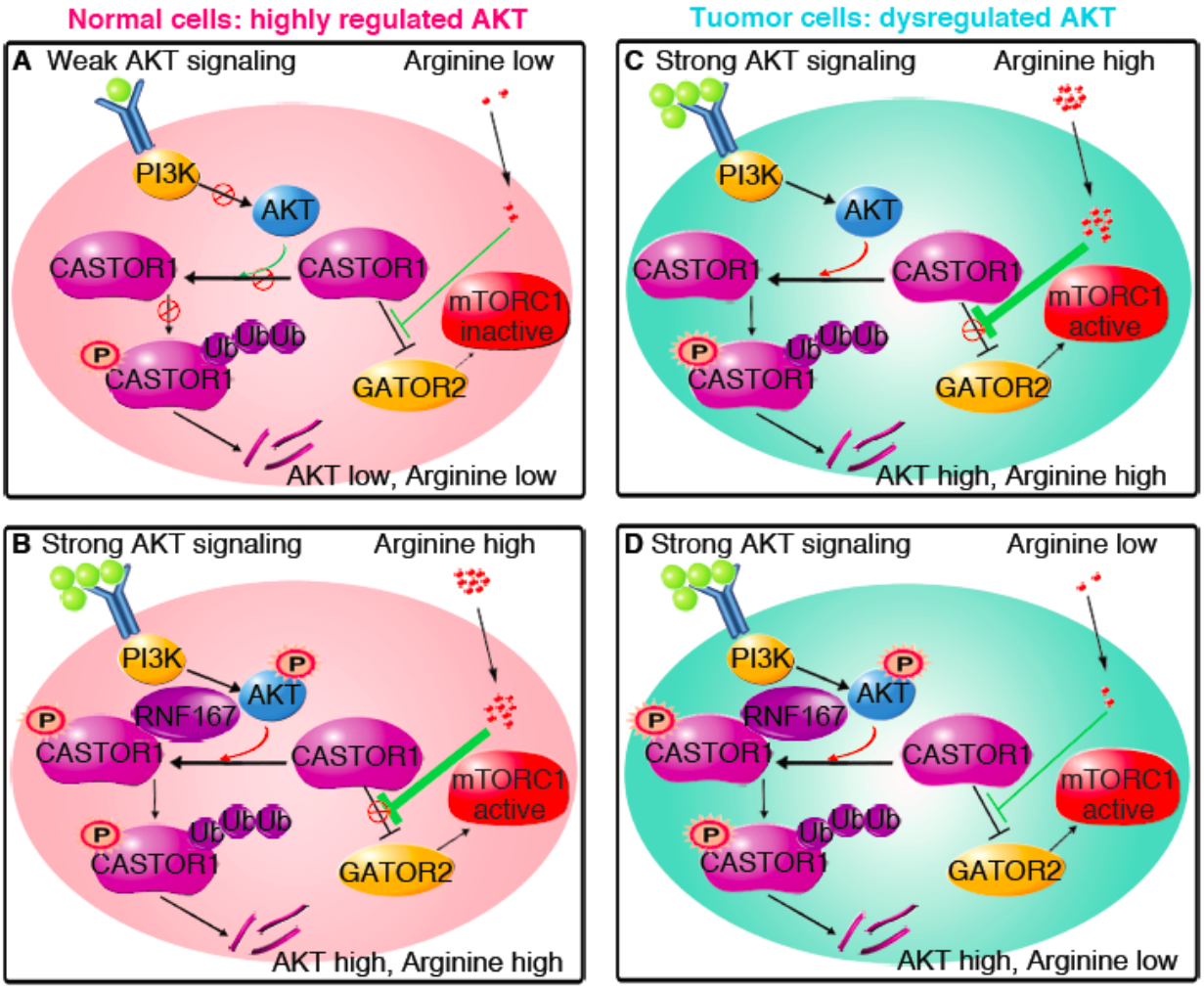

Figure 25: Proposed model of AKT-mediated phosphorylation and RNF167-dependent ubiquitination of CASTOR1 and mTORC1 activation in normal and cancer cells.

(**A** and **B**) mTORC1 activity is highly regulated in response to growth factors and nutrients in normal cells. In quiescent or slow growing cells, cells are exposed to low levels of nutrients and growth factors. AKT is not or only weakly activated, and CASTOR1 is dephosphorylated and stabilized to sequester GATOR2 complex, leading to mTORC1 inactivation and slow growth or arrest of the cells (**A**). In fast growing cells, cells are exposed to high levels of growth factors and nutrients. On one hand, AKT is highly activated, which induces CASTOR1 phosphorylation followed by RNF167-mediated CASTOR1 degradation. On the other hand, high levels of growth factors also stimulate uptake of nutrients including arginine, which interrupts CASTOR1-GATOR2 interaction leading to mTORC1 activation and anabolic growth of the cells (**B**). (**C** and **D**) mTORC1 activity is dysregulated and constitutively active as a result of dysregulated AKT signaling in cancer cells. Dysregulated AKT signaling as a

result of mutation in AKT or its upstream pathways of growth factors could increase cell uptake of nutrients including arginine and strong AKT activation. CASTOR1 function is suppressed by both AKT and arginine. Specifically, AKT-mediated CASTOR1 phosphorylation results in its increased binding to RNF167 and hence its degradation while arginine dissociates CASTOR1 from GATOR2 complex, a positive regulator of mTORC1, leading to robust mTORC1 activation and anabolic growth of cancer cells (**C**). In fast growing solid tumors, cancer cells are often deprived of nutrients including arginine, which fail to inhibit CASTOR1's function. However, constitutive AKT activation would continue to induce CASTOR1 destruction leading to mTORC1 activation and anabolic growth of cancer cells (**D**).

4.1 RNF167 mediates K29-linked polyubiquitination and degradation of CASTOR1 in response to growth factors

To reveal which environmental cue activates mTORC1 by modulating the expression of CASTOR1, we deprived cells of either fetal bovine serum (FBS) or arginine. FBS deprivation or AKT inhibitor MK2206 increased CASTOR1 expression at a protein but not mRNA level, resulting in decreased mTORC1 activity as shown by the reduced phosphorylation level of its downstream target 4EBP1 (**Figure 26A** and **Supplementary Figure 7A**). In contrast, chronic arginine deprivation decreased mTORC1 activity as previously reported but also enhanced AKT activation as a result of the feedback effect of mTORC1 inhibition [264, 265], leading to decreased CASTOR1 protein level (**Figure 26A**). Consistent with the observed negative correlation of CASTOR1 protein level with FBS, FBS deprivation reduced CASTOR1 ubiquitination, while arginine deprivation had no noticeable effect (**Figure 26B**). FBS re-stimulation after deprivation reversed the effect, restoring CASTOR1 ubiquitination, which correlated with the reduced CASTOR1 protein level (**Supplementary Figure 7B**). Together,

these results indicated that arginine did not affect CASTOR1 protein level but FBS targeted CASTOR1 for ubiquitination and proteasome-dependent degradation.

Covalent conjugation of ubiquitin is a key step in proteasome-mediated degradation of target proteins [266]. CASTOR1 was only labelled by wild type ubiquitin or K29 ubiquitin (a ubiquitin mutant containing only the K29 lysine) but not K48 and K63 ubiquitin (**Figure 26C**, **Supplementary Figure 7C** and **D**). To identify the E3 ubiquitin ligase(s) that might regulate CASTOR1 polyubiquitination and degradation, we screened a panel of E3 ubiquitin ligases implicated in mTORC1 regulation [120]. Although ectopic expression of numerous E3 ubiquitin ligases decreased CASTOR1 protein level (**Supplementary Figure 7E**), only RNF167 increased CASTOR1 ubiquitination (**Figure 26D** and **Supplementary Figure 7F**). Consistently, knockdown of RNF167 decreased CASTOR1 ubiquitination and increased CASTOR1 protein level (**Figure 26E** and **F**) while overexpression of RNF167 decreased CASTOR1 protein level in a dose-dependent manner (**Figure 26G**). Neither overexpression nor knockdown of RNF167 had notable effect on CASTOR1 mRNA level (**Supplementary Figure 7G** and **H**). Additionally, treatment with MG132 partially rescued RNF167-mediated downregulation of CASTOR1 protein (**Supplementary Figure 7I**). These results support model that RNF167 targets CASTOR1 for ubiquitination and proteasome-dependent degradation (**Figure 26H**).

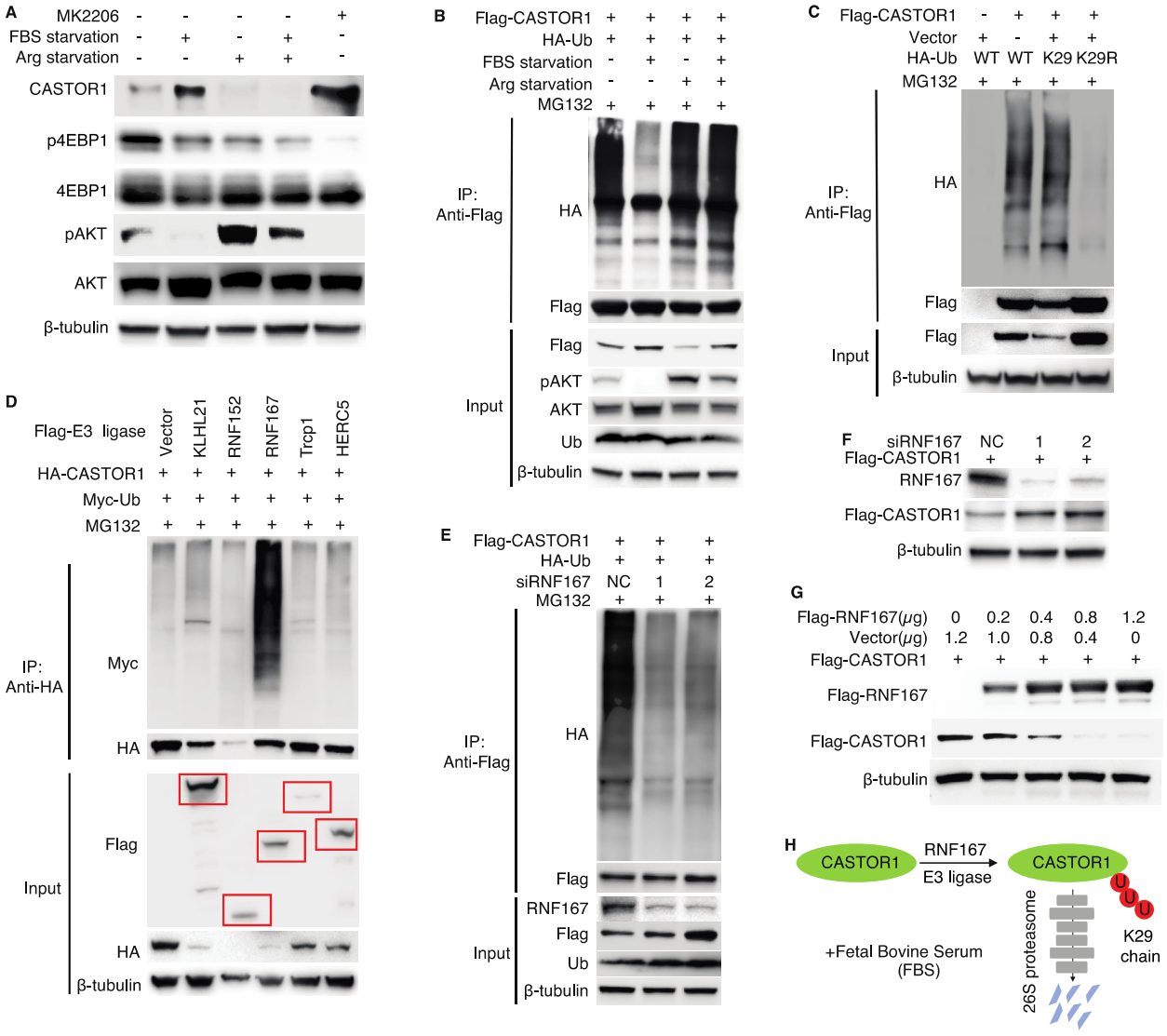

Figure 26: RNF167 mediates K29-linked polyubiquitination and degradation of CASTOR1 in response to growth factors.

(A) CASTOR1 level is regulated by fetal bovine serum (FBS). (**B**) FBS, but not arginine, stimulates CASTOR1 ubiquitination. **(C)** CASTOR1 is labelled by K29-linked polyubiquitination. (**D** and **E**) Ectopic expression of RNF167 increases (**D**) whereas knock down of RNF167 decreases (**E**) CASTOR1 ubiquitination. (**F** and **G**) RNF167 overexpression increases (**F**) whereas RNF167 knockdown decreases (**G**) CASTOR1 degradation. (**H**) Schematic depiction of the K29-marked polyubiquitination and degradation of CASTRO1 by RNF167 in response to FBS.

4.2 AKT1 phosphorylation of CASTOR1 promotes RNF167 ubiquitination and degradation of CASTOR1

By providing growth factors, FBS activates numerous kinases, which could be the reason that it regulates CASTOR1 level. Since the effect of AKT inhibitor MK2206 on CASTOR protein level was the same as FBS starvation, we used kinase prediction algorithms and identified an AKT phosphorylation site on CASTOR1 containing a consensus AKT1 phosphorylation motif R-V-R-V-L-S14. Proteomic analysis indeed identified CASTOR1 phosphorylation at S14 [267, 268], suggesting AKT1 might directly phosphorylate CASTOR1. Indeed, CASTOR1 interacted with both ectopically expressed AKT1 and endogenous AKT, and preferentially bound to AKT1 kinase domain (**Supplementary Figure 8A-F**). An antibody specific to the AKT phosphorylation consensus motif (R-X-R-X-X-pS/T) detected strong signal in the wild-type (WT) Flag-CASTOR1 protein expressed in 293T cells, confirming that CASTOR1 is phosphorylated at physiological condition (**Figure 27A**). Alanine substitution at S14 (Flag-CASTOR1 S14A) and AKT inhibitor MK2206 significantly reduced the motif-specific phosphorylation (**Figure 27A** and **B**), confirming AKT-mediated phosphorylation of CASTOR1 at S14. Alignment of CASTOR1 protein sequences from human with other vertebrates revealed that the CASTOR1 R-X-R-X-X-S14 motif was highly conserved (**Supplementary Figure 8G**). As expected, AKT interacted with and phosphorylated CASTOR1 at the AKT phosphorylation motif in rat (MM and KMM) cells [209] (**Supplementary Figure 8H**).

We performed *in vitro* kinase assay to confirm AKT direct phosphorylation of CASTOR1. Purified glutathione S-transferase (GST)-AKT1 efficiently phosphorylated purified GST-tagged CASTOR1 (GST-CASTOR1) recombinant protein only in the presence of ATP, which was

abolished by AKT inhibitor MK2206 (**Figure 27C, Supplementary Figure 8G** and **H**). Interestingly, Flag-CASTOR1 S14D, a mimic of constitutively phosphorylated mutant, had a much higher affinity to AKT1 than Flag-CASTOR1 WT and Flag-CASTOR1 S14A (**Supplementary Figure 8J-M**), suggesting possible CASTOR1 conformational changes following phosphorylation. Collectively, these results demonstrated that AKT directly bound to and phosphorylated CASTOR1.

As phosphorylation is intimately linked to protein ubiquitination and degradation [269], we examined the consequence of AKT1-mediated CASTOR1 phosphorylation and observed that myristoylated constitutively active AKT1 (myr-HA-AKT1) decreased CASTOR1 protein level in a dose-dependent manner (**Figure 27D**). Neither the kinase-dead AKT1 mutant (K179M) nor the AKT1 PH domain had any effects while overexpression of the AKT1 kinase domain alone was sufficient to reduce the CASTOR1 protein level albeit to a lesser degree than the WT AKT1 [270] (**Supplementary Figure 9A** and **B**). Hence, AKT-mediated CASTOR1 downregulation required its kinase activity. Neither the WT AKT1, AKT1 PH and kinase domains nor the kinase-dead mutant affected CASTOR1 mRNA level (**Supplementary Figure 9C-E**). Consistently, AKT1 silencing was sufficient to inhibit pan AKT activity, and increased CASTOR1 protein level (**Figure 27E**) but had no effect on the CASTOR1 mRNA expression (**Supplementary Figure 9F**).

To test if AKT1 regulated CASTOR1 stability, we first co-transfected cells with both Flag-CASTOR1 WT and myr-HA-AKT1, then treated them with *de novo* protein synthesis inhibitor cycloheximide (CHX), and observed faster degradation of CASTOR1 protein in cells expressing myr-HA-AKT1 than the vector control (**Supplementary Figure 9G**). Treatment with proteasome inhibitor MG132 increased the accumulation of CASTOR1 protein in cells

expressing myr-HA-AKT1 but only had a marginal effect on cells expressing the vector control (**Supplementary Figure 9H**). Furthermore, overexpression of myr-HA-AKT1 but not AKT1 mutant (K179M) enhanced whereas knockdown of AKT1 reduced CASTOR1 ubiquitination (**Figure 27F** and **G**). Together, these results indicated that AKT1 targeted CASTOR1 for ubiquitination and proteasome-dependent degradation.

We constructed 293T cells stably expressing Flag-CASTOR1 WT, S14A or S14D, and observed that cells expressing Flag-CASTOR1 S14D had lower protein level than those expressing CASTOR1 WT and S14A despite there was no significant change at the mRNA level (**Supplementary Figure 10A**). Indeed, treatment with CHX reduced while treatment with MG132 increased S14D protein level but had minimal effects on WT and S14A (**Supplementary Figure 10B-D**). Accordingly, the level of ubiquitination was significantly increased for S14D protein compared to those of WT and S14A proteins (**Figure 27H** and **Supplementary Figure 10E**). These results demonstrated that AKT1 phosphorylation of CASTOR1 at S14 resulted in its ubiquitination and degradation.

To clarify the link between AKT1-mediated phosphorylation and RNF167-mediated ubiquitination of CASTOR1, we examined the effect of CASTOR1 phosphorylation on CASTOR1-RNF167 interaction. CASTOR1 S14D had a much stronger affinity to RNF167 and a higher level of ubiquitination than WT or S14A had (**Figure 27H-J** and **Supplementary Figure 10E**), indicating that AKT-mediated phosphorylation promoted CASTOR1 degradation by specifically enhancing the CASTOR1-RNF167 interaction. Collectively, these results support a model that AKT1 phosphorylation of CASTOR1 at S14 enhances RNF167-targeting ubiquitination and degradation of CASTOR1 protein (**Figure 27K**).

Examination of CASTOR1 with the Ubisite and UbPreb program identified numerous lysine residues as putative ubiquitination sites including K61, K96 and K213 [271] (**Supplementary Figure 11A**). Whereas mutation of one or two of these sites to arginine in the CASTOR1 S14D failed to stabilize the protein, mutation of all three sites to arginine (3KR) significantly blocked CASTOR1 ubiquitination and degradation (**Supplementary Figure 11B-D**). Importantly, while all single and double lysine mutants of CASTOR1 S14D remained sensitive to RNF167-mediated downregulation, the 3KR mutant was resistant (**Supplementary Figure 11E**), indicating that RNF167 catalyzed CASTOR1 ubiquitination at multiple lysines.

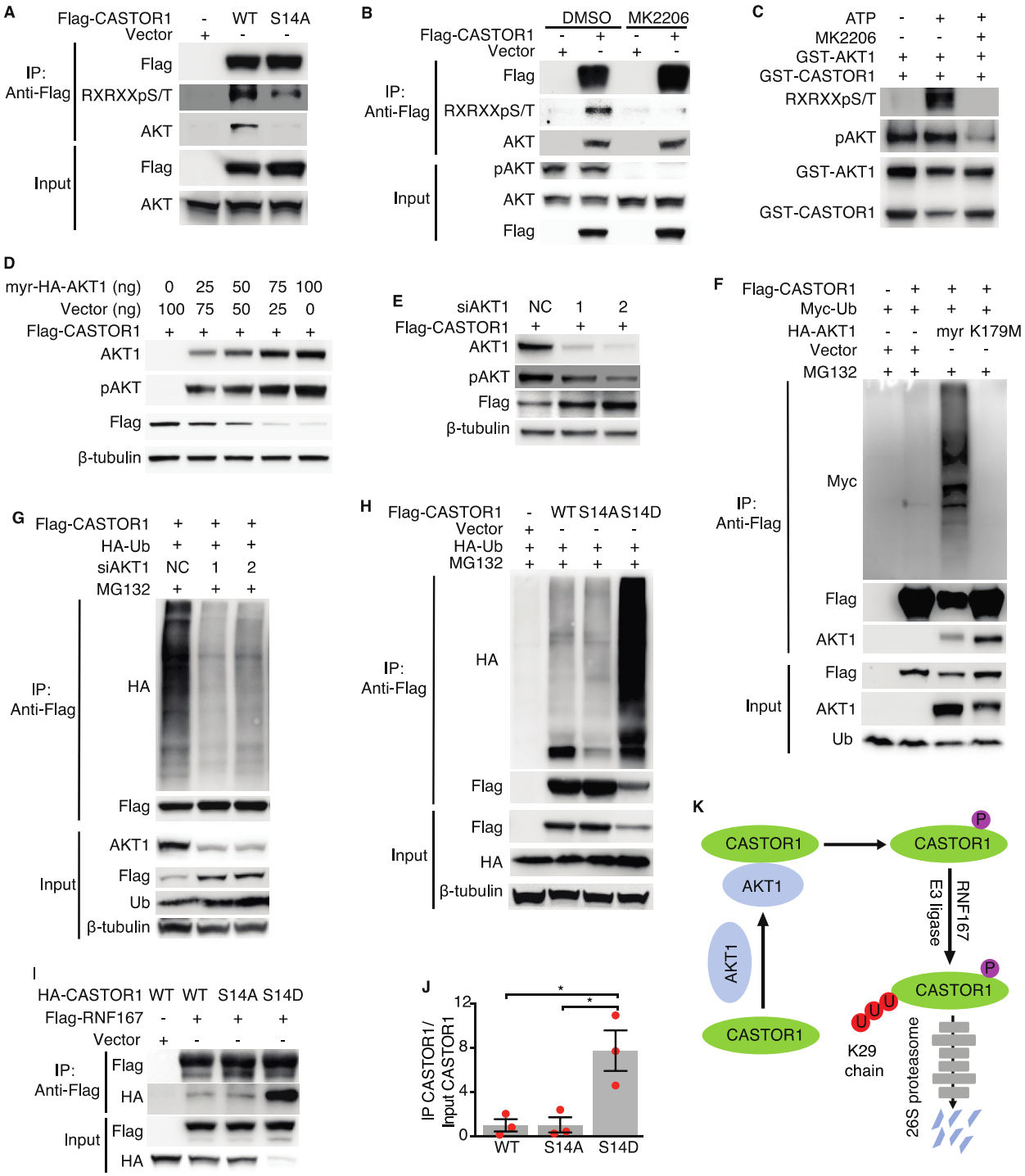

Figure 27: AKT1 phosphorylation of CASTOR1 promotes RNF167 ubiquitination and degradation of CASTOR1.

(**A**) CASTOR1 is physiologically phosphorylated at S14, which is abolished by alanine substitution of S14. (**B**) AKT inhibition decreases CASTOR1 phosphorylation at S14 *in vivo*. (**C**) AKT1 directly phosphorylates CASTOR1

in vitro. (**D** and **E**) AKT overexpression increases (**D**) and AKT1 silence decreases (**E**) CASTOR1 degradation. (**F** and **G**) AKT1 knockdown decreases (**F**) and AKT1 overexpression (**G**) increases CASTOR1 ubiquitination. (**H**) CASTOR1 S14D has increased ubiquitination level compared to WT and S14A**.** (**I** and **J**) The phosphorylation of CASTOR1 at S14 increases its affinity to RNF167 (**I**) and quantifications of results from three independent experiments were presented in (**J**), **P*<0.05, one-way ANOVA followed by Tukey post-hoc test (**J**). (**K**) A scheme illustrating that the K29-marked polyubiquitination and degradation of CASTOR1 by RNF167 is enhanced by AKT1.

4.3 AKT phosphorylation and RNF167 ubiquitination of CASTOR1 release arginine-deficiency mediate mTORC1 inactivation by arginine

Next, we assessed the downstream effects of AKT1-mediated phosphorylation and RNF167-targeting degradation of CASTOR1 protein. Consistent with the previous report [145], a high level of CASTOR1 protein rendered cells insensitive to arginine-mediated activation of mTORC1 (**Figure 28A**). Binding of CASTOR1 to MIOS, the core component of GATOR2 complex, was positively correlated to CASTOR1 protein level, indicating that mTORC1 activation was regulated by CASTOR1 protein level in addition to arginine (**Figure 28B**). As expected, ectopic expression of RNF167 degraded CASTOR1 and activated mTORC1 regardless the presence or absence of arginine (**Figure 28C**). In fact, cells with overexpression of RNF167 became insensitive to arginine-mediated mTORC1 activation (**Figure 28C**), affirming the essential role of RNF167 and regulation of CASTOR1 protein level in the control of mTORC1 activation. As expected, myr-HA-AKT1 but not its kinase-dead mutant K179M decreased CASTOR1 protein level and hence its binding to MIOS, resulting in increased mTORC1 activation (**Figure 28D**).

Since CASTOR1 S14D is constitutively phosphorylated and hence is prone to degradation whereas CASTOR1 S14A is non-phosphorylable and resistant to degradation, we utilized these constructs to assess the effect on mTORC1 activation. Consistently, the protein level was lower, which led to a lower pull down yield in co-immunoprecipitation, for S14D than WT and S14A (**Figure 28E** and **F**). Furthermore, S14D binding to MIOS was significantly weaker than that of WT or S14A even after taking consideration of its lower protein level and pull down efficiency in co-immunoprecipitation (**Figure 28E** and **F**). Hence, a lower protein level and a lower affinity to MIOS might lead to a more robust mTORC1 activation for S14D than WT and S14A (**Figure 28E**). These differences persisted even with arginine concentration reaching 50 μM indicating that the combined effects of AKT1 phosphorylation and RNF167-targeting degradation had a stronger role than arginine inhibition of CASTOR1 in regulating mTORC1 activation, particularly at condition with low concentrations of arginine, which is common in tumor microenvironment (**Figure 28G**).

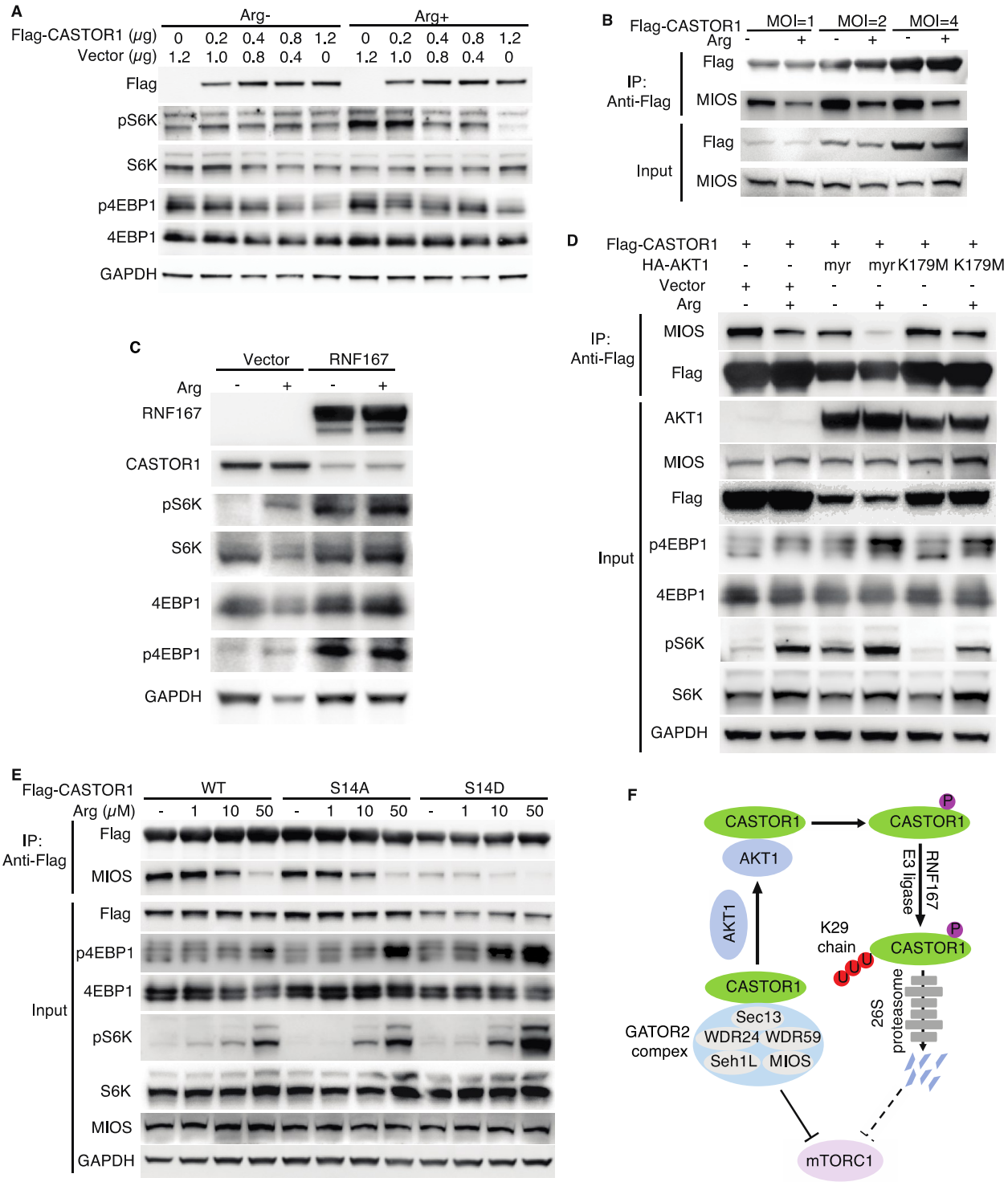

Figure 28: AKT phosphorylation and RNF167 ubiquitination of CASTOR1 release arginine-deficiency mediate mTORC1 inactivation by arginine.

(**A**) A higher CASTOR1 protein level overrides arginine-mediated mTORC1 activation. (B) CASTOR1 binds to MIOS in a dose-dependent manner. (**C**) RNF167-mediated CASTOR1 degradation activates mTORC1. (D) AKT1-

mediated CASTOR1 degradation decreases its binding to MIOS and activates mTORC1. (**E**) CASTOR1 S14D had a weaker binding to MIOS, hence a less inhibitory effect on mTORC1 than WT and S14A had. (**F**) A scheme depicting that AKT phosphorylation and RNF167 ubiquitination of CASTOR1 reverse arginine-deficiency mediated mTORC1 inactivation by CASTOR1.

4.4 RNF167 ubiquitination and AKT1 phosphorylation of CASTOR1 promotes breast cancer progression

We examined the prognostic value of CASTOR1 mRNA expression in cancer using the TCGA database. Consistent with its CASTOR1 inhibitory function and tumor suppressive role [151, 272], a lower CASTOR1 expression level was correlated with overall poor survival in pan-cancer analyses (**Supplementary Figure 12A** and **B**). At least 10 types of cancer showed a strong negative correlation (**Supplementary Figure 12C**), of these, high RNF167 expression predicted a poor prognosis in 5 of them (**Supplementary Figure 12D**).

Breast cancer represents 12% of cancer diagnosed and is a major life threat for women in the United States [273]. We found a high RNF167 expression level in breast tumors compared to its adjacent normal tissues [274] (**Supplementary Figure 12E**). Furthermore, a lower CASTOR1 expression level (**Supplementary Figure 12F** and **G**) and a higher RNF167 expression level (**Supplementary Figure 12H** and **I**) were correlated with poor survival in ER+ and HER2+ breast cancer, respectively. In two pairs of ER+ and HER2+ breast cancer cell lines, we found an inverse correlation of activated AKT level with CASTOR1 protein level (**Supplementary Figure 13A**). AKT interacted with CASTOR1 in MCF cells (**Supplementary Figure 13B**). Overexpression of myr-HA-AKT1 but not the AKT kinase dead mutant K179M in MCF7 and T47D cells resulted in a dose-dependent reduction in CASTOR1 protein level

(**Supplementary Figure 13C** and **D**). Consistently, silencing of AKT1 and AKT inhibitor MK2206 enhanced exogenous and endogenous CASTOR1 protein levels in these cells, respectively (**Supplementary Figure 13E** and **F**). In contrast, although chronic arginine deprivation activated AKT and hence decreased CASTOR1 protein level, mimicking the observations in 293T cells, FBS deprivation failed to inactivate AKT in MCF7 and T47D cells and thus had no impact on CASTOR1 protein level as demonstrated by the comparable phosphorylated AKT and CASTOR1 level before and after serum starvation (**Supplementary Figure 13G**). In fact, both MCF7 and T47D cells contain spontaneous mutation of AKT upstream genes such as PIK3CA [275], resulting in constitutive AKT activation, which is resistant to depletion of exogenous growth factors.

Consistent with 293T cells, we found that the affinity to exogenous and endogenous RNF167 was stronger for CASTOR1 S14D than WT and S14A in ER+ MCF7 and T47D cells, respectively (**Supplementary Figure 14A-C**). Likewise, RNF167 overexpression decreased whereas RNF167 knockdown increased CASTOR1 protein level in MCF7 cells (**Supplementary Figure 14D** and **E**). Together these results indicated that, similar to 293T cells, the CASTOR1 protein level was also regulated by AKT1 and RNF167 in breast cancer cells.

To examine the importance of AKT1-mediated phosphorylation and RNF167-mediated degradation of CASTOR1 in breast cancer cells, we overexpressed Flag-CASTOR1 WT, S14A and S14D in HCC1569, MCF7 and T47D cells. CASTOR1 S14D had much lower expression level than WT and S14A had in all three cell lines examined (**Supplementary Figure 15A-C**), indicating that S14D also had faster turnover in breast cancer cells. Importantly, ectopic expression of both CASTOR1 WT and S14A significantly inhibited mTORC1 whereas CASTOR1 S14D showed a much less inhibitory effect, confirming the fine-tuning of mTORC1

signaling pathway through CASTOR1 phosphorylation and degradation in breast cancer cells (**Supplementary Figure 15A-C**). Consistent with the mTORC1 activity, the proliferation and colony formation in softagar of breast cancer cells were significantly decreased by CASTOR1 WT and S14A, whereas CASTOR1 S14D had a less effect (**Figure 29A**, **B** and **Supplementary Figure 15E-G**). In T47D cells, which had a high endogenous level of CASTOR1 protein, silencing of CASTOR1 activated mTORC1 and significantly increased the colony formation efficiencies in softagar (**Figure 29C** and **Supplementary Figure 15D**). Moreover, overexpression of CASTOR1 WT and S14A had a stronger effect than S14D had in inhibiting cell cycle progression in MCF7 and HCC1569 cells (**Supplementary Figure 15H-I**). None of the CASTOR1 construct had significant effect on apoptosis (**Supplementary Figure 15J-K**), which recapitulated the characteristic phenotype of mTORC1 inhibition.

We then subcutaneously engrafted MCF7 cells that were transduced with a vector control, Flag-tagged CASTOR1 WT, S14A or S14D into both flanks of nude mice. Ectopic expression of CASTOR1 WT and S14A significantly inhibited tumor growth *in vivo*, whereas S14D had a relatively less effect (**Figure 29D-F** and **Supplementary Figure 16A**). Additionally, mice injected with cells expressing CASTOR1 WT and S14A had higher survival rates than those of expressing vector control and S14D (**Figure 29G**). Consistently, silencing of CASTOR1 in T47D cells promoted tumor growth i*n vivo* and shortened the overall survival compared to a scrambled control group (**Figure 29H-I** and **Supplementary Figure 16B**). Taken together, these results revealed that AKT-mediated phosphorylation and RNF167-dependent ubiquitination led to decreased CASTOR1 protein level in breast cancer cells, resulting in enhanced mTORC1 activation, cell proliferation, and tumorigenesis.

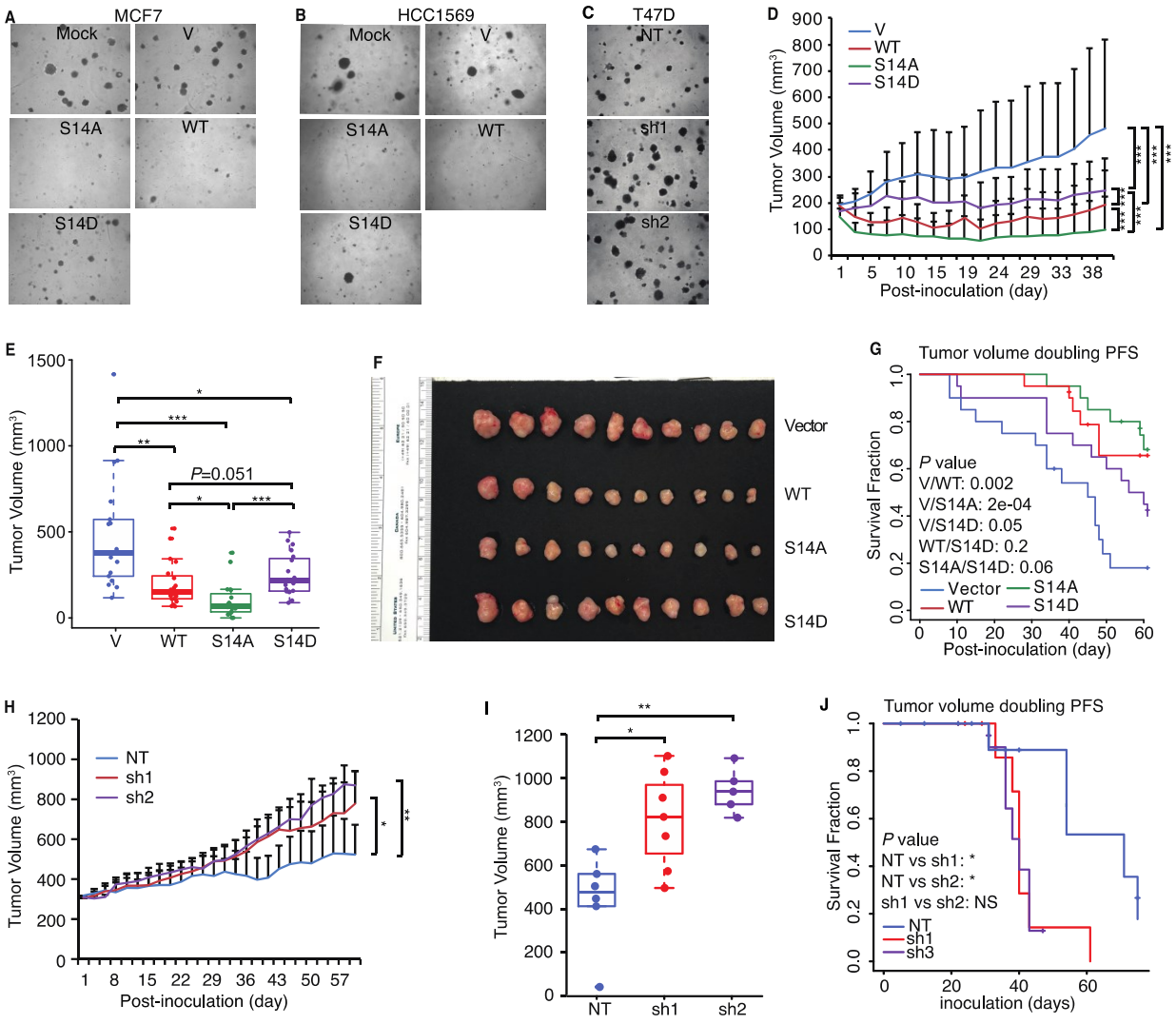

Figure 29: RNF167 ubiquitination and AKT1 phosphorylation of CASTOR1 promotes breast cancer progression.

(**A** and **B**) CASTOR1 WT and S14A had more stronger effects than S14D in suppressing colony formation of ER+ (**A**) and HER2+ (**B**) breast cancer cells in softagar. **c,** CASTOR1 silencing enhanced colony formation in softagar of T47D cells. (**D-G**) CASTOR1 WT and S14A showed more dramatic suppression in breast tumor growth in nude mice and had more extended animal survival rate than S14D did in a breast cancer xenograft model; the tumor volume at the indicated time point post-inoculation was measured (**D**). the tumor volume of the last time point (**E**), the actual tumors (**F**) and the survival rate (**G**) were shown. (**H-J**) CASTOR1 knockdown promoted tumor growth and shortened animal survival rate. The tumor volume at the indicated time point post-inoculation was measured (**H**). The tumor volume of the last time point (**I**), and the survival rate (**J**) were shown. (**D**, **E, H and I**) were presented as

mean ± SEM and analyzed by Student's t test. (**G** and **J**) was analyzed by Log-rank test. *P<0.05, **P<0.01 and ***P< 0.001 and NS means "not significant".

4.5 Discussion

In this study, we have shown that AKT directly interacts with and phosphorylates CASTOR1, which leads to ubiquitination and proteasome-dependent degradation of CASTOR1 and activation of the mTORC1. We have identified an AKT phosphorylation site in CASTOR1, which is present in other species analyzed, indicating its conserved function. Mutation of this site into a constitutively phosphorylated mutant (S14D) increases its interaction with AKT, suggesting a possible conformation change. In addition, we have identified a RING-type E3 ligase RNF167 that mediates CASTOR1 ubiquitination, and that multiple CASTOR1 lysines, *i.e.*, K61, K96 and K213, are marked by K29-linked polyubiquitination. Interestingly, the constitutively phosphorylated S14D mutant has a significantly higher affinity to RNF167, explaining why AKT-mediated CASTOR1 phosphorylation leads to its faster ubiquitination and degradation. Importantly, by manipulating extracellular nutrients (FBS and arginine), we have shown that AKT-mediated CASTOR1 degradation and activation of the mTORC1 is functional in physiological conditions.

mTORC1 is critical for maintaining cellular homeostasis in response to growth factors, stresses, energy status and amino acids [54]. By coordinating the cellular metabolism and the environmental nutrient signals, mTORC1 serves as a master regulator of cell growth and proliferation [54]. Thus, it is not surprising that mTORC1 activation is tightly regulated occurring in a cascade fashion initiated by the amino acids mediated mTORC1 translocation to

lysosomes followed by the AKT-induced Rheb phosphorylation of mTOR [72]. So far, several amino acid sensors including Sestrin2, SLC39A9, TM4SF5 and SMATOR are known to modulate mTORC1 activity in response to amino acid status [133, 138, 142, 153]. CASTOR1 is a newly discovered arginine sensor, which interplays with arginine to modulate mTORC1 signaling pathway [145, 146]. Hence, our findings reveal a crosstalk between two previously independent signaling pathways, *i.e.*, the growth factor-dependent AKT and arginine-regulated CASTOR1 signaling pathways, which fine-tunes mTORC1 activation. This regulatory mechanism is likely essential for controlling the homeostasis and proliferation of normal cells. In cells that are quiescent or at a low proliferating rate, a lower level of AKT activation as a result of minimal stimulation by growth factors would lead to a higher level of CASTOR1, a reduced level of mTORC1 activation, and a lower level of uptake of nutrients including arginine, which would have a minimal effect on CASTOR1 function and mTORC1 activation (**Figure 25A**). In hyperproliferating cells such as stimulated immune cells, a higher level of AKT activation as a result of stimulation by growth factors would lead to a lower level of CASTOR1, an increased level of mTORC1 activation, and a higher level of uptake of nutrients including arginine, which would also inhibit CASTOR1 function resulting in maximal mTORC1 activation (**Figure 25B**).

The mTORC1 pathway is often dysregulated in cancer, which is critical for the progression of cancer [120, 152, 276, 277]. While CASTOR1's mTORC1 inhibitory function is negated by arginine, a high level of CASTOR1 protein evades the effect of arginine and prevents arginine-mediated mTORC1 activation [145] (**Figure 28A**). Furthermore, cancer cells are often exposed to low nutrients including a low level of arginine [262]. Hence, it is expected that cancer cells would have evolved specific mechanisms to counter CASTOR1's inhibitory effect on mTORC1 in nutrients-deficient tumor microenvironment. In KSHV-transformed cells, KSHV-

encoded miRNAs downregulate CASTOR1 to activate mTORC1 [276]. In other types of cancer, the AKT pathway is persistently activated in tumor cells as a result of mutation of AKT itself or its upstream pathways of growth factors [278], which would phosphorylate CASTOR1 leading to its ubiquitination and degradation, and activation of mTORC1 regardless of the presence of high or low level of arginine (**Figure 25C and D**). Thus, cancer cells at least partially utilize constitutively active AKT to inhibit CASTOR1's function leading to constitutive mTORC1 activation.

While no consistent association of CASTOR1 mutation with any types of cancer has been identified so far, we have found that a lower mRNA expression level of CASTOR1 predicts a poor prognosis in 10 types of cancer (**Supplementary Figure 12C-F**). Importantly, a lower mRNA expression level of RNF167 is confirmed to predict a poor prognosis in 6 of these 10 types of cancer (**Supplementary Figure 12H-J**). The fact that a low mRNA expression levels of CASTOR1 and a high mRNA level of RNF167 predict a poor prognosis of these types of cancer suggest the existence of additional mechanisms regulating their mRNA expression. CASTOR1 is tumor suppressive in KSHV-induced cellular transformation and lung adenocarcinoma [152, 276]. In breast cancer cell lines, the protein level of CASTOR1 appears to be inversely correlated with the level of AKT activation (**Supplementary Figure 13A**). Genetic silencing of CASTOR1 increases cell proliferation and colony formation in softagar of breast cancer cells while overexpression of CASTOR1 has the opposite effect (**Figure 29A-C** and **Supplementary Figure 15E-G**). In a mouse tumor model, overexpression of WT CASTOR1 inhibits tumor growth and extends animal survival rate, whereas knockdown of CASTOR1 has the opposite effect (**Figure 29D-J**). While the constitutively phosphorylated mutant S14D has a much reduced effect, the dead phosphorylated mutant inhibits tumor growth even more effective than

the WT CASTOR1 (**Figure 29D-G**). Hence, our results have demonstrated a tumor suppressive function of CASTOR1 in breast cancer cells, which is negated by AKT-mediated phosphorylation. Whether CASTOR1 protein has a tumor suppressive function in other types of cancer remains to be investigated.

In addition to extracellular arginine deficiency commonly observed in tumor microenvironment, the rate-limiting enzyme ASS1 responsible for intracellular *de novo* arginine synthesis is also frequently silenced in most cancer types [238, 263]. These cancer cells are arginine auxotrophic, which are the basis for clinical trials using pegylated arginine deiminase (ADI-PEG20) and human recombinant arginase [238]. These regimens are expected to deprive cancer cells of arginine, leading to CASTOR1 activation, mTORC1 suppression and tumor regression. While tumors initially respond to ADI-PEG20, ASS1-deficient tumors eventually become resistant to the treatment at least in part by activating the PI3K/AKT pathway [279]. It is expected that AKT activation would result in CASTOR1 degradation and mTORC1 activation, contributing to the resistance of the therapy. Hence AKT-mediated degradation of CASTOR1 could be an important mechanism in resistance to cancer therapies designed to deplete cancer cells of arginine. In this context, combining arginine deprivation and AKT inhibition could be an attractive approach to overcome resistance to the cancer therapy.

5.0 Methods and materials

5.1 Cell culture

TIVE and KTIVE cells were obtained from Dr. Rolf Renne at the University of Florida, Gainesville [280]. TIVE cells were cultured in VascuLife VEGF complete media (Lifeline Cell Technology LM-0024) plus 10% fetal bovine serum (FBS, Sigma). KTIVE cells were cultured as TIVE cells in the presence of 10 μg/ml hygromycin. MM and KMM cells were cultured as previously described [209]. 293T cells were obtained from ATCC (CRL-3216). 293T cells were maintained in DMEM supplemented with 10% FBS. MCF7, T47D, HCC1569 and HCC202 cells were obtained from Dr. Xiaosong Wang at the University of Pittsburgh, and were cultured in RPMI1640 with 10% FBS.

5.2 Plasmids

The reporter construct of the wild-type full-length CASTOR1 3'UTR (CASTOR1 3'UTR) was generated by cloning the CASTOR1 3'UTR sequence downstream of the luciferase sequence into the pGL3-Control plasmid using primers 5'AGTGGTACCGGAACA GCAGACCCAACC3' (forward) and 5'AGTCTCGAGTCGGAACCAGAGGGCACAGC3' (reverse). The 35 bp and 26 bp DNA fragments from CASTOR1 3'UTR containing putative miRNA targeting sites, and the mutated 26 bp fragment were synthesized by Integrated DNA Technology, and cloned into the pGL3-Control plasmid. The coding sequence of CASTOR1 and

2 with a flag tag at the C-terminus was amplified by PCR using the cDNA prepared from MM cells as PCR templates, and cloned into the NotI/BamHI sites of the pITA-puro lentiviral vector to generate CASTOR1 and 2 expression vectors.

Plasmids that were purchased from Addgene included: pLKO1-TRC (10878), pcDNA3-myr-HA-AKT1 (46969), pcDNA3-HA-AKT1 (73408), pcDNA3-HA-AKT1-K179M (73409), pcDNA3-HA-AKT1-1-149aa (73410), pcDNA3-HA-AKT1-120-433aa (73411), pRK5-HA-Ubiquitin-WT (17608), pRK5-HA-Ubiquitin-K29 (22903) and pRK5-HA-Ubiquitin-K29R (17602). Plasmids provided by Jie Chen in Beijing University in China included p3.3 empty vector, p3.3-Myc-Ubiquitin-WT, p3.3-Myc-Ubiquitin-K48, p3.3-Myc-Ubiquitin-K63, p3.3-flag-KLHL19, p3.3-flag-KLHL21, p3.3-flag-KLHL22, p3.3-flag-ZNRF1, p3.3-flag-ZNRF2, p3.3-flag-BACURD1, p3.3-flag-BACURD2, p3.3-flag-RNF152, p3.3-flag-RNF167, p3.3-flag-β-Trcp1, p3.3-flag-FBW7, p3.3-flag-HERC5 and p3.3-flag-Skp2. pcDNA3 empty vector was manufactured from Invitrogen. pMD.G and p8.74 were made by PlasmidFactory. Human pITA-flag-CASTOR1 WT was cloned from 293T cells. Rat pITA-flag-CASTOR1 WT was cloned from MM cells. The mutants of human pITA-flag-CASTOR1 included S14A, S14D, K61R, K96R, K213R, K61R/K96R, K61R/K213R and K61R/K96R/K213R were generated using mutagenesis kit (NEB E0554) based on the manufacturer's instructions. The sequences of primers used for overpexression and shRNAs were listed in **Table 1** and the sequences of all plasmids were confirmed by direct sequencing.

5.3 *In vitro* kinase assay

Recombinant GST-AKT1 protein (Novus Biologicals 1775-KS) was mixed with GST-CASTOR1 protein (Novus Biologicals H00652968-P01) in 30 µl reaction mixture at room temperature for 1h. The reaction mixture contained protease inhibitors, 100 mM HEPES (pH 7.4), 150 mM NaCl, 50 mM $MgCl_2$,1 mM DTT, 0.01% NaN_3, 1 mM ATP, 0.2 µg GST-AKT1 and 1 µg GST-CASTOR1.

5.4 Lentiviral overexpression and knockdown of genes

Human CASTOR1 shRNAs, non-targeting control (NT), Flag-tagged CASTOR2 and CASTOR1 WT, S14A and S14D expression lentiviral plasmid pITA and rat ASS1 shRNAs, iNOS shRNAs, pITA-ASS1 expression lentiviral plasmid or empty vector pITA expression plasmid was cotransfected with pMDG and p8.74 packaging plasmids into 293T cells using the Lipofectamine 2000 Transfection Reagent (Thermo Fisher 11668019). At day 3 post-transfection, the supernatant of 293T cells was collected and filtered with a 0.45 µM filter. Cells were transduced by spinning infection at 1,500 rpm for 1 h in the presence of 10 µg/ml polybrene. Expression of CASTOR1 or 2 protein was confirmed by Western-blotting at day 2 post-transduction.

5.5 Colony formation in softagar

Softagar assay was performed as previously described [209]. Briefly, a total of $2x10^4$ cells suspended in 1 ml of 0.3% top agar (Sigma A5431) were plated onto one well of 0.5% base agar in 6 well-plates and maintained for 2 weeks. Colonies with a diameter of >50 μm were counted and photographed with a 4x objetive using a microscope.

5.6 Cell cycle analysis and apoptosis assay

Cell cycle was analyzed by propidium iodide (PI) staining and BrdU incorporation at the indicated time points as previously described [209]. Briefly, cells were pulsed with 10 μM BrdU (Sigma B5002) for 2 h, and then fixed and stained with a BrdU monoclonal antibody (Thermo Fisher Scientific B35129) and PI (Sigma P4864). Apoptotic cells were detected using the Fixable Viability Dye eFluor 660 Kit (eBioscience 650864) and PE-Cy7 Annexin V Apoptosis Detection Set (eBioscience 88810374) following the instructions of the manufacturer. Flow cytometry was performed in a FACS Canto System (BD Biosciences) and analysis was performed with FlowJo.

5.7 Reverse transcription real-time quantitative polymerase-chain reaction (RT-qPCR)

Total RNA was isolated with TRI Reagent (Sigma T9424) according to the instructions of the manufacturer. For coding genes, reverse transcription was performed with total RNA using the Maxima H Minus First Strand cDNA Synthesis Kit (Thermo Fisher Scientific K1652).

qPCR analysis was performed using the SsoAdvanced™ Universal SYBR® Green Supermix Kit (Bio-Rad 172-5272). For miRNAs, reverse transcription was performed with total RNA using the TaqMan miRNA Reverse Transcription Kit (Thermo Fisher Scientific 4366597). qPCR analysis was performed using the Power SYBR Green PCR Master Mix (Thermo Fisher Scientific 4367659). The relative expression levels of target genes were normalized to the expression level of an internal control gene, which yielded $2^{-\Delta\Delta Ct}$ values. All reactions were run in triplicates with cycle threshold (Ct) values within 0.5 Ct differences among the triplicates. The sequences of primers used for qPCR are listed in **Table 2**.

5.8 Antibodies

Primary antibodies included antibodies to S6K1 (Abcam 32359), pS6K (CST 9205), p4EBP1 (CST 9451), 4EBP1 (CST 9644), pan AKT (Cell Signaling Technology 4691), pAKT (CST 2965), AKT1 (CST 2938), pAKT substrate (RXRXXpS*/T*) (CST 10001), GAPDH (CST 5174), flag (Sigma F1804), flag (Sigma A9594), HA (CST 3724), HA (CST 3444), GST (CST 2625), Ub (Santa Cruz sc-8017), c-Myc (Santa Cruz sc-40), RNF167 (Santa Cruz sc-515405), RNF167 (Proteintech 24618-1-AP), ASS1 (cat. ab124465, Abcam), STAT3 (cat. 9139, 439 Cell Signaling Technology) and β-tubulin (7B9, Sigma), iNOS (cat. sc-651, Santa Cruz) and pSTAT3 (cat. 9145, Cell Signaling Technology), β-actin (Santa Cruz sc-47778) and β-tubulin (Sigma 7B9). Antibodies to CASTOR1were described as before. Secondary antibodies included mouse anti-Rabbit IgG (Light-Chain Specific) (CST 93702), rabbit anti-Mouse IgG (Light Chain Specific) (CST 58802), goat anti-rabbit HRP conjugated IgG (CST 7074), horse anti-mouse IgG

HRP conjugated IgG (CST 7076), goat anti-mouse IgG DyLight 800 (Bio-Rad STAR117D800GA) and goat anti-rabbit IgG StarBright Blue700 (Bio-Rad 12004161).

5.9 Immunoprecipitation

Cells were lysed in lysis buffer (50 mM Tris-HCl, with 150 mM NaCl, 1 mM EDTA, and 1% Triton X-100, pH 7.4) supplemented with a complete protease inhibitor cocktail (Thermo 78438) and phosphatase inhibitor (Thermo 78427), followed by centrifugation at 4°C for 5min. The supernatant was then precleared with mouse agarose IgG (Sigma A0919) at 4 ºC for 4 h, and subsequently mixed with washed anti-Flag (Sigma A2220), anti-HA (Thermo 26182), anti-Myc (Sigma A7470, anti-AKT (Cell Signaling Technology 3653) or mouse IgG agarose beads (Sigma A0919) at 4 C° overnight. Immunocomplexes were washed extensively 3 times with washing buffer (50 mM Tris-HCl,150 mM NaCl, pH 7.4). The immunoprecipates were eluted with 2xSDS and then were subjected to Immunoblotting analysis.

5.10 Western-blotting analysis

All other proteins were separated with 4%-20% SDS-polyacrylamide gels (Genscript M00656 and M00657) except CASTOR1, which was resolved with 10% SDS-polyacrylamide gels (Genscript M00665 and M00666). Gels were sequentially transferred to nitrocellulose membranes (GE Healthcare 10600004), which were then incubated with primary and secondary antibodies overnight and 1 h room temperature, respectively. The signals were developed using

chemiluminence substrates Luminiata Crescendo Western HRP substrate (EMD Millipore WBLUR0500) and SuperSignal West Femto Maximum Sensitivity Substrate (Thermo 34096) or fluroscent secondary antibodies. The images were recorded with a ChemiDoc MP imaging system (Bio-Rad 17001402) at either Chemi, Dylight 500, DyLight 800 or StarBright B700 channels.

5.11 Transfection and dual-luciferase reporter assay

The locked nucleic acid (LNA)-based suppressors for KSHV miRNAs were previously described [211, 217]. Transfections of siRNAs(Sigma), LNA-based miRNA suppressors (Exiqon) or plasmids were performed with Lipofectamine RNAiMAX (Thermo Fisher 13778150) or Lipofectamine 2000 Transfection Reagent (Thermo Fisher 11668019) following the manufacturer's instructions, respectively. For luciferase assay, MM, KMM or 293T cells transfected with DNAs of a luciferase reporter plasmid and the Renilla vector pRL-TK (Promega) together with a miRNA expression construct pSuper-miR-K1 or -K4, or a LNA-based miRNA suppressor for 48 h were harvested. The relative luciferase activity was assayed using the Dual-Luciferase Reporter Assay System (Promega E1960). The sequences for siRNA can be found based on the catalog No listed in **Table 3**.

5.12 Mouse experiments

Athymic Nude-Foxn1nu mice were purchased from Envigen. Mice were raised under 12 hour light/dark cycle and standard diet at the University of Pittsburgh. MCF7 cells transduced with either a vector control, Flag-CASTOR1 WT, S14A or S14D were trypsinized and concentrated by centrifugation to $5x10^6$ per 100 µl in DMEM supplemented with 10% FBS. An equal volume of cells was mixed with an equal volume of Matrigel (VWR 47743-720), and then $5x10^6$ cells were subcutaneously injected into each flank of the mouse. The mice were inserted with estrogen pellet (Sigma 8875) before injection. Tumor volume was measured twice a week and calculated based on the formula ($V = L \times W \times W \times 0.5$). Mice were euthanized when the tumor size reached the upper limit of 1,500 mm^3. All mouse experiments were done following the protocol approved by the University of Pittsburgh Institutional Animal Care and Use Committee (IACUC).

5.13 Live cell imaging

Live cell imaging was performed to detect intracellular NO as previously described [226]. Cells grown on 24 well plate at 37 °C in 5% CO2 were treated with 5 µM DAR-4M AM for 1 h at 37 °C, followed by washing with PBS for 4 times at 5 min per time at room temperature. Plates were then examined with a Nikon Eclipse Ti-S fluorescent microscope (Nikon instruments Inc, Melvile, NY, USA). SNAP (NO donor) was purchased from Cayman Chemical and used as a positive control. Imaging was taken with a 20x objective len. ImageJ was used for fluorescent quantification.

5.14 ROS detection

CellROX Deep Red Reagent (Thermo Fisher, Cat. C10422) is a fluorogenic probe designed to measure ROS in living cells. The cell-permeable CellROX Deep Red dye is non-fluorescent in a reduced state but exhibits fluorescence upon oxidation with excitation/emission maxima at 640/665 nm. Cells were incubated with CellROX Deep Red Reagent at a final concentration of 5 μM for 30 min at 37 °C. The cells were washed with PBS for three times, and examined with a FACS Canto II flow cytometer.

5.15 Quantification and statistical analysis

The intensity of a protein band was quantified with ImageJ. Data were presented as mean ± SEM (standard error of the mean) and analyzed by Student's t test or one-way analysis of variance (ANOVA) if multiple samples were involved followed by Tukey post-hoc test if $P < 0.05$. All statistical analyses were done with Prism software package (PRISM 6.0, GraphPad Software, USA). A $P < 0.05$ was considered as statistically significant. Statistical symbols "*", "**" and "***" indicate *P*-values < 0.05, < 0.01 and < 0.001, respectively, and "NS" denotes "not significant".

6.0 Conclusion and future directions

6.1 KSHV reprograms metabolic pathways and sensors

Cancer cells sustain their uncontrolled proliferation in nutrients- and oxygen-deficient tumor microenvironment through reprogramming the cellular metabolic sensors that consequently alter the ways that cancer cells respond to environmental inputs. While most studies concentrate on the glucose and glutamine metabolisms, cancer cells usurp a great variety of other nutrients, cysteines, vitamins, trace metals and proline for example. The diversity of nutrients and the complexity of cellular responding circuits complicate our understanding how nutrients contribute to tumorigenesis. Viruses are absolute parasites that depend on the energy and macromolecules from host cells in favor of their infection and spread. Oncogenic KSHV infection induces cellular transformation by altering host cell metabolism, which is essential to maintain cell survival and viral genome. However, the delineation of the underpinning mechanisms is instead confounded by the multiple stages of KSHV infection. A simple example is the differential glucose catabolism observed by two groups in short-term KSHV- infected endothelial and KSHV-transformed cells respectively. The application of ^{18}F-FDG PET/CT technique to monitor the glycolytic efflux in KS and PEL patients might solve this controversy. Several KSHV products have been involved in reprogramming the glycolysis, glutaminolysis and FAS, however how exactly viral genes manipulate these pathways is unknown. Further a better understanding of the underlying mechanisms and a global screening of host cell metabolites and gene profiles to pinpoint other metabolic changes in normal and KSHV-infected/-transformed cells are required to develop therapies against KS and PEL tumors.

Despite substantial progress that has been made towards cancer metabolism, we are only beginning to understand how KSHV-mediated host cell metabolic alterations contributes to tumorigenesis.

Studies have been done to investigate how KSHV has evolved to usurp the host metabolic products, funneling them towards reproducing virion progeny and transforming host cells. However, how normal cells develop countermeasures to sense and antagonize these viral alterations is less studied. Additionally, whether KSHV's intervention of metabolic sensors like mTOR, AMPK and SIRT1, accounts for the metabolic alterations in host cells is unknown. A comprehensive mapping of the KSHV targeted host cell metabolic network can be exploited for therapeutic intervention of KSHV-induced human diseases.

6.2 The central role of mTORC1 in nutrients sensing

mTORC1 is a central controller of cell growth by coordinating multiple environment cues and it is widely accepted now that mTORC1 is regulated by a coincidence event, with mTORC1 activation only happening when both nutrients and growth factors are sufficient. The growth-factors mediated mTORC1 activation has been well studied since mTOR is copurified with rapamycin-FKBP12 in 1995, nevertheless the amino acids transduction to mTORC1 is obscure until the discovery of Rag GTPases as indispensable proteins anchoring mTORC1 in lysosomes in 2008. Until now, there are more than thirty new players identified as the components of the amino acids mediated mTORC1 signaling pathways, such as v-ATPase, Rag, Ragulator, FLCN, GATOR1, GATOR2, KICSTOC complexes and amino acids sensors (SESN2, SLC38A9, TM4SF5, CASTOR1 and SAMTOR). Most of these genes have not been well studied although

some are reported to have genetic changes in cancer, indicating their potentially important roles in cancer progression. It might be interesting to investigate what are their exact roles in human diseases by modulating mTORC1 signaling pathway and how they coordinate with each other and finally give a command to mTORC1. Yet the amino acids metabolism is highly intertwined and our understanding about amino acids sensing is far from complete. Although arginine, leucine and SAM sensors have been defined, whether there are sensors for other amino acids remain unknown. Whereas the metabolites are highly different in normal and tumor cells, how these sensor proteins differentially interplay with each other in normal and cancer cells are interesting. Moreover, current studies more focus on the short-term nutrients deprivation since it was initially shown the mTORC1 has a maximal activity when cells were starved for 50 min and re-stimulated for 10 min. However, cancer cells have persistently limited supply in nutrients, how well these studies mimic cancer *in vivo* are debatable. It is worthwhile trying a long-term deprivation of nutients and checking how players are being regulated and participate in mTORC1 network. As human bodies are compartmentalized, it will be intriguing to know the concentration of nutrients circulating to each organ and then define the activities or functions of mTORC1 accordingly. The paper detecting metabolites including glucoses and amino acids in individual cell compartments is a good beginning. Additionally, a prerequisite for mTORC1 activation is its lysosomal localization, it is mysterious how this megadolton mTORC1 moves onto lysosome within minutes in response to nutrients stimulation. The understanding of the underlying mechanism might advance the development of inhibitors specifically targeting the mTORC1 translocation.

The eventual goal of mTOR research is still clinical translation. How to better antagonizing cancer, aging and even diabetes still requires a better encoding of the complicated mTORC1 regulatory circuits.

Appendix A Supplementary figures

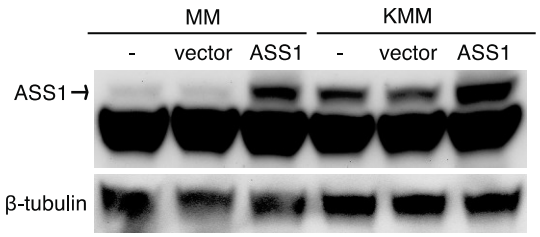

Supplementary Figure 1: Validation of the specificity of ASS1 antibody.

Western-blotting examination of MM and KMM cells stably expressing ASS1 or a vector control. The intensity of the upper band was dramatically increased in cells expressing ASS1 but not the vector control, indicating that the upper band is specific for the ASS1 protein.

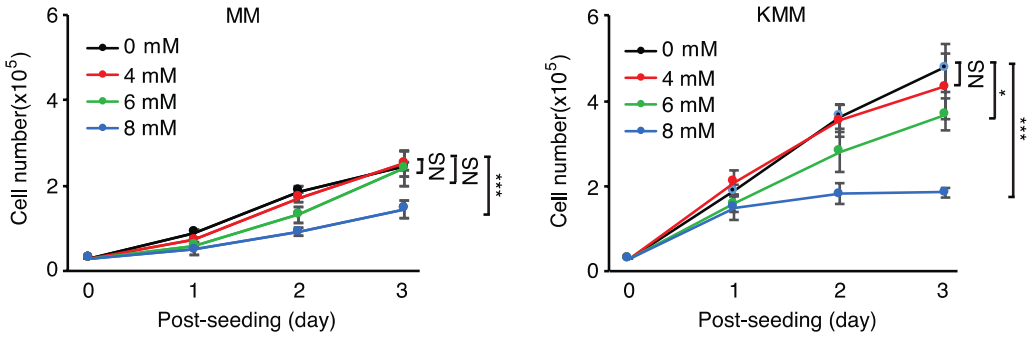

Supplementary Figure 2: iNOS inhibitor L-NAME reduced cell proliferation.

Proliferation of MM and KMM cells treated with 0, 4, 6 or 8 mM of L-NAME. Three independent experiments were repeated and results were shown as mean ± SEM; Data were analyzed by Student's t-test; * for $P < 0.05$, and *** for $P < 0.001$.

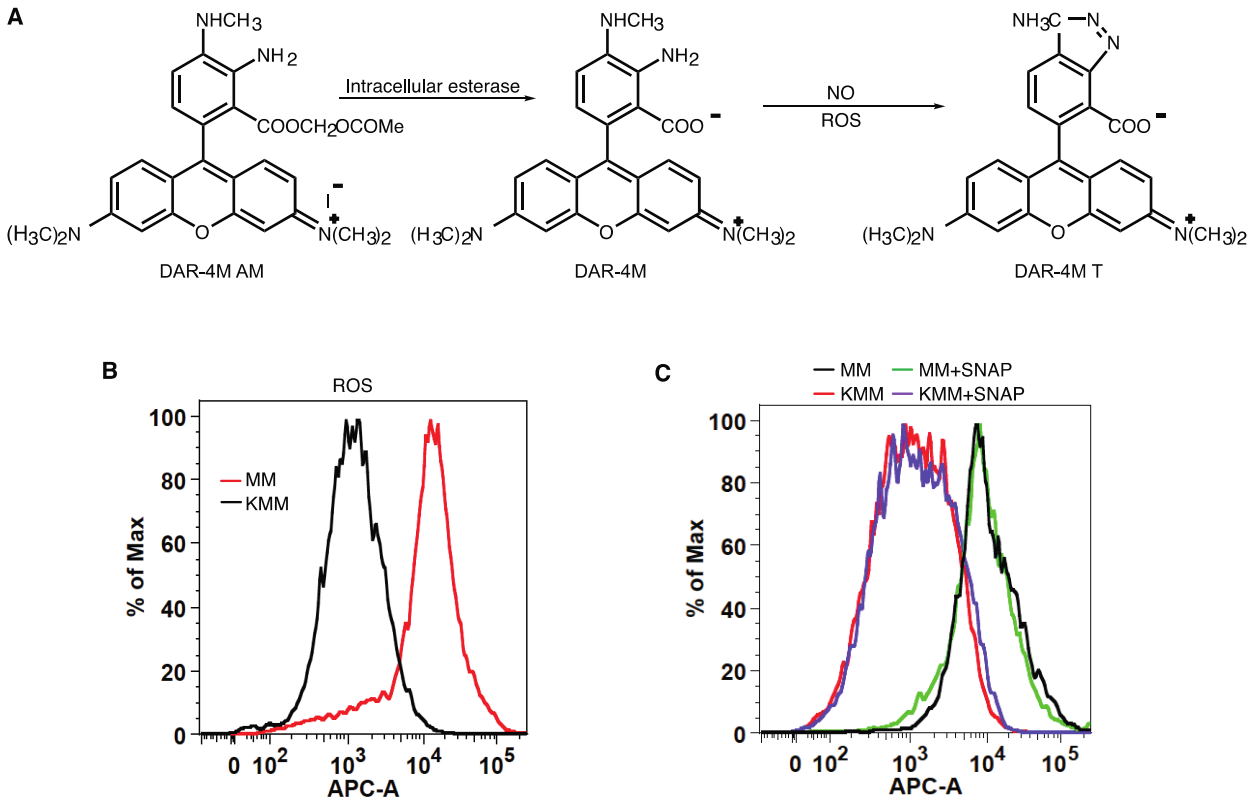

Supplementary Figure 3: Detection of intracellular NO level with DAR is not altered by different intracellular ROS levels.

(A) The chemical equation showed that the reaction of DAR with NO required ROS. **(B)** MM cells had higher intracellular ROS than KMM cells. **(C)** FACS analysis showed that NO donor SNAP did not alter intracellular ROS levels in MM and KMM cells.

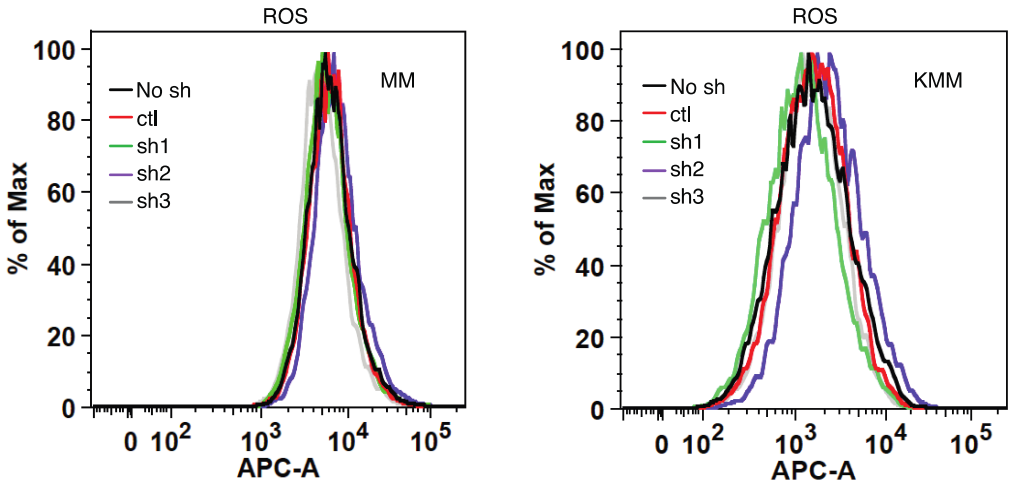

Supplementary Figure 4: ASS1 knockdown had no effect on ROS production.

MM and KMM cells transduced with 3 ASS1 shRNAs (sh1, sh2 or sh3) or a scrambled shRNA (ctl) for 2 days were examined for intracellular ROS levels.

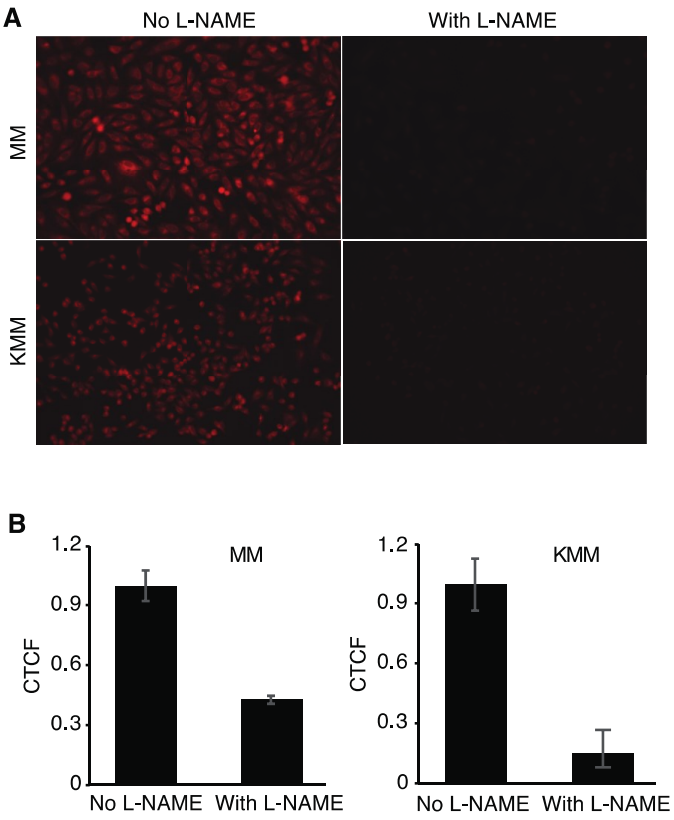

Supplementary Figure 5: iNOS inhibitor L-NAME reduced intracellular NO levels in MM and KMM cells.

(A) Detection of intracellular NO levels with DAR in MM and KMM cells with or without treatment with the NO donor L-NAME. Representative images were captured at 20x magnification with a fluorescent microscope. **(B)** Quantification of intracellular NO levels in MM and KMM cells with Image J. CTCF represented the corrected total cell fluorescence by ImageJ.

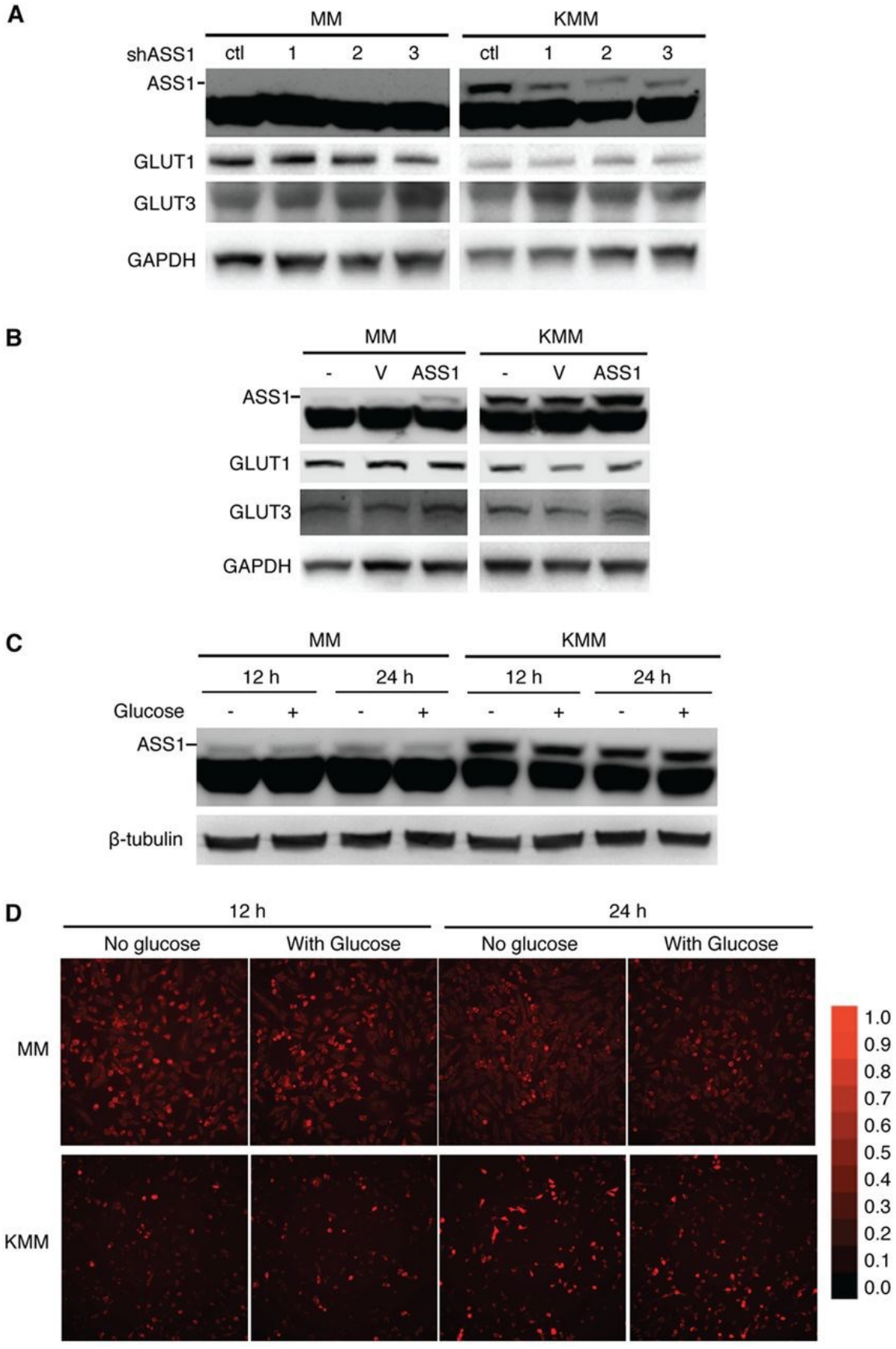
A
MM
KMM
shASS1
ctl
1
2
3
ctl
1
2
3
ASS1
GLUT1
GLUT3
GAPDH
B
MM
KMM
-
V
ASS1
-
V
ASS1
ASS1
GLUT1
GLUT3
GAPDH
C
MM
KMM
12 h
24 h
12 h
24 h
Glucose
-
+
-
+
-
+
-
+
ASS1
β-tubulin
D
12 h
24 h
No glucose
With Glucose
No glucose
With Glucose
MM
KMM
1.0
0.9
0.8
0.7
0.6
0.5
0.4
0.3
0.2
0.1
0.0

Supplementary Figure 6: ASS1 does not regulate the expression of GLUT1 and GLUT3, and glucose deprivation does not affect ASS1 protein and intracellular NO levels.

(A) ASS1 knockdown has no effect on the expression of GLUT1 and GLUT3 proteins. MM and KMM cells transduced with 3 ASS1 shRNAs (shRNA1, -2, or -3) or a scrambled shRNA (ctl) for 2 days were examined for the levels of GLUT1 and GLUT3 proteins. (B) Overexpression of ASS1 has no effect on the expression of GLUT1 and GLUT3 proteins. MM and KMM cells overexpressing ASS1 or a vector control (V) for 2 days were examined for the levels of GLUT1 and GLUT3 proteins. GAPDH, glyceraldehyde-3-phosphate dehydrogenase. (C and D) Glucose deprivation does not affect ASS1 protein and intracellular NO levels. MM and KMM cells were seeded overnight in full medium, cultured in medium with and without glucose for 12 and 24 h, and examined for the level of ASS1 protein (C) or intracellular NO (D).

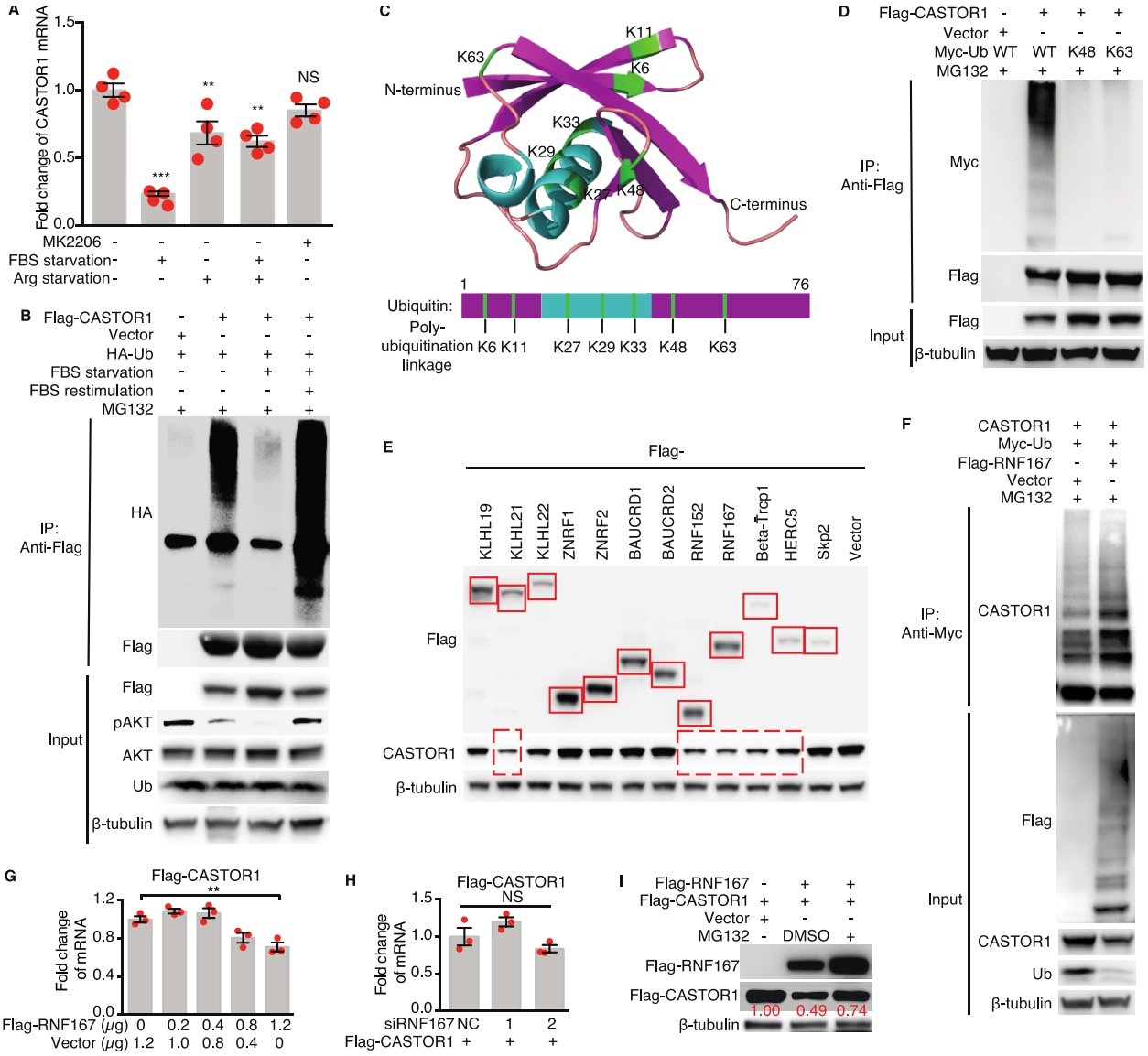

Supplementary Figure 7: RNF167 mediates K29-linked polyubiquitination and degradation of CASTOR1 in response to growth factors.

(**A**) FBS or arginine deprivation but not AKT inhibition decreased endogenous CASTOR1 mRNA level. (**B**) FBS re-stimulation restored CASTOR1 ubiquitination. (**C**) A schematic illustration of ubiquitin structure and the seven lysine residues in ubiquitin responsible for polyubiquitination linkage. (**D**) CASTOR1 was not tagged by K48- or K63-linked polyubiquitination. (**E**) Screening of E3 ligases that regulated CASTOR1 protein level. (**F**) RNF167 overexpression increased CASTOR1 ubiquitination. (**G** and **H**) RNF167 overexpression had no effect on CASTOR1 mRNA level except at higher doses (>0.8 μg), which showed a marginal reduction (**G**), while RNF167 knockdown

had no effect on CASTOR1 mRNA level (**H**). (**I**) MG132 partially rescued RNF167-mediated CASTOR1 downregulation.

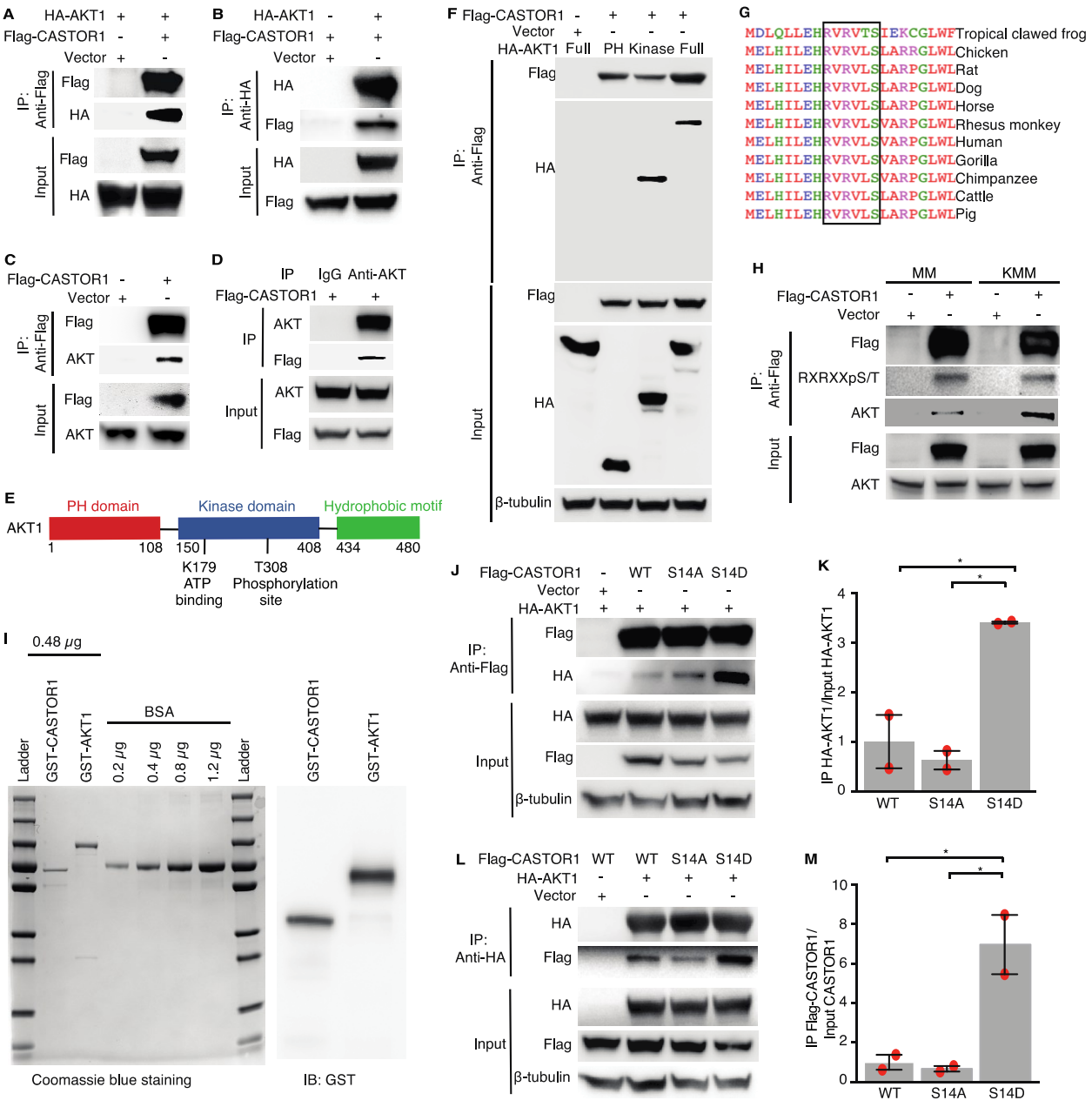

Supplementary Figure 8: AKT1 promotes CASTOR1 protein degradation but has no effect on CASTOR1 mRNA expression.

(**A-D**) CASTOR1 interacted with exogenous (**A** and **B**) and endogenous AKT (**C** and **D**). (**E**) Schematic illustration depicting AKT1 domains consisting of PH and kinase domains and a hydrophobic motif. K179 is the ATP binding site and T308 is the phosphorylation site required for AKT kinase functionality. (**F**) CASTOR1 preferentially interacted with AKT1 kinase domain. (**G**) AKT phosphorylation consensus motif in CASTOR1 was conserved among various vertebrates. Alignment of the CASTOR1 protein sequence using MUSCLE algorithm[271]. (**H**)

AKT interacted with and phosphorylated CASTOR1 in rat cells. **i,** Coomassie blue staining and immunoblotting analysis with an anti-GST antibody to examine the purity of recombinant GST-AKT1 and GST-CASTOR1 proteins. This was from one experiment. (**J** and **M**) CASTOR1 S14D had stronger binding to AKT1 than WT and S14A. Results from two independent experiments were quantified and examined by one-way ANOVA followed by Tukey post-hoc test (**J** and **M**), **P*<0.05.

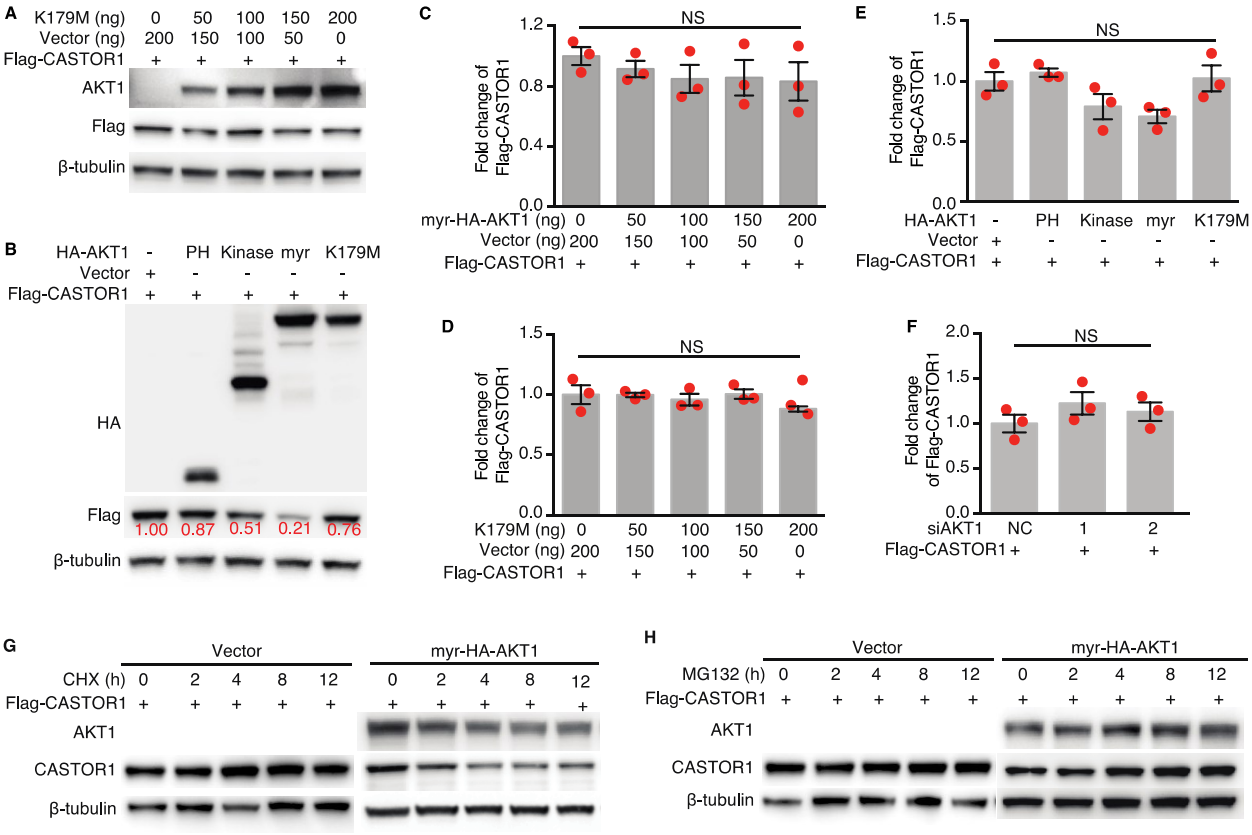

Supplementary Figure 9: AKT1-mediated CASTOR1 phosphorylation promotes its proteasome-dependent degradation.

(**A**) AKT1 kinase dead mutant K179M did not affect CASTOR1 protein level. (**B**) AKT1 kinase domain was sufficient to decrease CASTOR1 protein level, but to a lesser extent than the AKT1 WT. (**C-F**) myr-HA-AKT1, AKT1-K179M, different AKT1 domains and different siRNAs to AKT1 (siAKT1s) did not affect CASTOR1 mRNA level, one-way ANOVA followed by Tukey post-hoc test was used for the statistical analysis. NS, not significant; $^{**}P< 0.01$; $^{***}P< 0.001$. (**G** and **H**) AKT1 accelerated CASTOR1 degradation. 293T cells co-transfected with Flag-CASTOR1 and myr-HA-AKT1 for 36 h were treated with either cycloheximide (CHX) (**G**) or MG132 (**H**).

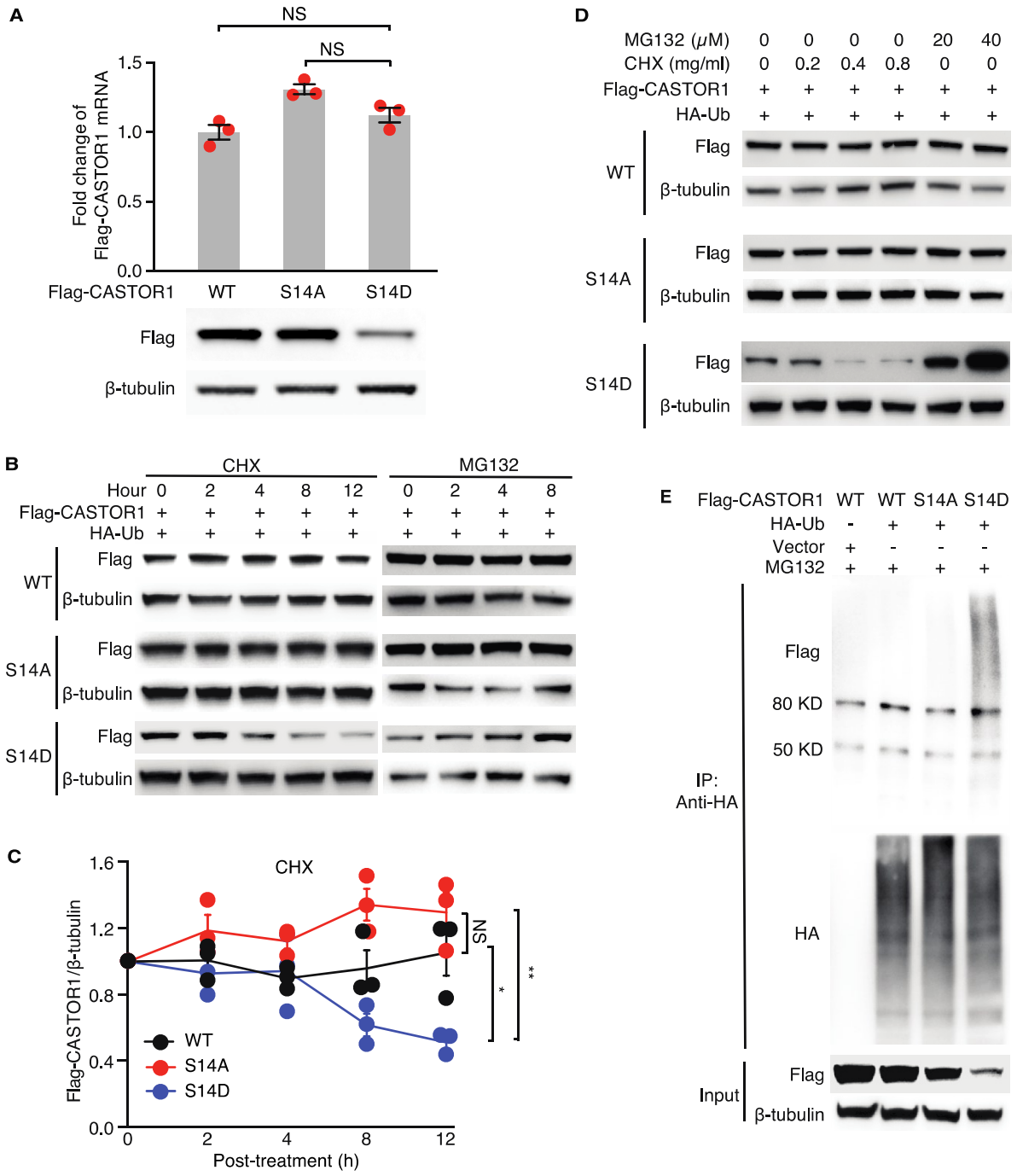

Supplementary Figure 10: AKT1-mediated CASTOR1 phosphorylation promotes its proteasome-dependent degradation.

(**A**) AKT1-mediated phosphorylation of CASTOR1 decreased protein but not mRNA level. NS, not significant; (**B** and **C**) CASTOR1 S14D had faster turnover than WT and S14A had. The protein level of CASTOR1 WT, S14A or S14D was examined following treatment with either CHX or MG132 for the indicated time (**B**), and the relative

levels were quantified and presented in (**C**), NS, not significant, **P*<0.01; ***P*<0.001. **d,** AKT-mediated CATOR1 phosphorylation induces ubiquitination and proteasome-dependent degradation for 12h at indicated concentration. **e,** CASTOR1 S14D had increased ubiquitination level compared to WT and S14A.

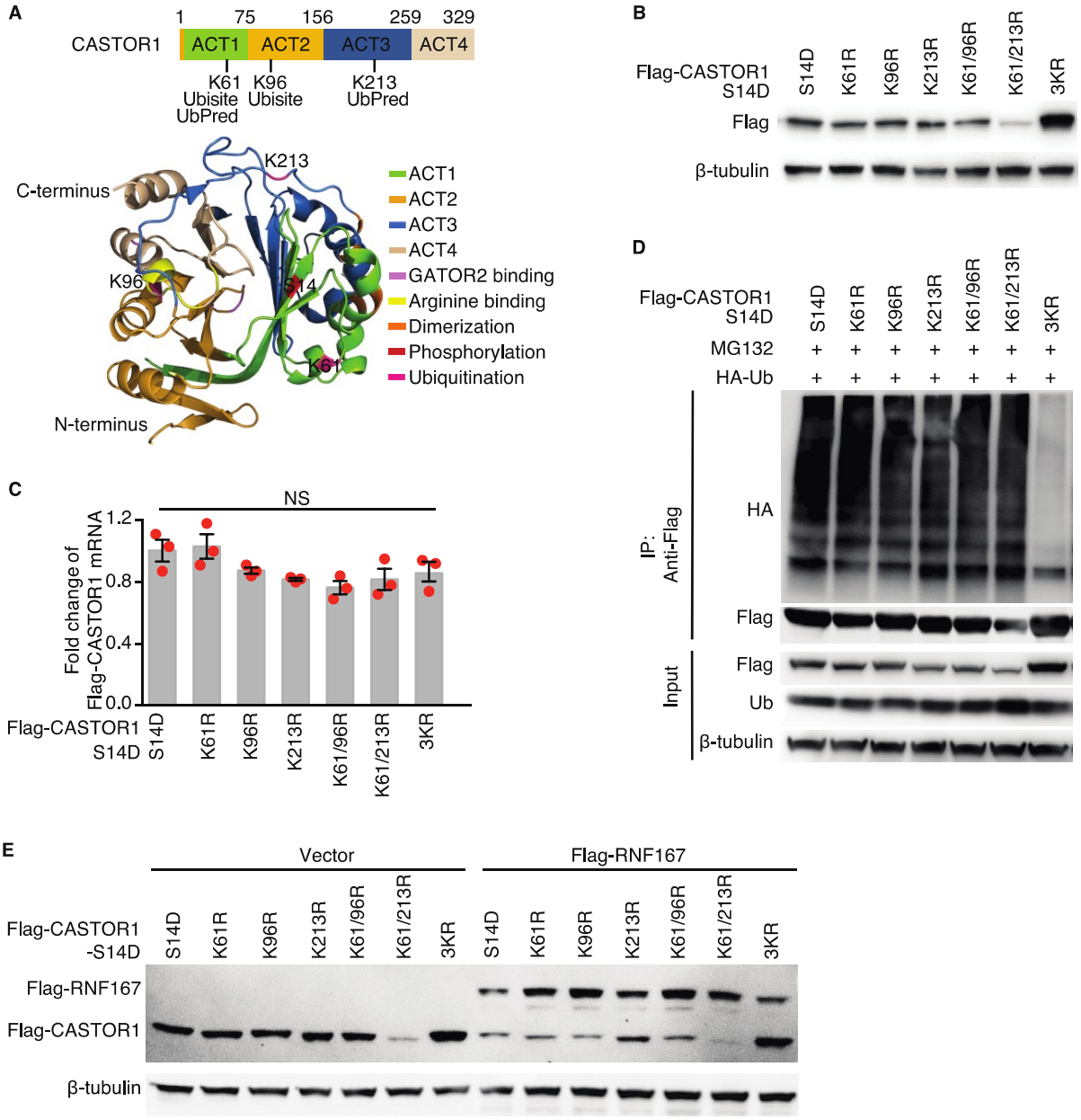

Supplementary Figure 11: CASTOR1 is marked by K29-linked polyubiquitination at K61, K96 and K213.

(**A**) A schematic illustration of ubiquitin structure and the seven lysine residues in ubiquitin responsible for polyubiquitination linkage. (**B** and **C**) Simultaneous mutations of CASTOR1 lysines K61, K96 and K213 to arginines (3KR) are required to stabilize the protein (**B**) but had no effect on mRNA level (**C**), (**C**) was shown as mean± SEM from three independent replicates, and one-way ANOVA followed by Tukey post-hoc test was used for the statistical analysis. NS, not significant. (**D** and **E**) The K61, K96 and K213 triple mutant 3KR of Flag-CASTOR1 S14D was resistant to RNF167-mediated ubiquitination (**D**) and degradation (**E**).

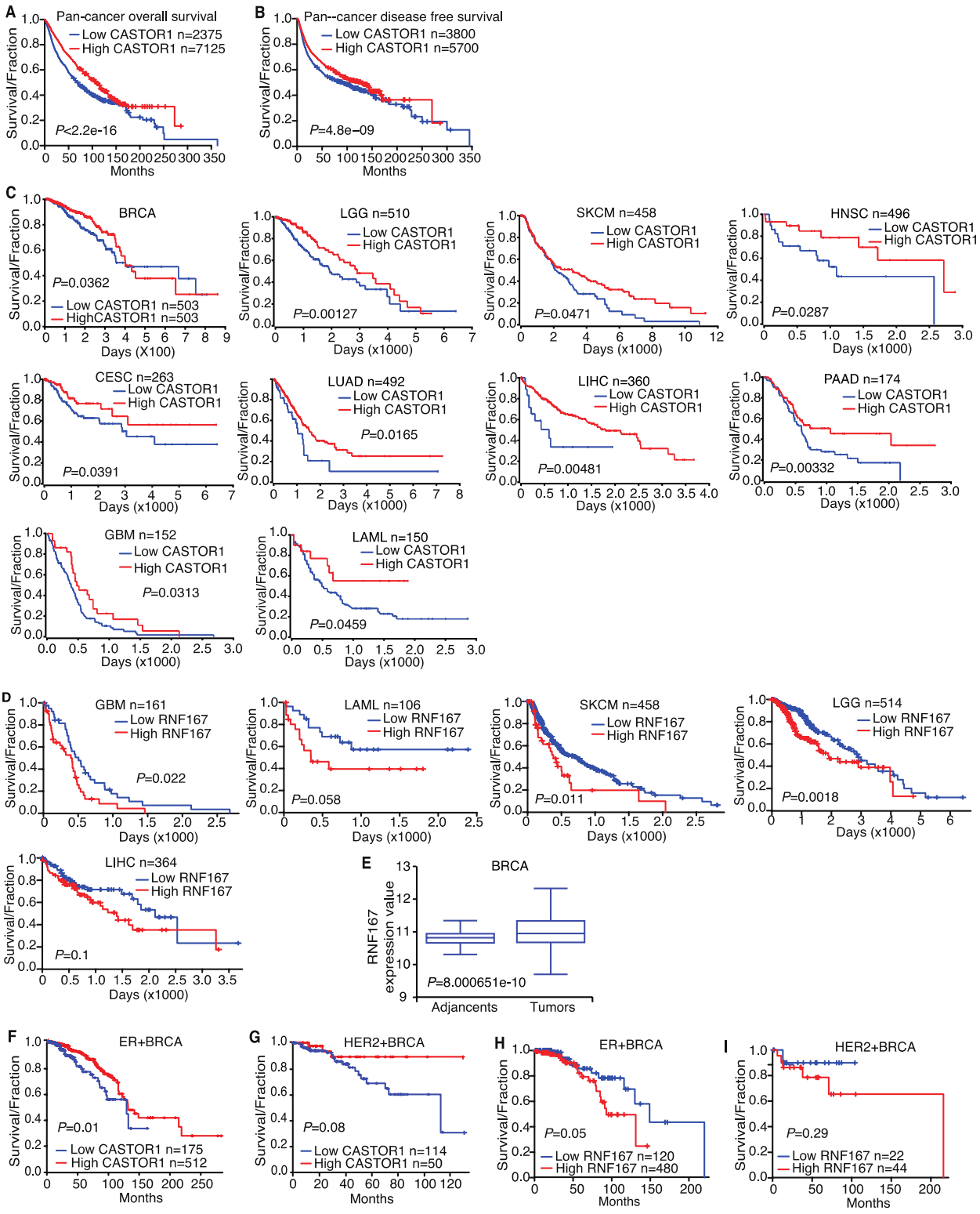

Supplementary Figure 12: Expression levels of CASTOR1 and RNF167 regulate mTORC1 and predict cancer survival in different types of cancer.

(**A** and **B**) Low CASTOR1 expression level was associated with poor overall survival (**A**) and disease-free survival (**B**) in pan-cancer analysis. (**C-E**) Low CASTOR1 expression level was associated with poor survival of breast cancer (**C**), and specific breast cancer subtypes including HER2-positive (HER2+) (**D**) and ER positive (ER+) (**E**) subtypes. (**F**) Low CASTOR1 mRNA expression level is associated with poor survival in multiple types of cancer. Analyses were performed with the TCGA database. **(G)** RNF167 expression level was higher in breast cancer tumors than the adjacent normal tissues. (**H** and **I**) High RNF167 expression level was associated with poor survival of ER+ (**H**) and HER2+ (**I**) subtypes of breast cancer. (**J**) Low CASTOR1 mRNA expression level and high RNF167 mRNA expression level are associated with poor survival in multiple types of cancer.

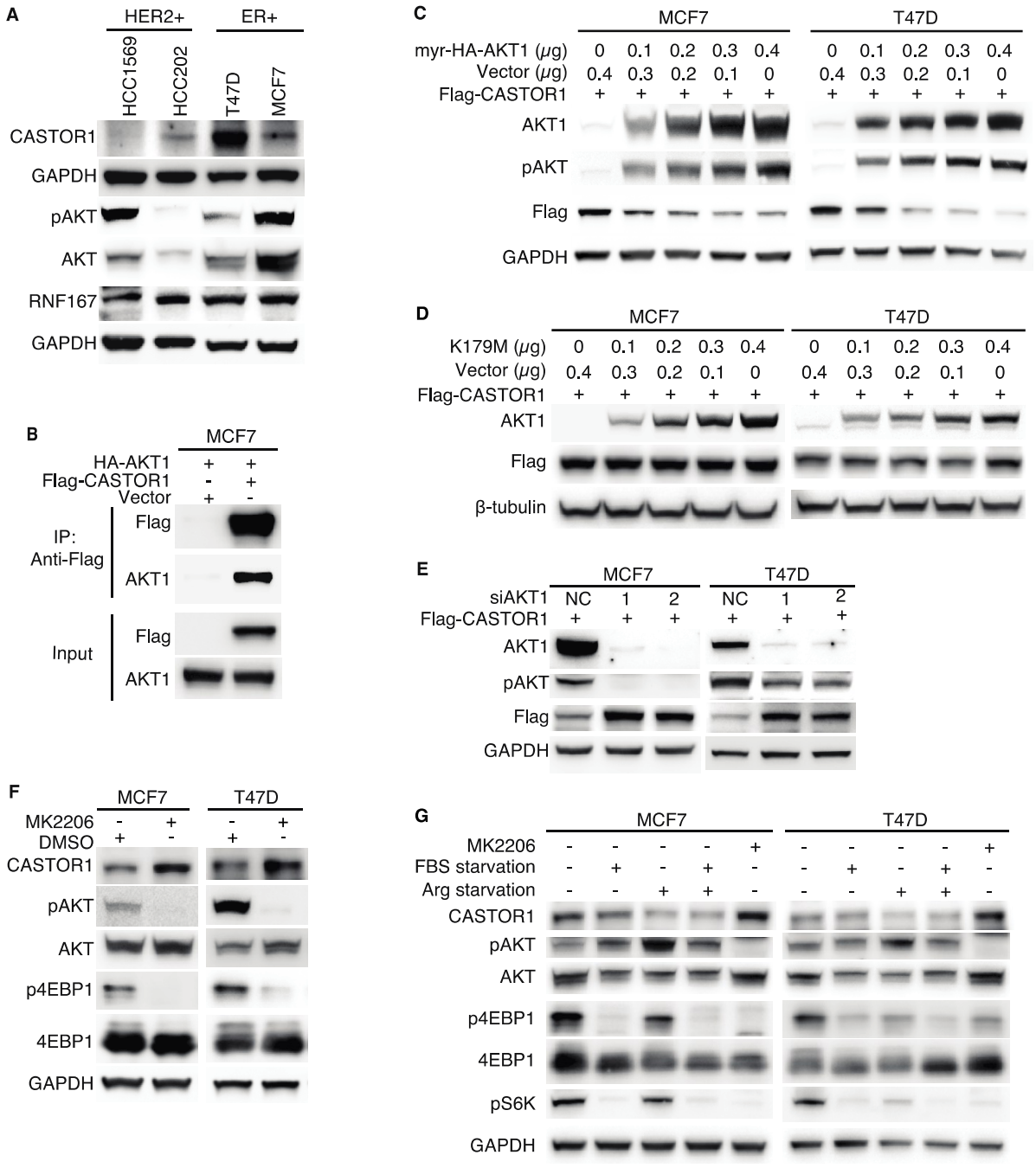

Supplementary Figure 13: AKT1-mediated phosphorylation and degradation of CASTOR1 in breast cancer cells.

(**A**) CASTOR1 protein level was negatively correlated to AKT activation in ER+ and HER2+ breast cells, respectively. (**B**) CASTOR1 interacted with AKT1 in MCF7 cells. (**C** and **D**) overexpression of myr-HA-AKT1 (**C**) but not the AKT kinase dead mutant K179M (**D**) in MCF7 and T47D cells resulted in a dose-dependent reduction in CASTOR1 protein level. **(E)** AKT1 silencing increased CASTOR1 protein level in ER+ breast cancer cells. (**F**)

AKT inhibitor MK2206 increased the endogenous CASTOR1 protein level in ER+ breast cancer cells. (**G**) AKT inhibitor MK2206 increased CASTOR1 protein level and inactivated AKT-mTORC1 signaling pathway in ER+ breast cancer cells, whereas FBS and arginine deprivation did not.

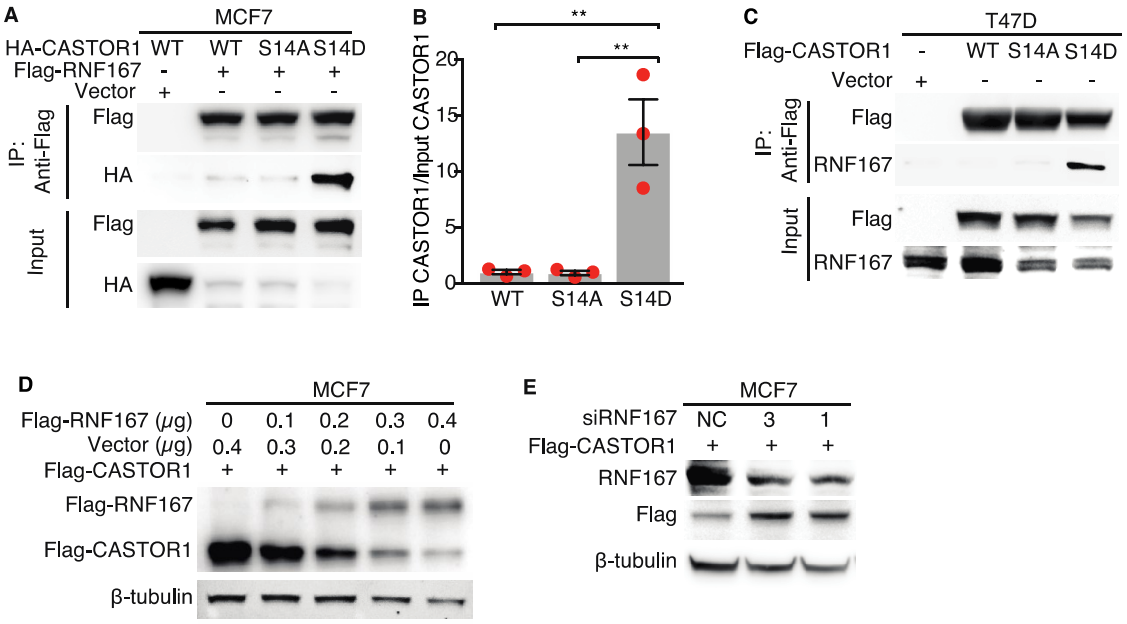

Supplementary Figure 14: AKT phosphorylation of CASTOR1 promoted RNF167-mediated CASTOR1 degradation in breast cancer.

(A-C) CASTOR1 S14D had higher affinity to RNF167 than WT and S14A had in MCF7 cells (**A**) and T47D (**C**). The results from three independent experiments were quantified and presented (**B**). **(D** and **E)** RNF167 overexpression (**D**) decreased while RNF167 knockdown (**E**) increased CASTOR1 expression in MCF7 cells.

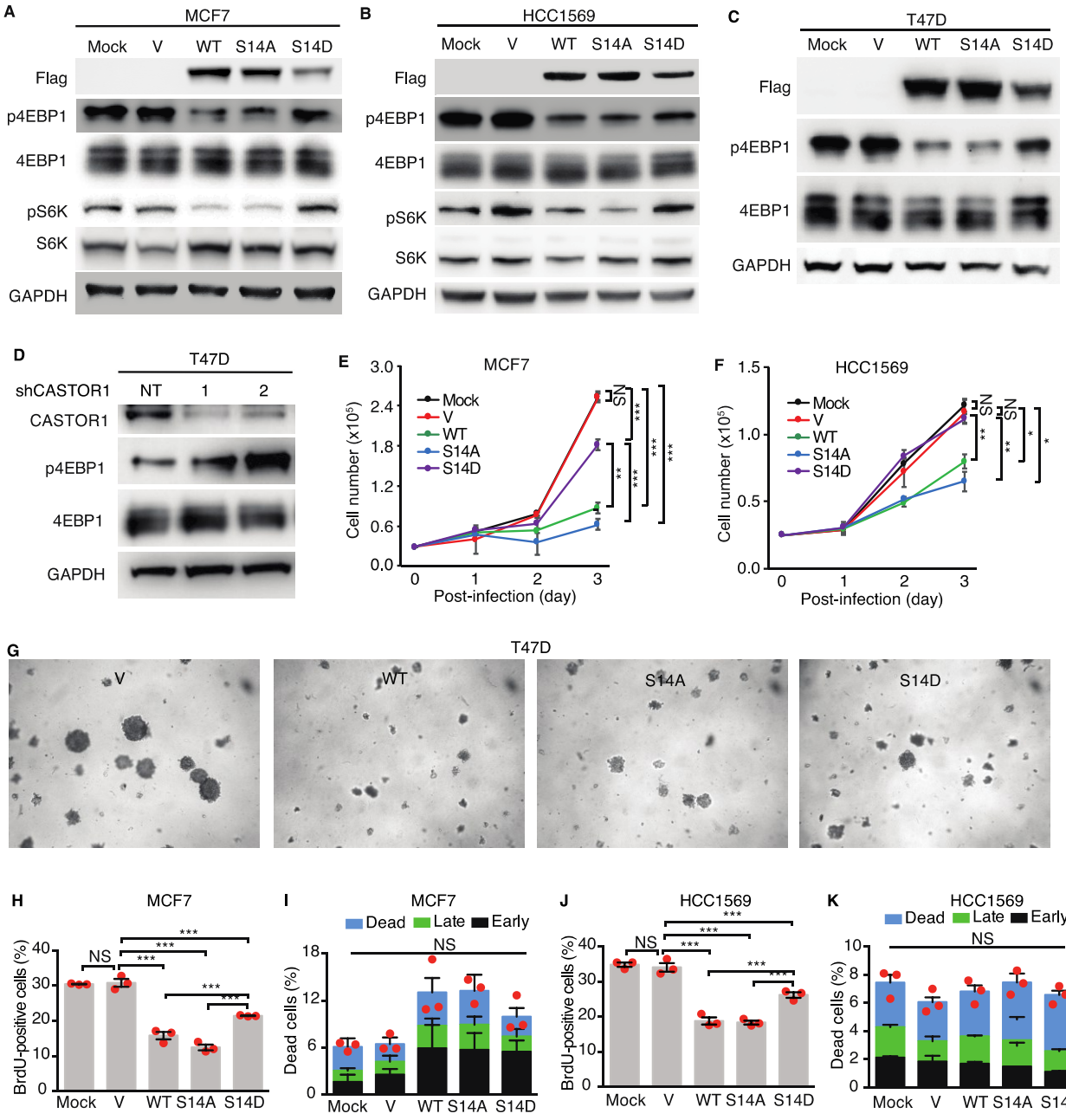

Supplementary Figure 15: CASTOR1 inhibits cell cycle progression and colony formation in softagar of breast cancer cells, and suppresses tumor growth by inactivating mTORC1.

(**A-C**) Inhibition of mTORC1 activation was stronger by Flag-CASTOR1 WT and S14A than S14D in MCF7 (**A**), HCC1569 cells (**B**) and T47D (**C**). (**D**) CASTOR1 silencing activated the mTORC1 signaling pathway. (**E-G**) CASTOR1 WT and S14A had stronger effects than S14D had in suppressing cell proliferation (**E** and **F**) and colony formation in softagar (**G**) of T47D cells. (**H** and **I**) Overexpression of Flag-CASTOR1 WT and S14A induced cell

cycle arrest in HER2+ HCC1569 (**H**) and ER+ MCF7 (**I**) breast cancer cells while S14D had only a marginal inhibitory effect. (**J** and **K**) Overexpression of Flag-CASTOR1 WT, S14A or S14D had minimal effect on apoptosis in HER2+ HCC1569 (**J**) and ER+ MCF7 (**K**) breast cancer cells. One-way ANOVA followed by Tukey post-hoc test was used for the statistical analysis **(E, F, H-K),** NS, not significant; *** $P< 0.001$.

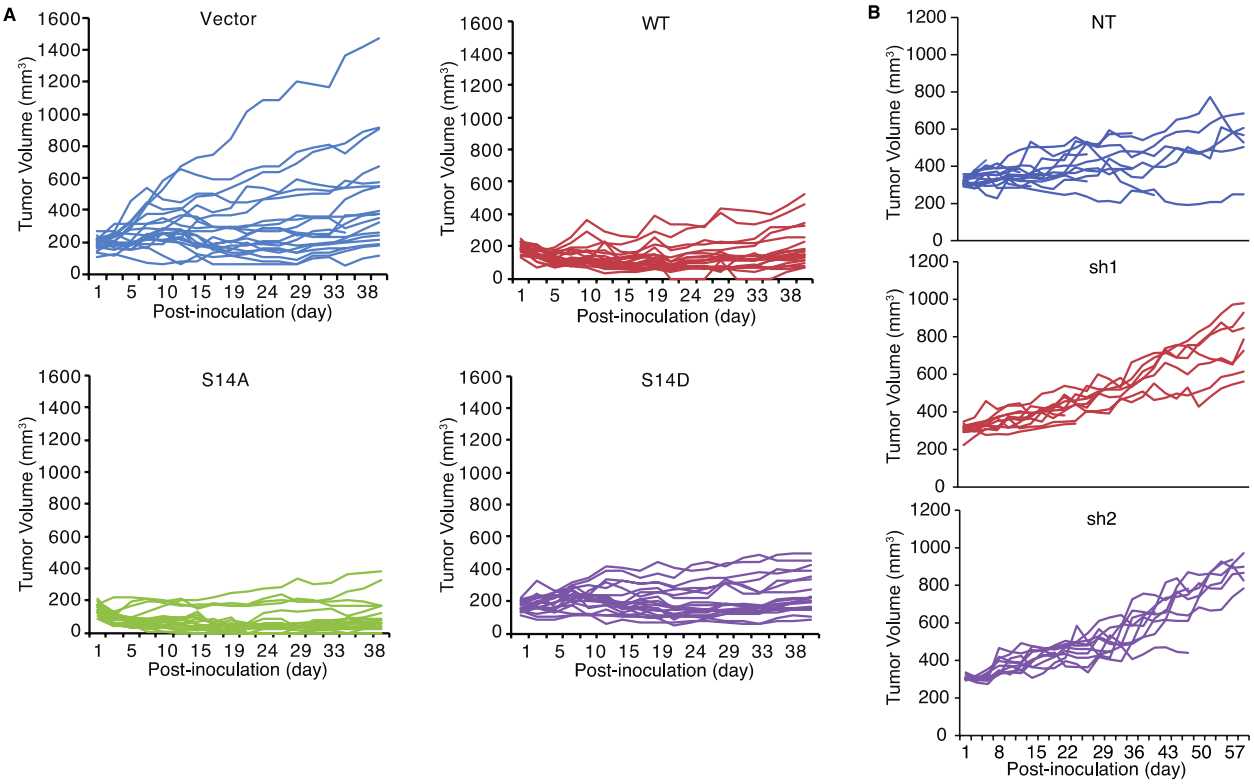

Supplementary Figure 16: AKT1-mediated phosphorylation and degradation of CASTOR1 promote breast cancer progression.

(**A**) Individual tumor growth curves indicated that CASTOR1 WT and S14A had more inhibitory effect on tumor growth than S14D had. (**B**) Individual tumor growth curve after CASTOR1 silencing suggested that CASTOR1 deletion promoted tumor growth. Results were shown as mean± SEM from three independent replicates.

Appendix B List of tables

Table 1 Summary of PCR primers and shRNAs

Rat Flag-CASTOR1-forward	5′TATGCGGCCGCGCCACCATGGACTACAAAGACGATGACGACAAGATGGAACTTCACATCCAGAGC3′
Rat Flag-CASTOR1-reverse	5′ATAGGATCCCTATGGATCTTTGGAAGCCAGG3′
Human CASTOR1-forward	5’TATGCGGCCGCGCCACCATGGAGCTGCACATCCTAGAAC3'
Human CASTOR1-reverse	5'ATAGGATCCTCAGGAAGCCAGGCCTTCCT3'
Human HA-CASTOR1-forward	5'TATGCGGCCGCGCCACCATGTACCCATACGATGTTCCAGATTACGCTATGGAGCTGCACATCCTAGAAC3'
Human HA-CASTOR1-reverse	5'ATAGGATCCTCAGGAAGCCAGGCCTTCCT3'
Human Flag-CASTOR1-forward	5’TATGCGGCCGCGCCACCATGGACTACAAAGACGATGACGACAAGATGGAGCTGCACATCCTAGAAC3’
Human Flag-CASTOR1-reverse	5’ATAGGATCCTCAGGAAGCCAGGCCTTCCT3'
Human Flag-CASTOR1-S14A-forward	5'GCGGGTGCTGGCTGTCGCCCGTC3'
Human Flag-CASTOR1-S14A-reverse	5'ACCCGGTGTTCTAGGATG3'
Human Flag-CASTOR1-S14D-forward	5'GCGGGTGCTGGATGTCGCCCGTC3'
Human Flag-CASTOR1-S14D-reverse	5'ACCCGGTGTTCTAGGATG3'
Human Flag-CASTOR1-K61R-forward	5'GGAGGGCTTTCGAGAGCTGCCCC3'
Human Flag-CASTOR1-K61R-reverse	5'TCGTCCACCATAAGCGTG3'
Human Flag-CASTOR1-K96R-forward	5'TGGGGTCACCCGGATCGCCCGTTCGG3'
Human Flag-CASTOR1-K96R-reverse	5'GCAGCCTGCACTGCCGCA3'
Human Flag-CASTOR1-K213R-forward	5'CAGCACCCCCCGGGAGGCAGCCT3'

Table 1 continued

Human Flag-CASTOR1-	5'TGCGAGTAGAAGAGGACATCTATG3'

K213R-reverse	
shRNA non-targeting (NT) control	5'TTGTACTACACAAAAGTACTG3'
Human CASTOR1-sh1	5'GGAGCTGCACATCCTAGAACA3'
Human CASTOR1-sh2	5'GCTTTGATGAATGTGGCATCG3'
Rat ASS1-sh1	5' GCTCGCAAACAAGTGGAAATT3'
Rat ASS1-sh2	5' GCACATCCTTGGACCTCTTCA3'
Rat ASS1-sh1	5' GCATGGATGAGAACCTTATGC3'
Rat iNOS-sh1	5' GCACAGAATGTTCCAGAATCC3'
Rat iNOS-sh1	5' GCATATCTGCAGACACATACT3'
Rat iNOS-sh1	5' GCTGAAATCCCTCCAGAATCT3'

Table 2 Summary of qPCR primers

Rat CASTOR1-F	5′-TCCATAGGGAACAGCAGACC-3′
Rat CASTOR1-R	5′-GCAGACATGTCCACAACCAC-3′
Rat CASTOR2-F	5′-AGAGGTTGGGGACAA GAGGT-3′
Rat CASTOR2-R	5′-TTGGAGACTGACCCTGCTCT-3′
Human CASTOR1-F	5′-GCCACCACCCTCATAGATGT-3′
Human CASTOR1-R	5′-AGGAGGTCACTGGGGAACTT-3′
Human CASTOR2-F	5′-AACTCCACATCCTGGAGCAC-3′
Human CASTOR2-R	5′-GGAATCCTTCCTCATCGACA-3′
Human β-actin-F	5′-ATCATTGCTCCTCCTGAGCG-3′
Human β-actin-R	5′-CGGACTCGTCATACTCCTGC-3′
Rat ASS1-F	5'CTGGAGGATGCCCGAGTTTT3'
Rat ASS1-R	5'TCCAGGATTCGAGCCTGGTA3'
Rat iNOS-F	5'CACCTTGGAGTTCACCCAGT3'
Rat iNOS-R	5'ACCACTCGTACTTGGGATGC3'
Rat β-actin-F	5' CCATGTACCCAGGCATTGCT 3'
Rat β-actin-R	5' AGCCACCAATCCACACAGAG3'

Table 3 Summary of siRNAs

siRNA negative control (NC)	Sigma	Cat#SIC001
Human AKT1 siRNA-1	Sigma	Cat#SASI_Hs01_00105954
Human AKT1 siRNA-2	Sigma	Cat#SASI_Hs01_00105953
Human RNF167 siRNA-1	Sigma	Cat#SASI_Hs01_00201491
Human RNF167 siRNA-2	Sigma	Cat#SASI_Hs01_00201493

Appendix C List of academic achievements

Appendix C.1 Publications related to my thesis

1. **Li T**, Wang X, Ju EG, Zhang XQ, da Silva SR, Gao S-J. RNF167 activates mTORC1 and promotes tumorigenesis by targeting CASTOR1 for ubiquitination and degradation, **submitted.**
2. **Li T**, Ju EG, Gao S-J. Suppression of mTORC1 inhibitor CASTOR1 by oncogenic KSHV-encoded miRNAs promotes cell proliferation and growth transformation. **Journal of Clinical Investigation, 2019**, 130: 3310-3323.
3. **Li T**, Zhu Y, Cheng F, Lu C, Jung JU, Gao S-J. Oncogenic KSHV upregulates argininosuccinate synthase 1, a rate-limiting enzyme of the citrulline-nitric oxide cycle, to activate STAT3 pathway and promote growth transformation. **Journal of Virology, 2019**, 93: e01599-18.

Appendix C.2 Co-author publications

1. Ju EG, **Li T**, Liu Z, Silva S. R., Wei S., Zhang X., Wang X., Gao S-J., Specific Inhibition of Viral miRNAs by Carbon Dots-Mediated Delivery of Locked Nucleic Acids for Therapy of Virus-Induced Cancer. **ACS Nano, 2020,** 14, 476-487.

2. Ju EG, **Li T**, Gao S-J. Efficient targeting of HPV-induced cervical cancer by gold nanoparticle delivery of Cas9 mRNA. **ACS Appl. Mater. Interfaces, 2019,** 113834717-34724.
3. Gao RY, **Li T**, Ramos da Silva S, Jung JU, Feng PH, Gao S-J. FoxO1 suppresses Kaposi's sarcoma-associated herpesvirus lytic replication and controls viral latency. **Journal of Virology, 2019,** 93: e01681-18.
4. Zhu Y, **Li T**, Ramos da Silva S, Lee J-J, Lu C, Eoh H, Jung JU, Gao S-J. A critical role of glutamine and asparagine γ-nitrogen in nucleotide biosynthesis in cancer cells hijacked by an oncogenic virus. **mBio, 2017,** 8: e01179-17.
5. He ML, Tan B, Cheng F, da Silva SR, Graffaz M, Oceane S, **Li T**, Gao SJ. Molecular biology of KSHV in relation to AIDS-associated oncogenesis. In: AIDS-Associated Viral Oncogenesis, **Cancer Treatment and Research Book Series. 2019**, 177: 23-62. doi: 10.1007/978-3-030-03502-0_2. Craig Meyers (Ed.) (2nd Edition), Springer.
6. Zhang F, Xu X, **Li T**, Liu Z. Shellfish Toxins Targeting Voltage-Gated Sodium Channels; **Marine Drugs**, **2013**(11), 4698-4723.

Appendix C.3 Attended international conference

1. 2019 International Conference on KSHV, **Jul 2019 (Oral Presentation)**
2. Cell Symposium, Metabolites as Signaling Molecules, Seattle, **Dec 2018 (Poster)**
3. 2018 International Conference on EBV & KSHV, Madison, **Jul 2018 (Oral Presentation)**
4. 2016 International Conference on KSHV, Los Angeles, **Jul 2016 (Attendee)**

Bibliography

1. Seyfried, T.N. and L.M. Shelton, *Cancer as a metabolic disease.* Nutrition & Metabolism, 2010. **7**.
2. Vazquez, A., et al., *Cancer metabolism at a glance.* Journal of Cell Science, 2016. **129**(18): p. 3367-3373.
3. de Martel, C., et al., *Global burden of cancers attributable to infections in 2008: a review and synthetic analysis.* Lancet Oncology, 2012. **13**(6).
4. Ye, F., X. Lei, and S.J. Gao, *Mechanisms of Kaposi's Sarcoma-Associated Herpesvirus Latency and Reactivation.* Adv Virol, 2011. **2011**.
5. Claus, C. and U.G. Liebert, *A renewed focus on the interplay between viruses and mitochondrial metabolism.* Archives of Virology, 2014. **159**(6): p. 1267-1277.
6. Warburg, O., *On respiratory impairment in cancer cells.* Science, 1956. **124**(3215): p. 269-70.
7. Pavlova, N.N. and C.B. Thompson, *The Emerging Hallmarks of Cancer Metabolism.* Cell Metab, 2016. **23**(1): p. 27-47.
8. Mehrmohamadi, M., et al., *Characterization of the usage of the serine metabolic network in human cancer.* Cell Rep, 2014. **9**(4): p. 1507-19.
9. Nilsson, R., et al., *Metabolic enzyme expression highlights a key role for MTHFD2 and the mitochondrial folate pathway in cancer.* Nat Commun, 2014. **5**: p. 3128.
10. Maddocks, O.D., et al., *Serine Metabolism Supports the Methionine Cycle and DNA/RNA Methylation through De Novo ATP Synthesis in Cancer Cells.* Mol Cell, 2016. **61**(2): p. 210-21.
11. Chang, Y., et al., *Identification of herpesvirus-like DNA sequences in AIDS-associated Kaposi's sarcoma.* Science, 1994. **266**(5192): p. 1865-9.
12. Bhutani, M., et al., *Kaposi sarcoma-associated herpesvirus-associated malignancies: epidemiology, pathogenesis, and advances in treatment.* Semin Oncol, 2015. **42**(2): p. 223-46.

13. Soulier, J., et al., *Kaposi's sarcoma-associated herpesvirus-like DNA sequences in multicentric Castleman's disease.* Blood, 1995. **86**(4): p. 1276-80.
14. Zhu, Y., et al., *gamma-Herpesvirus-encoded miRNAs and their roles in viral biology and pathogenesis.* Curr Opin Virol, 2013. **3**(3): p. 266-75.
15. Verma, S.C., K. Lan, and E. Robertson, *Structure and function of latency-associated nuclear antigen.* Curr Top Microbiol Immunol, 2007. **312**: p. 101-36.
16. Ganem, D., *KSHV and the pathogenesis of Kaposi sarcoma: listening to human biology and medicine.* Journal of Clinical Investigation, 2010. **120**(4): p. 939-949.
17. Som, P., et al., *A Fluorinated Glucose Analog, 2-Fluoro-2-Deoxy-D-Glucose (F-18) - Nontoxic Tracer for Rapid Tumor-Detection.* Journal of Nuclear Medicine, 1980. **21**(7): p. 670-675.
18. Almuhaideb, A., N. Papathanasiou, and J. Bomanji, *18F-FDG PET/CT imaging in oncology.* Ann Saudi Med, 2011. **31**(1): p. 3-13.
19. Delgado, T., et al., *Induction of the Warburg effect by Kaposi's sarcoma herpesvirus is required for the maintenance of latently infected endothelial cells.* Proc Natl Acad Sci U S A, 2010. **107**(23): p. 10696-701.
20. Singh, R.K., et al., *Metabolic reprogramming of Kaposi's sarcoma associated herpes virus infected B-cells in hypoxia.* PLoS Pathog, 2018. **14**(5): p. e1007062.
21. Ma, T., et al., *KSHV induces aerobic glycolysis and angiogenesis through HIF-1-dependent upregulation of pyruvate kinase 2 in Kaposi's sarcoma.* Angiogenesis, 2015. **18**(4): p. 477-488.
22. Yogev, O., et al., *Kaposi's Sarcoma Herpesvirus MicroRNAs Induce Metabolic Transformation of Infected Cells.* Plos Pathogens, 2014. **10**(9).
23. Jones, T., et al., *Direct and efficient cellular transformation of primary rat mesenchymal precursor cells by KSHV*. Journal of Clinical Investigation, 2012. **122**(3): p. 1076-1081.
24. Zhu, Y., et al., *An Oncogenic Virus Promotes Cell Survival and Cellular Transformation by Suppressing Glycolysis.* Plos Pathogens, 2016. **12**(5).
25. Bannai, S. and T. Ishii, *A Novel Function of Glutamine in Cell-Culture - Utilization of Glutamine for the Uptake of Cystine in Human-Fibroblasts.* Journal of Cellular Physiology, 1988. **137**(2): p. 360-366.

26. Timmerman, L.A., et al., *Glutamine Sensitivity Analysis Identifies the xCT Antiporter as a Common Triple-Negative Breast Tumor Therapeutic Target.* Cancer Cell, 2013. **24**(4): p. 450-465.
27. Gross, M.I., et al., *Antitumor Activity of the Glutaminase Inhibitor CB-839 in Triple-Negative Breast Cancer.* Molecular Cancer Therapeutics, 2014. **13**(4): p. 890-901.
28. Jacque, N., et al., *Targeting glutaminolysis has antileukemic activity in acute myeloid leukemia and synergizes with BCL-2 inhibition.* Blood, 2015. **126**(11): p. 1346-56.
29. Shroff, E.H., et al., *MYC oncogene overexpression drives renal cell carcinoma in a mouse model through glutamine metabolism.* Proc Natl Acad Sci U S A, 2015. **112**(21): p. 6539-44.
30. Qin, Z., et al., *Upregulation of xCT by KSHV-encoded microRNAs facilitates KSHV dissemination and persistence in an environment of oxidative stress.* PLoS Pathog, 2010. **6**(1): p. e1000742.
31. Timmerman, L.A., et al., *Glutamine sensitivity analysis identifies the xCT antiporter as a common triple-negative breast tumor therapeutic target.* Cancer Cell, 2013. **24**(4): p. 450-65.
32. Shin, C.S., et al., *The glutamate/cystine xCT antiporter antagonizes glutamine metabolism and reduces nutrient flexibility.* Nat Commun, 2017. **8**: p. 15074.
33. Valiya Veettil, M., et al., *Glutamate secretion and metabotropic glutamate receptor 1 expression during Kaposi's sarcoma-associated herpesvirus infection promotes cell proliferation.* PLoS Pathog, 2014. **10**(10): p. e1004389.
34. Sanchez, E.L., et al., *Latent KSHV Infected Endothelial Cells Are Glutamine Addicted and Require Glutaminolysis for Survival.* PLoS Pathog, 2015. **11**(7): p. e1005052.
35. Zhu, Y., et al., *A Critical Role of Glutamine and Asparagine gamma-Nitrogen in Nucleotide Biosynthesis in Cancer Cells Hijacked by an Oncogenic Virus.* MBio, 2017. **8**(4).
36. Li, T., et al., *Oncogenic Kaposi's Sarcoma-Associated Herpesvirus Upregulates Argininosuccinate Synthase 1, a Rate-Limiting Enzyme of the Citrulline-Nitric Oxide Cycle, To Activate the STAT3 Pathway and Promote Growth Transformation.* J Virol, 2019. **93**(4).

37. Bhatt, A.P., et al., *Dysregulation of fatty acid synthesis and glycolysis in non-Hodgkin lymphoma.* Proc Natl Acad Sci U S A, 2012. **109**(29): p. 11818-23.
38. Qin, Z., et al., *Targeting sphingosine kinase induces apoptosis and tumor regression for KSHV-associated primary effusion lymphoma.* Mol Cancer Ther, 2014. **13**(1): p. 154-64.
39. Angius, F., et al., *Neutral lipid alterations in human herpesvirus 8-infected HUVEC cells and their possible involvement in neo-angiogenesis.* BMC Microbiol, 2015. **15**: p. 74.
40. Delgado, T., et al., *Global metabolic profiling of infection by an oncogenic virus: KSHV induces and requires lipogenesis for survival of latent infection.* PLoS Pathog, 2012. **8**(8): p. e1002866.
41. Sychev, Z.E., et al., *Integrated systems biology analysis of KSHV latent infection reveals viral induction and reliance on peroxisome mediated lipid metabolism.* PLoS Pathog, 2017. **13**(3): p. e1006256.
42. Sanchez, E.L., et al., *Glycolysis, Glutaminolysis, and Fatty Acid Synthesis Are Required for Distinct Stages of Kaposi's Sarcoma-Associated Herpesvirus Lytic Replication.* J Virol, 2017. **91**(10).
43. Wang, Y.P. and Q.Y. Lei, *Metabolite sensing and signaling in cell metabolism.* Signal Transduct Target Ther, 2018. **3**: p. 30.
44. Wang, L. and B. Damania, *Kaposi's sarcoma-associated herpesvirus confers a survival advantage to endothelial cells.* Cancer Research, 2008. **68**(12): p. 4640-4648.
45. Roy, D., et al., *mTOR Inhibitors Block Kaposi Sarcoma Growth by Inhibiting Essential Autocrine Growth Factors and Tumor Angiogenesis.* Cancer Research, 2013. **73**(7): p. 2235-2246.
46. Stallone, G., et al., *Sirolimus for Kaposi's sarcoma in renal-transplant recipients.* N Engl J Med, 2005. **352**(13): p. 1317-23.
47. Chang, H.H. and D. Ganem, *A unique herpesviral transcriptional program in KSHV-infected lymphatic endothelial cells leads to mTORC1 activation and rapamycin sensitivity.* Cell Host Microbe, 2013. **13**(4): p. 429-40.
48. Martin, D., et al., *PI3Kgamma mediates kaposi's sarcoma-associated herpesvirus vGPCR-induced sarcomagenesis.* Cancer Cell, 2011. **19**(6): p. 805-13.
49. Tomlinson, C.C. and B. Damania, *The K1 protein of Kaposi's sarcoma-associated herpesvirus activates the Akt signaling pathway.* J Virol, 2004. **78**(4): p. 1918-27.

50. Bhatt, A.P., et al., *A viral kinase mimics S6 kinase to enhance cell proliferation.* Proceedings of the National Academy of Sciences of the United States of America, 2016. **113**(28): p. 7876-7881.
51. Li, T.T., E.G. Ju, and S.J. Gao, *Kaposi sarcoma-associated herpesvirus miRNAs suppress CASTOR1-mediated mTORC1 inhibition to promote tumorigenesis.* Journal of Clinical Investigation, 2019. **129**(8): p. 3310-3323.
52. Kim, J. and K.L. Guan, *mTOR as a central hub of nutrient signalling and cell growth.* Nature Cell Biology, 2019. **21**(1): p. 63-71.
53. Saxton, R.A. and D.M. Sabatini, *mTOR Signaling in Growth, Metabolism, and Disease (vol 168, pg 960, 2017).* Cell, 2017. **169**(2): p. 362-362.
54. Mossmann, D., S. Park, and M.N. Hall, *mTOR signalling and cellular metabolism are mutual determinants in cancer.* Nat Rev Cancer, 2018. **18**(12): p. 744-757.
55. Herzig, S. and R.J. Shaw, *AMPK: guardian of metabolism and mitochondrial homeostasis.* Nat Rev Mol Cell Biol, 2018. **19**(2): p. 121-135.
56. Garcia, D. and R.J. Shaw, *AMPK: Mechanisms of Cellular Energy Sensing and Restoration of Metabolic Balance.* Mol Cell, 2017. **66**(6): p. 789-800.
57. Inoki, K., T. Zhu, and K.L. Guan, *TSC2 mediates cellular energy response to control cell growth and survival.* Cell, 2003. **115**(5): p. 577-90.
58. Gwinn, D.M., et al., *AMPK phosphorylation of raptor mediates a metabolic checkpoint.* Mol Cell, 2008. **30**(2): p. 214-26.
59. Anders, P.M., et al., *The KSHV K1 Protein Modulates AMPK Function to Enhance Cell Survival.* Plos Pathogens, 2016. **12**(11).
60. Cheng, F., et al., *Suppression of Kaposi's Sarcoma-Associated Herpesvirus Infection and Replication by 5 '-AMP-Activated Protein Kinase.* Journal of Virology, 2016. **90**(14): p. 6515-6525.
61. Lin, Z. and D. Fang, *The Roles of SIRT1 in Cancer.* Genes Cancer, 2013. **4**(3-4): p. 97-104.
62. He, M.L., et al., *SIRT1 and AMPK pathways are essential for the proliferation and survival of primary effusion lymphoma cells.* Journal of Pathology, 2017. **242**(3): p. 309-321.

63. He, M., et al., *SIRT1-mediated downregulation of p27(Kip1) is essential for overcoming contact inhibition of Kaposi's sarcoma-associated herpesvirus transformed cells.* Oncotarget, 2016. **7**(46): p. 75698-75711.
64. Li, Q., et al., *Activation of Kaposi's sarcoma-associated herpesvirus (KSHV) by inhibitors of class III histone deacetylases: identification of sirtuin 1 as a regulator of the KSHV life cycle.* J Virol, 2014. **88**(11): p. 6355-67.
65. Ye, F., et al., *High Glucose Induces Reactivation of Latent Kaposi's Sarcoma-Associated Herpesvirus.* J Virol, 2016. **90**(21): p. 9654-9663.
66. Brown, E.J., et al., *A mammalian protein targeted by G1-arresting rapamycin-receptor complex.* Nature, 1994. **369**(6483): p. 756-8.
67. Sabers, C.J., et al., *Isolation of a protein target of the FKBP12-rapamycin complex in mammalian cells.* J Biol Chem, 1995. **270**(2): p. 815-22.
68. Sabatini, D.M., et al., *RAFT1: a mammalian protein that binds to FKBP12 in a rapamycin-dependent fashion and is homologous to yeast TORs.* Cell, 1994. **78**(1): p. 35-43.
69. Sancak, Y., et al., *The Rag GTPases bind raptor and mediate amino acid signaling to mTORC1.* Science, 2008. **320**(5882): p. 1496-501.
70. Kim, E., et al., *Regulation of TORC1 by Rag GTPases in nutrient response.* Nature Cell Biology, 2008. **10**(8): p. 935-945.
71. Hara, K., et al., *Amino acid sufficiency and mTOR regulate p70 S6 kinase and eIF-4E BP1 through a common effector mechanism.* J Biol Chem, 1998. **273**(23): p. 14484-94.
72. Saxton, R.A. and D.M. Sabatini, *mTOR Signaling in Growth, Metabolism, and Disease.* Cell, 2017. **169**(2): p. 361-371.
73. Sarbassov, D.D., et al., *Phosphorylation and regulation of Akt/PKB by the rictor-mTOR complex.* Science, 2005. **307**(5712): p. 1098-101.
74. Gan, X., et al., *PRR5L degradation promotes mTORC2-mediated PKC-delta phosphorylation and cell migration downstream of Galpha12.* Nat Cell Biol, 2012. **14**(7): p. 686-96.
75. Garcia-Martinez, J.M. and D.R. Alessi, *mTOR complex 2 (mTORC2) controls hydrophobic motif phosphorylation and activation of serum- and glucocorticoid-induced protein kinase 1 (SGK1).* Biochem J, 2008. **416**(3): p. 375-85.

76. Li, X. and T. Gao, *mTORC2 phosphorylates protein kinase Czeta to regulate its stability and activity.* EMBO Rep, 2014. **15**(2): p. 191-8.
77. Thomanetz, V., et al., *Ablation of the mTORC2 component rictor in brain or Purkinje cells affects size and neuron morphology.* J Cell Biol, 2013. **201**(2): p. 293-308.
78. Malik, N., et al., *Mechanism of activation of SGK3 by growth factors via the Class 1 and Class 3 PI3Ks.* Biochem J, 2018. **475**(1): p. 117-135.
79. Lamming, D.W., et al., *Rapamycin-induced insulin resistance is mediated by mTORC2 loss and uncoupled from longevity.* Science, 2012. **335**(6076): p. 1638-43.
80. Toschi, A., et al., *Regulation of mTORC1 and mTORC2 complex assembly by phosphatidic acid: competition with rapamycin.* Mol Cell Biol, 2009. **29**(6): p. 1411-20.
81. Mukaida, S., et al., *Adrenoceptors promote glucose uptake into adipocytes and muscle by an insulin-independent signaling pathway involving mechanistic target of rapamycin complex 2.* Pharmacol Res, 2017. **116**: p. 87-92.
82. Smith, E.M., et al., *The tuberous sclerosis protein TSC2 is not required for the regulation of the mammalian target of rapamycin by amino acids and certain cellular stresses.* J Biol Chem, 2005. **280**(19): p. 18717-27.
83. Long, X., et al., *Rheb binds and regulates the mTOR kinase.* Curr Biol, 2005. **15**(8): p. 702-13.
84. Kim, E., et al., *Regulation of TORC1 by Rag GTPases in nutrient response.* Nat Cell Biol, 2008. **10**(8): p. 935-45.
85. Tee, A.R., et al., *Tuberous sclerosis complex gene products, tuberin and hamartin, control mTOR signaling by acting as a GTPase-activating protein complex toward Rheb.* Current Biology, 2003. **13**(15): p. 1259-1268.
86. Fawal, M.A., M. Brandt, and N. Djouder, *MCRS1 binds and couples Rheb to amino acid-dependent mTORC1 activation.* Dev Cell, 2015. **33**(1): p. 67-81.
87. Li, Y., et al., *TSC2: filling the GAP in the mTOR signaling pathway.* Trends Biochem Sci, 2004. **29**(1): p. 32-8.
88. Inoki, K., T.Q. Zhu, and K.L. Guan, *TSC2 mediates cellular energy response to control cell growth and survival.* Cell, 2003. **115**(5): p. 577-590.
89. Inoki, K., et al., *TSC2 is phosphorylated and inhibited by Akt and suppresses mTOR signalling.* Nature Cell Biology, 2002. **4**(9): p. 648-657.

90. Dibble, C.C., et al., *TBC1D7 Is a Third Subunit of the TSC1-TSC2 Complex Upstream of mTORC1.* Molecular Cell, 2012. **47**(4): p. 535-546.
91. Garami, A., et al., *Insulin activation of Rheb, a mediator of mTOR/S6K/4E-BP signaling, is inhibited by TSC1 and 2.* Molecular Cell, 2003. **11**(6): p. 1457-1466.
92. Inoki, K., et al., *Rheb GTPase is a direct target of TSC2 GAP activity and regulates mTOR signaling.* Genes & Development, 2003. **17**(15): p. 1829-1834.
93. Manning, B.D., et al., *Identification of the tuberous sclerosis complex-2 tumor suppressor gene product tuberin as a target of the phosphoinositide 3-kinase/akt pathway.* Mol Cell, 2002. **10**(1): p. 151-62.
94. Potter, C.J., L.G. Pedraza, and T. Xu, *Akt regulates growth by directly phosphorylating Tsc2.* Nat Cell Biol, 2002. **4**(9): p. 658-65.
95. Roux, P.P., et al., *Tumor-promoting phorbol esters and activated Ras inactivate the tuberous sclerosis tumor suppressor complex via p90 ribosomal S6 kinase.* Proc Natl Acad Sci U S A, 2004. **101**(37): p. 13489-94.
96. Li, Y., et al., *The p38 and MK2 kinase cascade phosphorylates tuberin, the tuberous sclerosis 2 gene product, and enhances its interaction with 14-3-3.* J Biol Chem, 2003. **278**(16): p. 13663-71.
97. Lee, D.F., et al., *IKK beta suppression of TSC1 links inflammation and tumor angiogenesis via the mTOR pathway.* Cell, 2007. **130**(3): p. 440-55.
98. Inoki, K., et al., *TSC2 integrates Wnt and energy signals via a coordinated phosphorylation by AMPK and GSK3 to regulate cell growth.* Cell, 2006. **126**(5): p. 955-68.
99. Brugarolas, J., et al., *Regulation of mTOR function in response to hypoxia by REDD1 and the TSC1/TSC2 tumor suppressor complex.* Genes Dev, 2004. **18**(23): p. 2893-904.
100. Cota, D., et al., *The role of hypothalamic mammalian target of rapamycin complex 1 signaling in diet-induced obesity.* J Neurosci, 2008. **28**(28): p. 7202-8.
101. Reiling, J.H. and E. Hafen, *The hypoxia-induced paralogs Scylla and Charybdis inhibit growth by down-regulating S6K activity upstream of TSC in Drosophila.* Genes Dev, 2004. **18**(23): p. 2879-92.

102. Zhang, C.S., et al., *The lysosomal v-ATPase-Ragulator complex is a common activator for AMPK and mTORC1, acting as a switch between catabolism and anabolism.* Cell Metab, 2014. **20**(3): p. 526-40.
103. Feng, Z., et al., *The coordinate regulation of the p53 and mTOR pathways in cells.* Proc Natl Acad Sci U S A, 2005. **102**(23): p. 8204-9.
104. Stambolic, V., et al., *Regulation of PTEN transcription by p53.* Mol Cell, 2001. **8**(2): p. 317-25.
105. Budanov, A.V. and M. Karin, *p53 target genes sestrin1 and sestrin2 connect genotoxic stress and mTOR signaling.* Cell, 2008. **134**(3): p. 451-60.
106. Nobukuni, T., et al., *Amino acids mediate mTOR/raptor signaling through activation of class 3 phosphatidylinositol 3OH-kinase.* Proc Natl Acad Sci U S A, 2005. **102**(40): p. 14238-43.
107. Sekiguchi, T., et al., *Novel G proteins, Rag C and Rag D, interact with GTP-binding proteins, Rag A and Rag B.* J Biol Chem, 2001. **276**(10): p. 7246-57.
108. Efeyan, A., et al., *Regulation of mTORC1 by the Rag GTPases is necessary for neonatal autophagy and survival.* Nature, 2013. **493**(7434): p. 679-83.
109. Bar-Peled, L., et al., *Ragulator is a GEF for the rag GTPases that signal amino acid levels to mTORC1.* Cell, 2012. **150**(6): p. 1196-208.
110. Sancak, Y., et al., *Ragulator-Rag complex targets mTORC1 to the lysosomal surface and is necessary for its activation by amino acids.* Cell, 2010. **141**(2): p. 290-303.
111. Shen, K. and D.M. Sabatini, *Ragulator and SLC38A9 activate the Rag GTPases through noncanonical GEF mechanisms.* Proc Natl Acad Sci U S A, 2018. **115**(38): p. 9545-9550.
112. Zoncu, R., et al., *mTORC1 senses lysosomal amino acids through an inside-out mechanism that requires the vacuolar H(+)-ATPase.* Science, 2011. **334**(6056): p. 678-83.
113. Mindell, J.A., *Lysosomal Acidification Mechanisms.* Annual Review of Physiology, Vol 74, 2012. **74**: p. 69-86.
114. Abu-Remaileh, M., et al., *Lysosomal metabolomics reveals V-ATPase- and mTOR-dependent regulation of amino acid efflux from lysosomes.* Science, 2017. **358**(6364): p. 807-+.

115. Tsun, Z.Y., et al., *The folliculin tumor suppressor is a GAP for the RagC/D GTPases that signal amino acid levels to mTORC1.* Mol Cell, 2013. **52**(4): p. 495-505.

116. Petit, C.S., A. Roczniak-Ferguson, and S.M. Ferguson, *Recruitment of folliculin to lysosomes supports the amino acid-dependent activation of Rag GTPases.* J Cell Biol, 2013. **202**(7): p. 1107-22.

117. Shen, K., et al., *Cryo-EM Structure of the Human FLCN-FNIP2-Rag-Ragulator Complex.* Cell, 2019.

118. Bar-Peled, L., et al., *A Tumor suppressor complex with GAP activity for the Rag GTPases that signal amino acid sufficiency to mTORC1.* Science, 2013. **340**(6136): p. 1100-6.

119. Shen, K., et al., *Arg-78 of Nprl2 catalyzes GATOR1-stimulated GTP hydrolysis by the Rag GTPases.* J Biol Chem, 2019. **294**(8): p. 2970-2975.

120. Chen, J., et al., *KLHL22 activates amino-acid-dependent mTORC1 signalling to promote tumorigenesis and ageing.* Nature, 2018. **557**(7706): p. 585-589.

121. Deng, L., et al., *The ubiquitination of rag A GTPase by RNF152 negatively regulates mTORC1 activation.* Mol Cell, 2015. **58**(5): p. 804-18.

122. Jin, G., et al., *Skp2-Mediated RagA Ubiquitination Elicits a Negative Feedback to Prevent Amino-Acid-Dependent mTORC1 Hyperactivation by Recruiting GATOR1.* Mol Cell, 2015. **58**(6): p. 989-1000.

123. Wolfson, R.L., et al., *KICSTOR recruits GATOR1 to the lysosome and is necessary for nutrients to regulate mTORC1.* Nature, 2017. **543**(7645): p. 438-442.

124. Peng, M., N. Yin, and M.O. Li, *SZT2 dictates GATOR control of mTORC1 signalling (vol 543, pg 433, 2017).* Nature, 2018. **558**(7710): p. E2-E2.

125. Blommaart, E.F., et al., *Phosphorylation of ribosomal protein S6 is inhibitory for autophagy in isolated rat hepatocytes.* J Biol Chem, 1995. **270**(5): p. 2320-6.

126. Nicklin, P., et al., *Bidirectional transport of amino acids regulates mTOR and autophagy.* Cell, 2009. **136**(3): p. 521-34.

127. Sanli, T., et al., *Sestrin2 modulates AMPK subunit expression and its response to ionizing radiation in breast cancer cells.* PLoS One, 2012. **7**(2): p. e32035.

128. Morrison, A., et al., *Sestrin2 promotes LKB1-mediated AMPK activation in the ischemic heart.* FASEB J, 2015. **29**(2): p. 408-17.

129. Chantranupong, L., et al., *The Sestrins interact with GATOR2 to negatively regulate the amino-acid-sensing pathway upstream of mTORC1.* Cell Rep, 2014. **9**(1): p. 1-8.

130. Parmigiani, A., et al., *Sestrins inhibit mTORC1 kinase activation through the GATOR complex.* Cell Rep, 2014. **9**(4): p. 1281-91.

131. Kim, J.S., et al., *Corrigendum: Sestrin2 inhibits mTORC1 through modulation of GATOR complexes.* Sci Rep, 2015. **5**: p. 14029.

132. Peng, M., N. Yin, and M.O. Li, *Sestrins function as guanine nucleotide dissociation inhibitors for Rag GTPases to control mTORC1 signaling.* Cell, 2014. **159**(1): p. 122-133.

133. Wolfson, R.L., et al., *Sestrin2 is a leucine sensor for the mTORC1 pathway.* Science, 2016. **351**(6268): p. 43-8.

134. Saxton, R.A., et al., *Structural basis for leucine sensing by the Sestrin2-mTORC1 pathway.* Science, 2016. **351**(6268): p. 53-8.

135. Lee, J.H., U.S. Cho, and M. Karin, *Sestrin regulation of TORC1: Is Sestrin a leucine sensor?* Sci Signal, 2016. **9**(431): p. re5.

136. Lee, J.H., A.V. Budanov, and M. Karin, *Sestrins orchestrate cellular metabolism to attenuate aging.* Cell Metab, 2013. **18**(6): p. 792-801.

137. Sundberg, B.E., et al., *The evolutionary history and tissue mapping of amino acid transporters belonging to solute carrier families SLC32, SLC36, and SLC38.* J Mol Neurosci, 2008. **35**(2): p. 179-93.

138. Wang, S., et al., *Metabolism. Lysosomal amino acid transporter SLC38A9 signals arginine sufficiency to mTORC1.* Science, 2015. **347**(6218): p. 188-94.

139. Rebsamen, M., et al., *SLC38A9 is a component of the lysosomal amino acid sensing machinery that controls mTORC1.* Nature, 2015. **519**(7544): p. 477-+.

140. Wyant, G.A., et al., *mTORC1 Activator SLC38A9 Is Required to Efflux Essential Amino Acids from Lysosomes and Use Protein as a Nutrient.* Cell, 2017. **171**(3): p. 642-+.

141. Castellano, B.M., et al., *Lysosomal cholesterol activates mTORC1 via an SLC38A9-Niemann-Pick C1 signaling complex.* Science, 2017. **355**(6331): p. 1306-1311.

142. Jung, J.W., et al., *Transmembrane 4 L Six Family Member 5 Senses Arginine for mTORC1 Signaling.* Cell Metab, 2019. **29**(6): p. 1306-1319 e7.

143. Wright, M.D., J. Ni, and G.B. Rudy, *The L6 membrane proteins--a new four-transmembrane superfamily.* Protein Sci, 2000. **9**(8): p. 1594-600.

144. Abu-Remaileh, M., et al., *Lysosomal metabolomics reveals V-ATPase- and mTOR-dependent regulation of amino acid efflux from lysosomes.* Science, 2017. **358**(6364): p. 807-813.

145. Chantranupong, L., et al., *The CASTOR Proteins Are Arginine Sensors for the mTORC1 Pathway.* Cell, 2016. **165**(1): p. 153-164.

146. Saxton, R.A., et al., *Mechanism of arginine sensing by CASTOR1 upstream of mTORC1.* Nature, 2016. **536**(7615): p. 229-33.

147. Gai, Z., et al., *Structural mechanism for the arginine sensing and regulation of CASTOR1 in the mTORC1 signaling pathway.* Cell Discov, 2016. **2**: p. 16051.

148. Xia, J., et al., *Structural insight into the arginine-binding specificity of CASTOR1 in amino acid-dependent mTORC1 signaling.* Cell Discov, 2016. **2**: p. 16035.

149. Zhou, Y., et al., *Crystal structures of arginine sensor CASTOR1 in arginine-bound and ligand free states.* Biochem Biophys Res Commun, 2019. **508**(2): p. 387-391.

150. Sun, L., et al., *Seeking mTORC1 Inhibitors Through Molecular Dynamics Simulation of Arginine Analogs Inhibiting CASTOR1.* Cancer Genomics Proteomics, 2019. **16**(6): p. 465-479.

151. Li, T., E. Ju, and S.J. Gao, *Kaposi sarcoma-associated herpesvirus miRNAs suppress CASTOR1-mediated mTORC1 inhibition to promote tumorigenesis.* J Clin Invest, 2019. **129**(8): p. 3310-3323.

152. Zhou, X., et al., *CASTOR1 suppresses the progression of lung adenocarcinoma and predicts poor prognosis.* J Cell Biochem, 2018. **119**(12): p. 10186-10194.

153. Gu, X., et al., *SAMTOR is an S-adenosylmethionine sensor for the mTORC1 pathway.* Science, 2017. **358**(6364): p. 813-818.

154. Duran, R.V., et al., *Glutaminolysis activates Rag-mTORC1 signaling.* Mol Cell, 2012. **47**(3): p. 349-58.

155. Jewell, J.L., et al., *Metabolism. Differential regulation of mTORC1 by leucine and glutamine.* Science, 2015. **347**(6218): p. 194-8.

156. Crino, P.B., K.L. Nathanson, and E.P. Henske, *The tuberous sclerosis complex.* N Engl J Med, 2006. **355**(13): p. 1345-56.

157. Tee, A.R., et al., *Tuberous sclerosis complex gene products, Tuberin and Hamartin, control mTOR signaling by acting as a GTPase-activating protein complex toward Rheb.* Curr Biol, 2003. **13**(15): p. 1259-68.

158. Zhao, S., et al., *A brain somatic RHEB doublet mutation causes focal cortical dysplasia type II.* Exp Mol Med, 2019. **51**(7): p. 84.

159. Grabiner, B.C., et al., *A Diverse Array of Cancer-Associated MTOR Mutations Are Hyperactivating and Can Predict Rapamycin Sensitivity.* Cancer Discovery, 2014. **4**(5): p. 554-563.

160. Nickerson, M.L., et al., *Mutations in a novel gene lead to kidney tumors, lung wall defects, and benign tumors of the hair follicle in patients with the Birt-Hogg-Dube syndrome.* Cancer Cell, 2002. **2**(2): p. 157-64.

161. Okosun, J., et al., *Corrigendum: Recurrent mTORC1-activating RRAGC mutations in follicular lymphoma.* Nat Genet, 2016. **48**(6): p. 700.

162. Brown, E.J., et al., *Control of p70 s6 kinase by kinase activity of FRAP in vivo.* Nature, 1995. **377**(6548): p. 441-6.

163. Brunn, G.J., et al., *Phosphorylation of the translational repressor PHAS-I by the mammalian target of rapamycin.* Science, 1997. **277**(5322): p. 99-101.

164. Beretta, L., et al., *Rapamycin blocks the phosphorylation of 4E-BP1 and inhibits cap-dependent initiation of translation.* EMBO J, 1996. **15**(3): p. 658-64.

165. Ruvinsky, I. and O. Meyuhas, *Ribosomal protein S6 phosphorylation: from protein synthesis to cell size.* Trends Biochem Sci, 2006. **31**(6): p. 342-8.

166. Hannan, K.M., et al., *mTOR-Dependent regulation of ribosomal gene transcription requires S6K1 and is mediated by phosphorylation of the carboxy-terminal activation domain of the nucleolar transcription factor UBF.* Molecular and Cellular Biology, 2003. **23**(23): p. 8862-8877.

167. Mayer, C., et al., *mTOR-dependent activation of the transcription factor TIMA links rRNA synthesis to nutrient availability.* Genes & Development, 2004. **18**(4): p. 423-434.

168. Michels, A.A., et al., *mTORC1 Directly Phosphorylates and Regulates Human MAF1.* Molecular and Cellular Biology, 2010. **30**(15): p. 3749-3757.

169. Shor, B., et al., *Requirement of the mTOR Kinase for the Regulation of Maf1 Phosphorylation and Control of RNA Polymerase III-dependent Transcription in Cancer Cells.* Journal of Biological Chemistry, 2010. **285**(20): p. 15380-15392.

170. Zhang, H., et al., *Regulation of cellular growth by the Drosophila target of rapamycin dTOR.* Genes Dev, 2000. **14**(21): p. 2712-24.

171. Barbet, N.C., et al., *TOR controls translation initiation and early G1 progression in yeast.* Mol Biol Cell, 1996. **7**(1): p. 25-42.

172. Hentges, K.E., et al., *FRAP/mTOR is required for proliferation and patterning during embryonic development in the mouse.* Proc Natl Acad Sci U S A, 2001. **98**(24): p. 13796-801.

173. Sengupta, S., et al., *mTORC1 controls fasting-induced ketogenesis and its modulation by ageing.* Nature, 2010. **468**(7327): p. 1100-4.

174. Guertin, D.A., et al., *Ablation in mice of the mTORC components raptor, rictor, or mLST8 reveals that mTORC2 is required for signaling to Akt-FOXO and PKC alpha but not S6K1.* Developmental Cell, 2006. **11**(6): p. 859-871.

175. Vega-Rubin-de-Celis, S., et al., *Multistep regulation of TFEB by MTORC1.* Autophagy, 2017. **13**(3): p. 464-472.

176. Settembre, C., et al., *TFEB links autophagy to lysosomal biogenesis.* Science, 2011. **332**(6036): p. 1429-33.

177. Roczniak-Ferguson, A., et al., *The transcription factor TFEB links mTORC1 signaling to transcriptional control of lysosome homeostasis.* Sci Signal, 2012. **5**(228): p. ra42.

178. Settembre, C., et al., *A lysosome-to-nucleus signalling mechanism senses and regulates the lysosome via mTOR and TFEB.* EMBO J, 2012. **31**(5): p. 1095-108.

179. Martina, J.A., et al., *MTORC1 functions as a transcriptional regulator of autophagy by preventing nuclear transport of TFEB.* Autophagy, 2012. **8**(6): p. 903-14.

180. Ganley, I.G., et al., *ULK1.ATG13.FIP200 complex mediates mTOR signaling and is essential for autophagy.* J Biol Chem, 2009. **284**(18): p. 12297-305.

181. Kim, J., et al., *AMPK and mTOR regulate autophagy through direct phosphorylation of Ulk1.* Nat Cell Biol, 2011. **13**(2): p. 132-41.

182. Puente, C., R.C. Hendrickson, and X.J. Jiang, *Nutrient-regulated Phosphorylation of ATG13 Inhibits Starvation-induced Autophagy.* Journal of Biological Chemistry, 2016. **291**(11): p. 6026-6035.

183. Yuan, H.X., R.C. Russell, and K.L. Guan, *Regulation of PIK3C3/VPS34 complexes by MTOR in nutrient stress-induced autophagy.* Autophagy, 2013. **9**(12): p. 1983-1995.

184. Ma, X., et al., *MTORC1-mediated NRBF2 phosphorylation functions as a switch for the class III PtdIns3K and autophagy.* Autophagy, 2017. **13**(3): p. 592-607.

185. Munson, M.J., et al., *mTOR activates the VPS34-UVRAG complex to regulate autolysosomal tubulation and cell survival.* Embo Journal, 2015. **34**(17): p. 2272-2290.

186. Laplante, M. and D.M. Sabatini, *mTOR signaling in growth control and disease.* Cell, 2012. **149**(2): p. 274-93.

187. Shaw, R.J., et al., *The LKB1 tumor suppressor negatively regulates mTOR signaling.* Cancer Cell, 2004. **6**(1): p. 91-99.

188. Wang, L., et al., *Hexokinase 2-mediated Warburg effect is required for PTEN- and p53-deficiency-driven prostate cancer growth.* Cell Rep, 2014. **8**(5): p. 1461-74.

189. Cunningham, J.T., et al., *Protein and Nucleotide Biosynthesis Are Coupled by a Single Rate-Limiting Enzyme, PRPS2, to Drive Cancer (vol 157, pg 1088, 2014).* Cell, 2014. **158**(3): p. 689-689.

190. Ben-Sahra, I., et al., *mTORC1 induces purine synthesis through control of the mitochondrial tetrahydrofolate cycle.* Science, 2016. **351**(6274): p. 728-733.

191. Ben-Sahra, I., et al., *Stimulation of de Novo Pyrimidine Synthesis by Growth Signaling Through mTOR and S6K1.* Science, 2013. **339**(6125): p. 1323-1328.

192. Robitaille, A.M., et al., *Quantitative Phosphoproteomics Reveal mTORC1 Activates de Novo Pyrimidine Synthesis.* Science, 2013. **339**(6125): p. 1320-1323.

193. Bakan, I. and M. Laplante, *Connecting mTORC1 signaling to SREBP-1 activation.* Curr Opin Lipidol, 2012. **23**(3): p. 226-34.

194. Porstmann, T., et al., *SREBP activity is regulated by mTORC1 and contributes to Akt-dependent cell growth.* Cell Metabolism, 2008. **8**(3): p. 224-236.

195. Duvel, K., et al., *Activation of a Metabolic Gene Regulatory Network Downstream of mTOR Complex 1.* Molecular Cell, 2010. **39**(2): p. 171-183.

196. Peterson, T.R., et al., *mTOR complex 1 regulates lipin 1 localization to control the SREBP pathway.* Cell, 2011. **146**(3): p. 408-20.
197. Lee, G., et al., *Post-transcriptional Regulation of De Novo Lipogenesis by mTORC1-S6K1-SRPK2 Signaling.* Cell, 2017. **171**(7): p. 1545-1558 e18.
198. Yip, C.K., et al., *Structure of the human mTOR complex I and its implications for rapamycin inhibition.* Mol Cell, 2010. **38**(5): p. 768-74.
199. Ming, M., et al., *Dose-Dependent AMPK-Dependent and Independent Mechanisms of Berberine and Metformin Inhibition of mTORC1, ERK, DNA Synthesis and Proliferation in Pancreatic Cancer Cells.* PLoS One, 2014. **9**(12): p. e114573.
200. Onken, B. and M. Driscoll, *Metformin induces a dietary restriction-like state and the oxidative stress response to extend C. elegans Healthspan via AMPK, LKB1, and SKN-1.* PLoS One, 2010. **5**(1): p. e8758.
201. Robida-Stubbs, S., et al., *TOR signaling and rapamycin influence longevity by regulating SKN-1/Nrf and DAF-16/FoxO.* Cell Metab, 2012. **15**(5): p. 713-24.
202. Hara, T., et al., *Suppression of basal autophagy in neural cells causes neurodegenerative disease in mice.* Nature, 2006. **441**(7095): p. 885-9.
203. Sarkar, S. and D.C. Rubinsztein, *Small molecule enhancers of autophagy for neurodegenerative diseases.* Mol Biosyst, 2008. **4**(9): p. 895-901.
204. Selman, C., et al., *Ribosomal protein S6 kinase 1 signaling regulates mammalian life span.* Science, 2009. **326**(5949): p. 140-4.
205. Kaeberlein, M., et al., *Regulation of yeast replicative life span by TOR and Sch9 in response to nutrients.* Science, 2005. **310**(5751): p. 1193-6.
206. Kapahi, P., et al., *Regulation of lifespan in Drosophila by modulation of genes in the TOR signaling pathway.* Curr Biol, 2004. **14**(10): p. 885-90.
207. Hansen, M., et al., *Lifespan extension by conditions that inhibit translation in Caenorhabditis elegans.* Aging Cell, 2007. **6**(1): p. 95-110.
208. Szlosarek, P.W., et al., *Aberrant regulation of argininosuccinate synthetase by TNF-alpha in human epithelial ovarian cancer.* Int J Cancer, 2007. **121**(1): p. 6-11.
209. Jones, T., et al., *Direct and efficient cellular transformation of primary rat mesenchymal precursor cells by KSHV.* J Clin Invest, 2012. **122**(3): p. 1076-81.

210. Jones, T., et al., *Viral cyclin promotes KSHV-induced cellular transformation and tumorigenesis by overriding contact inhibition.* Cell Cycle, 2014. **13**(5): p. 845-58.

211. Moody, R., et al., *KSHV microRNAs mediate cellular transformation and tumorigenesis by redundantly targeting cell growth and survival pathways.* PLoS Pathog, 2013. **9**(12): p. e1003857.

212. Ye, F.C., et al., *Kaposi's sarcoma-associated herpesvirus latent gene vFLIP inhibits viral lytic replication through NF-kappaB-mediated suppression of the AP-1 pathway: a novel mechanism of virus control of latency.* J Virol, 2008. **82**(9): p. 4235-49.

213. Zhu, Y., et al., *An oncogenic virus promotes cell survival and cellular transformation by suppressing glycolysis.* PLoS Pathog, 2016. **12**(5): p. e1005648.

214. Li, Q., et al., *Genetic disruption of KSHV major latent nuclear antigen LANA enhances viral lytic transcriptional program.* Virology, 2008. **379**(2): p. 234-44.

215. Ye, F.C., et al., *Disruption of Kaposi's sarcoma-associated herpesvirus latent nuclear antigen leads to abortive episome persistence.* J Virol, 2004. **78**(20): p. 11121-9.

216. Zhou, F.C., et al., *Efficient infection by a recombinant Kaposi's sarcoma-associated herpesvirus cloned in a bacterial artificial chromosome: application for genetic analysis.* J Virol, 2002. **76**(12): p. 6185-96.

217. Lei, X., et al., *Regulation of NF-kappaB inhibitor IkappaBalpha and viral replication by a KSHV microRNA.* Nat Cell Biol, 2010. **12**(2): p. 193-9.

218. Haines, R.J., L.C. Pendleton, and D.C. Eichler, *Argininosuccinate synthase: at the center of arginine metabolism.* Int J Biochem Mol Biol, 2011. **2**(1): p. 8-23.

219. Husson, A., et al., *Argininosuccinate synthetase from the urea cycle to the citrulline-NO cycle.* Eur J Biochem, 2003. **270**(9): p. 1887-99.

220. Morris, S.M., Jr., *Arginine metabolism: boundaries of our knowledge.* J Nutr, 2007. **137**(6 Suppl 2): p. 1602S-1609S.

221. Somasundaram, V., et al., *Nitric oxide and reactive oxygen species: Clues to target oxidative damage repair defective breast cancers.* Crit Rev Oncol Hematol, 2016. **101**: p. 184-92.

222. Keshet, R. and A. Erez, *Arginine and the metabolic regulation of nitric oxide synthesis in cancer.* Dis Model Mech, 2018. **11**(8).

223. Qualls, J.E., et al., *Sustained generation of nitric oxide and control of mycobacterial infection requires argininosuccinate synthase 1.* Cell Host Microbe, 2012. **12**(3): p. 313-23.

224. Goodwin, B.L., L.P. Solomonson, and D.C. Eichler, *Argininosuccinate synthase expression is required to maintain nitric oxide production and cell viability in aortic endothelial cells.* J Biol Chem, 2004. **279**(18): p. 18353-60.

225. Mun, G.I., et al., *Endothelial argininosuccinate synthetase 1 regulates nitric oxide production and monocyte adhesion under static and laminar shear stress conditions.* J Biol Chem, 2011. **286**(4): p. 2536-42.

226. Pandit, L., et al., *The physiologic aggresome mediates cellular inactivation of iNOS.* Proc Natl Acad Sci U S A, 2009. **106**(4): p. 1211-5.

227. Steinert, J.R., et al., *Nitric oxide is a volume transmitter regulating postsynaptic excitability at a glutamatergic synapse.* Neuron, 2008. **60**(4): p. 642-56.

228. Lacza, Z., et al., *The novel red-fluorescent probe DAR-4M measures reactive nitrogen species rather than NO.* J Pharmacol Toxicol Methods, 2005. **52**(3): p. 335-40.

229. Pan, X., et al., *Nitric oxide suppresses transforming growth factor-beta1-induced epithelial-to-mesenchymal transition and apoptosis in mouse hepatocytes.* Hepatology, 2009. **50**(5): p. 1577-87.

230. Shan, Y.S., et al., *Argininosuccinate synthetase 1 suppression and arginine restriction inhibit cell migration in gastric cancer cell lines.* Sci Rep, 2015. **5**: p. 9783.

231. Herrmann, A., et al., *Targeting Stat3 in the myeloid compartment drastically improves the in vivo antitumor functions of adoptively transferred T cells.* Cancer Res, 2010. **70**(19): p. 7455-64.

232. Kujawski, M., et al., *Stat3 mediates myeloid cell-dependent tumor angiogenesis in mice.* J Clin Invest, 2008. **118**(10): p. 3367-77.

233. Gruffaz, M., et al., *TLR4-Mediated Inflammation Promotes KSHV-Induced Cellular Transformation and Tumorigenesis by Activating the STAT3 Pathway.* Cancer Res, 2017. **77**(24): p. 7094-7108.

234. Lee, M.S., et al., *Exploitation of the complement system by oncogenic Kaposi's sarcoma-associated herpesvirus for cell survival and persistent infection.* PLoS Pathog, 2014. **10**(9): p. e1004412.

235. Huang, K., et al., *Arctigenin promotes apoptosis in ovarian cancer cells via the iNOS/NO/STAT3/survivin signalling.* Basic Clin Pharmacol Toxicol, 2014. **115**(6): p. 507-11.

236. Solomonson, L.P., et al., *The caveolar nitric oxide synthase/arginine regeneration system for NO production in endothelial cells.* J Exp Biol, 2003. **206**(Pt 12): p. 2083-7.

237. Wu, M.S., et al., *Gene expression profiling of gastric cancer by microarray combined with laser capture microdissection.* World J Gastroenterol, 2005. **11**(47): p. 7405-12.

238. Delage, B., et al., *Arginine deprivation and argininosuccinate synthetase expression in the treatment of cancer.* Int J Cancer, 2010. **126**(12): p. 2762-72.

239. Bateman, L.A., et al., *Argininosuccinate Synthase 1 is a Metabolic Regulator of Colorectal Cancer Pathogenicity.* ACS Chem Biol, 2017. **12**(4): p. 905-911.

240. Feun, L.G., et al., *Negative argininosuccinate synthetase expression in melanoma tumours may predict clinical benefit from arginine-depleting therapy with pegylated arginine deiminase.* Br J Cancer, 2012. **106**(9): p. 1481-5.

241. Szlosarek, P.W., et al., *In vivo loss of expression of argininosuccinate synthetase in malignant pleural mesothelioma is a biomarker for susceptibility to arginine depletion.* Clin Cancer Res, 2006. **12**(23): p. 7126-31.

242. Wu, G. and S.M. Morris, Jr., *Arginine metabolism: nitric oxide and beyond.* Biochem J, 1998. **336 (Pt 1)**: p. 1-17.

243. Xie, L. and S.S. Gross, *Argininosuccinate synthetase overexpression in vascular smooth muscle cells potentiates immunostimulant-induced NO production.* J Biol Chem, 1997. **272**(26): p. 16624-30.

244. McCormick, S.M., et al., *DNA microarray reveals changes in gene expression of shear stressed human umbilical vein endothelial cells.* Proc Natl Acad Sci U S A, 2001. **98**(16): p. 8955-60.

245. Bogdan, C., *Nitric oxide synthase in innate and adaptive immunity: an update.* Trends Immunol, 2015. **36**(3): p. 161-78.

246. Serio, R., M.G. Zizzo, and F. Mule, *Nitric oxide induces muscular relaxation via cyclic GMP-dependent and -independent mechanisms in the longitudinal muscle of the mouse duodenum.* Nitric Oxide, 2003. **8**(1): p. 48-52.

247. Lala, P.K. and C. Chakraborty, *Role of nitric oxide in carcinogenesis and tumour progression.* Lancet Oncol, 2001. **2**(3): p. 149-56.

248. Kielbik, M., et al., *Nitric oxide donors: spermine/NO and diethylenetriamine/NO induce ovarian cancer cell death and affect STAT3 and AKT signaling proteins.* Nitric Oxide, 2013. **35**: p. 93-109.

249. Hernandez-Sierra, A., et al., *Role of HHV-8 and mTOR pathway in post-transplant Kaposi sarcoma staging.* Transpl Int, 2016. **29**(9): p. 1008-16.

250. Stallone, G., et al., *Kaposi's sarcoma and mTOR: a crossroad between viral infection neoangiogenesis and immunosuppression.* Transpl Int, 2008. **21**(9): p. 825-32.

251. Kerr, D.A., et al., *mTOR, VEGF, PDGFR, and c-kit signaling pathway activation in Kaposi sarcoma.* Hum Pathol, 2017. **65**: p. 157-165.

252. Cai, X., et al., *Kaposi's sarcoma-associated herpesvirus expresses an array of viral microRNAs in latently infected cells.* Proc Natl Acad Sci U S A, 2005. **102**(15): p. 5570-5.

253. Marshall, V., et al., *Conservation of virally encoded microRNAs in Kaposi sarcoma--associated herpesvirus in primary effusion lymphoma cell lines and in patients with Kaposi sarcoma or multicentric Castleman disease.* J Infect Dis, 2007. **195**(5): p. 645-59.

254. Flamand, M.N., et al., *A non-canonical site reveals the cooperative mechanisms of microRNA-mediated silencing.* Nucleic Acids Res, 2017. **45**(12): p. 7212-7225.

255. Saxton, R.A. and D.M. Sabatini, *mTOR signaling in growth, metabolism, and disease.* Cell, 2017. **168**(6): p. 960-976.

256. Boulanger, E., et al., *Human herpesvirus-8 (HHV-8)-associated primary effusion lymphoma in two renal transplant recipients receiving rapamycin.* Am J Transplant, 2008. **8**(3): p. 707-10.

257. Sodhi, A., et al., *The TSC2/mTOR pathway drives endothelial cell transformation induced by the Kaposi's sarcoma-associated herpesvirus G protein-coupled receptor.* Cancer Cell, 2006. **10**(2): p. 133-43.

258. Bhatt, A.P., et al., *A viral kinase mimics S6 kinase to enhance cell proliferation.* Proc Natl Acad Sci U S A, 2016. **113**(28): p. 7876-81.

259. Sabatini, D.M., *Twenty-five years of mTOR: Uncovering the link from nutrients to growth.* Proc Natl Acad Sci U S A, 2017. **114**(45): p. 11818-11825.

260. Gottwein, E., et al., *A viral microRNA functions as an orthologue of cellular miR-155.* Nature, 2007. **450**(7172): p. 1096-9.

261. Xia, J., et al., *Structural insight into the arginine-binding specificity of CASTOR1 in amino acid-dependent mTORC1 signaling.* Cell Discovery, 2016. **2**.

262. Ward, P.S. and C.B. Thompson, *Metabolic reprogramming: a cancer hallmark even warburg did not anticipate.* Cancer Cell, 2012. **21**(3): p. 297-308.

263. Bean, G.R., et al., *A metabolic synthetic lethal strategy with arginine deprivation and chloroquine leads to cell death in ASS1-deficient sarcomas.* Cell Death Dis, 2016. **7**(10): p. e2406.

264. Yoon, S.O., et al., *Focal Adhesion- and IGF1R-Dependent Survival and Migratory Pathways Mediate Tumor Resistance to mTORC1/2 Inhibition.* Molecular Cell, 2017. **67**(3): p. 512-+.

265. Hara, K., et al., *Amino acid sufficiency and mTOR regulate p70 S6 kinase and eIF-4E BP1 through a common effector mechanism. (vol 273, pg 14484, 1998).* Journal of Biological Chemistry, 1998. **273**(34): p. 22160-22160.

266. Komander, D. and M. Rape, *The ubiquitin code.* Annu Rev Biochem, 2012. **81**: p. 203-29.

267. Obenauer, J.C., L.C. Cantley, and M.B. Yaffe, *Scansite 2.0: Proteome-wide prediction of cell signaling interactions using short sequence motifs.* Nucleic Acids Res, 2003. **31**(13): p. 3635-41.

268. Hornbeck, P.V., et al., *PhosphoSitePlus, 2014: mutations, PTMs and recalibrations.* Nucleic Acids Res, 2015. **43**(Database issue): p. D512-20.

269. Hunter, T., *The age of crosstalk: phosphorylation, ubiquitination, and beyond.* Mol Cell, 2007. **28**(5): p. 730-8.

270. Hanada, M., J. Feng, and B.A. Hemmings, *Structure, regulation and function of PKB/AKT--a major therapeutic target.* Biochim Biophys Acta, 2004. **1697**(1-2): p. 3-16.

271. Radivojac, P., et al., *Identification, analysis, and prediction of protein ubiquitination sites.* Proteins, 2010. **78**(2): p. 365-80.

272. Zhou, X.F., et al., *CASTOR1 suppresses the progression of lung adenocarcinoma and predicts poor prognosis.* Journal of Cellular Biochemistry, 2018. **119**(12): p. 10186-10194.

273. Waks, A.G. and E.P. Winer, *Breast Cancer Treatment A Review.* Jama-Journal of the American Medical Association, 2019. **321**(3): p. 288-300.

274. Costa, R.L.B., H.S. Han, and W.J. Gradishar, *Targeting the PI3K/AKT/mTOR pathway in triple-negative breast cancer: a review.* Breast Cancer Research and Treatment, 2018. **169**(3): p. 397-406.

275. Mukohara, T., *PI3K mutations in breast cancer: prognostic and therapeutic implications.* Breast Cancer-Targets and Therapy, 2015. **7**: p. 111-123.

276. Li, T., E. Ju, and S.J. Gao, *Kaposi sarcoma-associated herpesvirus miRNAs suppress CASTOR1-mediated mTORC1 inhibition to promote tumorigenesis.* J Clin Invest, 2019. **130**.

277. Sabatini, D.M., *mTOR and cancer: insights into a complex relationship.* Nat Rev Cancer, 2006. **6**(9): p. 729-34.

278. Manning, B.D. and A. Toker, *AKT/PKB Signaling: Navigating the Network.* Cell, 2017. **169**(3): p. 381-405.

279. Tsai, W.B., et al., *Activation of Ras/PI3K/ERK pathway induces c-Myc stabilization to upregulate argininosuccinate synthetase, leading to arginine deiminase resistance in melanoma cells.* Cancer Res, 2012. **72**(10): p. 2622-33.

280. An, F.Q., et al., *Long-term-infected telomerase-immortalized endothelial cells: a model for Kaposi's sarcoma-associated herpesvirus latency in vitro and in vivo.* J Virol, 2006. **80**(10): p. 4833-46.